Technical University of Munich

TUM School of Life Sciences

Principles in Homeostatic Navigation

Virginia Palieri

Complete reprint of the dissertation approved by the TUM School of Life Sciences of the Technical University of Munich for the award of the

Doktorin der Naturwissenschaften

Chair: Prof. Julijana Gjorgjieva, Ph.D.

Examiners:

1. Prof. Dr. Ruben Portugues
2. Prof. Dr. Ilona Grunwald Kadow

The dissertation was submitted to the Technical University of Munich on 04.07.2023 and accepted by the TUM School of Life Sciences on 05.10.2023.

Zusammenfassung

Eine der grundlegendsten Herausforderungen, denen Tiere gegenüberstehen, besteht darin, ihre physiologischen Prozesse in einem gesunden Bereich zu halten. Um dies zu gewährleisten, haben sie verschiedene Strategien entwickelt, um schnell auf interne und externe Störungen zu reagieren und ein dynamisches Gleichgewicht, das allgemein als Homöostase bezeichnet wird, aufrechtzuerhalten. Ein prototypisches Beispiel für einen Umweltfaktor, der physiologische Prozesse in der Tierwelt tiefgreifend beeinflusst, ist die Temperatur. Da das Versagen der Reaktion auf thermischen Stress schwerwiegende Folgen haben kann, haben Tiere verschiedene Möglichkeiten entwickelt, die Thermoregulation zu erreichen. Endotherme Tiere wie Vögel und Säugetiere können autonome Mechanismen mit freiwilligen Strategien verknüpfen. Ektotherme Tiere hingegen, die den überwiegenden Teil der Tierwelt ausmachen, haben keine internen homöostatischen Prozesse und ihre Kernkörpertemperatur schwankt entsprechend den Umgebungsbedingungen. Daher ist die Umsiedlung, um einen günstigeren Ort zu finden, die einzige Option, die Ektothermen zur Thermoregulation haben. Die Erreichung der Homöostase durch Navigation ist nicht nur auf die Temperatur beschränkt, sondern stellt auch einen Mechanismus dar, der mit anderen homöostatischen Bedrohungen wie pH- und Salzgehaltsschwankungen sowie der Nahrungssuche geteilt wird. Im Rahmen dieser Arbeit werde ich diesen Prozess als homöostatische Navigation bezeichnen.

Unabhängig von der spezifischen Strategie und den beteiligten Umweltfaktoren spielt das Nervensystem eine entscheidende Rolle bei der Aufrechterhaltung der Homöostase, indem es externe Hinweise, sensorische Erfahrungen und den aktuellen physiologischen Zustand mit motorischen Handlungen kombiniert, um erfolgreich in der Umgebung zu navigieren. Eine umfangreiche Literatur, die sich mit vielen verschiedenen Tieren, sowohl Wirbeltieren als auch Nicht-Wirbeltieren, befasst, hat gezeigt, dass Organismen, wenn eine Ressource oder eine homöostatische Bedrohung in einem Gradienten organisiert ist, eine sehr konservierte Verhaltensstrategie verwenden. Sie halten ihre aktuelle Richtung bei, wenn sie sich ihrem homöostatischen Ziel annähern, oder sie reorientieren sich, wenn sie wahrnehmen, dass sie sich von ihrem beabsichtigten Ziel entfernen. In dieser Arbeit habe ich versucht, die Verhaltenskomponenten und Gehirnregionen aufzudecken, die die homöostatische Navigation bei Zebrafischlarven unterstützen. Ich habe mich hauptsächlich auf die Thermoregulation konzentriert (Kapitel 2 und 3), aber auch andere homöostatische Bedrohungen getestet, um zu sehen, ob der zugrunde liegende neuronale Schaltkreis teilweise über verschiedene Modalitäten hinweg überlappt (Kapitel 4). Aus dem Whole-Brain-Screening, das ich durchgeführt habe, wurde der

Präoptische Bereich des Hypothalamus (PoA) als eine stark reaktive Gehirnregion auf thermische Reize hervorgehoben. Da der PoA bei Endothermen die interne Körpertemperatur durch autonome Maßnahmen reguliert, war ich besonders daran interessiert, potenzielle Funktionen dieses Gehirnbereichs bei der Thermoregulation von Ektothermen zu erforschen. Ich habe auch die Funktion der dorsalen Habenula (dHb) weiter untersucht, nachdem sie in unserem Whole-Brain-Screening als eine Region identifiziert wurde, die durch verschiedene homöostatische Bedrohungen mit sehr ähnlicher Dynamik aktiviert wird. Chemogenetische und laserbasierte Manipulationen in Kapitel 5 zeigen, dass sowohl der PoA als auch die dHb die homöostatische Navigation gemeinsam unterstützen. Ersterer fungiert als "Homöostat", indem er eine Reorientierung veranlasst, wenn schnelle sensorische Veränderungen dem Tier signalisieren, dass es sich von seinem homöostatischen Sollwert entfernt; letzterer wirkt auf längeren Zeitskalen und berücksichtigt intermittierende sensorische Hinweise, um downstream Regionen eine abstraktere Darstellung der relativen Wertigkeit des Reizes unabhängig von der Reizidentität zu vermitteln. Schließlich habe ich in Kapitel 6 auch überprüft, ob eine erhöhte Reorientierung bei Verschlechterung der Bedingungen in einem thermischen Gradienten in evolutionär entfernten Organismen, die sich an unterschiedliche Umweltstatistiken angepasst haben, erhalten bleibt. Zu diesem Zweck habe ich sowohl die homöostatische Navigation durch Thermoregulation bei Zebrafischlarven als auch bei der Fruchtfliege unter nahezu identischen experimentellen Bedingungen betrachtet und präsentiere Beweise dafür, dass Fliegen und Fische dieselbe Verhaltensstrategie verwenden, wenn sie zeitlichen thermischen Gradienten ausgesetzt sind.

Summary

One of the most fundamental challenges animals face is to keep their physiological processes in a healthy range. To ensure this happens they evolved different strategies to quickly react to internal and external perturbations to preserve a dynamic equilibrium, commonly referred to as homeostasis. One prototypical example of an environmental factor deeply affecting physiological processes across the animal kingdom is temperature. Since failure to react to thermal stress can lead to severe consequences, animals have evolved different ways of achieving thermoregulation. Endotherms, such as birds and mammals, can couple autonomic mechanisms with volitional strategies. Ectotherms, on the other hand, which account for the vast majority of animals, lack internal homeostatic processes and their core temperature fluctuates matching environmental conditions. Therefore, relocation in space to find a more favorable spot is the only option ectotherms have to achieve thermoregulation. Achieving homeostasis through navigation is not just confined to temperature but it is a mechanism shared with other homeostatic threats, such as pH and salinity changes and food-seeking behaviors. Throughout this work I will refer to this process as **homeostatic navigation**.

Regardless of the specific strategy and environmental factors involved, the nervous system plays a crucial role in preserving homeostasis by combining external cues, sensory experience and current physiological state with motor actions to promote successful navigation in the surrounding environment. An extensive body of literature, in many different animals, vertebrates and non, has shown that when a resource or a homeostatic threat is organized in a gradient, organisms use a very conserved behavioral strategy. They keep the current direction of traveling if they are moving closer to their homeostatic goal or they reorient when they perceive they are getting away from their intended target. Starting from this observation, in this work, I aimed to uncover the behavioral components and brain regions supporting homeostatic navigation in larval zebrafish. I mostly focused on thermoregulation (Chapter 3, 4 and 6) but I also tested other homeostatic threats to see whether the underlying neural circuit showed partial overlap across modalities (Chapter 5). I primarily took advantage of the larval zebrafish transparent brain to perform a whole-brain imaging screen with a lightsheet microscope. From this functional screen the Preoptic Area of the Hypothalamus (PoA) was highlighted as a strongly responsive brain region to thermal stimuli. Since the PoA, in endotherms, regulates internal body temperature through autonomic measures I was particularly interested in exploring potential roles of this brain area in thermoregulation in ectotherms. I also further investigated the function of the dorsal Habenula (dHb) after it emerged in our whole-brain screen as a region activated with very similar dynamics by different homeostatic threats. Chemogenetic and laser

manipulations in Chapter 6 show that both the PoA and dHb jointly support homeostatic navigation. The former acting as a "homeostat" by driving reorientation when fast sensory changes signal the animal that it is moving away from its homeostatic setpoint; while the latter acts on longer timescales accounting for intermittent sensory cues, coupling the sensory with the motor history and conveying to downstream regions a more abstract representation of the stimulus relative valence regardless of stimulus identity. Finally, in Chapter 7 I also investigated whether the increase in reorientation in response to worsening conditions is conserved among evolutionarily distant organisms that have adapted to different environmental conditions. To this end, I looked at thermoregulation through homeostatic navigation in both larval zebrafish and the fruitfly under almost identical experimental conditions and I present evidence that fly and fish use the same behavioral strategy when exposed to thermal gradients.

Table of contents

List of Figures

Principles in Homeostatic Navigation

There are these two young fish swimming along, and they happen to meet an older fish swimming the other way, who nods at them and says, “Morning, boys. How’s the water?” And the two young fish swim on for a bit, and then eventually one of them looks over at the other and goes, “What the hell is water?”

—David Foster Wallace (Kenyon College, 2005)

1. Introduction

1.1 Homeostasis: a summary

Homeostasis can be broadly defined as a self-regulating process by which systems achieve stability adapting to changing environmental conditions (Billman 2020). It is a concept tightly linked to biological systems and, in particular, with how the body achieves a constant internal environment (Cannon 1932; Davies 2016).

Cannon wrote, "*The constant conditions which are maintained in the body might be termed equilibria. That word, however, has come to have fairly exact meaning as applied to relatively simple physico-chemical states, in closed systems, where known forces are balanced. The coordinated physiological processes which maintain most of the steady states in the organism are so complex and so peculiar to living beings - involving, as they may, the brain and nerves, the heart, lungs, kidneys and spleen, all working cooperatively - that I have suggested a special designation for these states, homeostasis. The word does not imply something set and immobile, a stagnation. It means a condition - a condition which may vary, but which is relatively constant.*"

- (Cannon 1932)

The last two sentences are particularly insightful. They highlight the dynamical nature of homeostatic mechanisms. By using the word "condition", it is stressed how, for living beings, successful survival means constantly compromising between fluctuating environmental conditions and internal needs. It is also important to point out that cells and organisms often get exposed to sudden and steep changes in various environmental factors which pose serious physiological threats; such as thermal stress, food deprivation, chemical toxins, salt and pH fluctuations. Considering that organisms can cope with these transient changes quite well, it has been proposed that homeostasis is an adaptive process where also the range of homeostatic values can be dynamically adapted (Davies 2016).

The study of physiology and homeostasis has been deeply influenced by control theory. Briefly, the core of any control system is the variable that is being controlled (Carpenter 2004). In the most general terms the goal is to get the value of this variable as close as possible to a certain desired value x, commonly referred to as setpoint. Assuming one has perfect knowledge of how the variable will behave to different commands, the set of inputs that will give the desired output can be computed in advance. However, in this scenario there is no way of knowing whether the system *actually* reached the intended value and, especially in biological systems, this knowledge would

never be exact (Carpenter 2004). Therefore, all biological systems need to monitor whether the actual outcome was, in fact, moving the system in the right direction and incorporate in the process possible environmental perturbations and mistakes.

Generally speaking, there are two ways of adjusting the output until the system reaches homeostasis (i.e. the setpoint). Either through feedback systems or feedforward mechanisms (Billman 2020). When the sensory results from current actions are used to control future actions we talk about sensorimotor feedback. This is, for example, how a thermostat works. When the room temperature crosses a certain threshold the device turns on and stays on until the temperature doesn't fall again into the specified range. This type of control is called negative feedback loop. The organism, or the object, tries to achieve the desired output (e.g. maintain a stable temperature) and it responds only when there is a failure in meeting such a goal. Organisms can also build on the results that generate a favorable outcome to produce still greater actions (i.e. positive feedback). However, in this work, I will focus on the negative feedback mechanisms.

Homeostasis can also be controlled through feed forward mechanisms. In this case, contrary to what happens with feedback regulation, the system gets updated before detecting any actual change in the controlled variable. This is similar to switching on the heating as soon as a window is open, and before detecting an actual change in temperature. It is important to highlight that these mechanisms heavily rely on the assumption that the world is coherent and structured. Furthermore, they still need sensory information about the nature and the extent of the potential disturbance. For example, the number of windows and doors in the house must be monitored and sensors must detect when they are opened. Without this information a response cannot be elicited before the temperature moves significantly away from the setpoint and the entire system is then better described as negative feedback control.

For animals that have evolved a central nervous system, it is beyond any doubt that the brain plays a crucial role in preserving homeostasis. Animals take actions to alter their own state with respect to the environment or to alter the environment itself in response to external sensory stimuli or internal needs. Regardless of the specific strategy adopted, the brain shapes future actions and autonomic responses, by comparing environmental and internal signals relative to past and ongoing experience with the animal's physiological state (Goodman 1980).

In this scenario multiple types of control are likely to happen in parallel and it is difficult to incorporate more abstract concepts such as adaptation, learning and decision-making with the classical framework of control theory (Goodman 1980). To circumvent this problem frameworks such as *hierarchical control* (Mesarović 1964) have been proposed (Figure 1). In this framework, first-level components such as organs and muscles are the targets of the homeostatic processes.

They ultimately mediate the responses to internal and external stimuli. The second level is where changes in a given variable are detected and autonomous regulation is initiated. Finally, the third level (i.e. the central nervous system) integrates the information coming from lower levels to coordinate the physiological and behavioral responses to changing environmental conditions and internal needs (Goodman 1980).

Figure 1: Hierarchical organization of homeostatic navigation

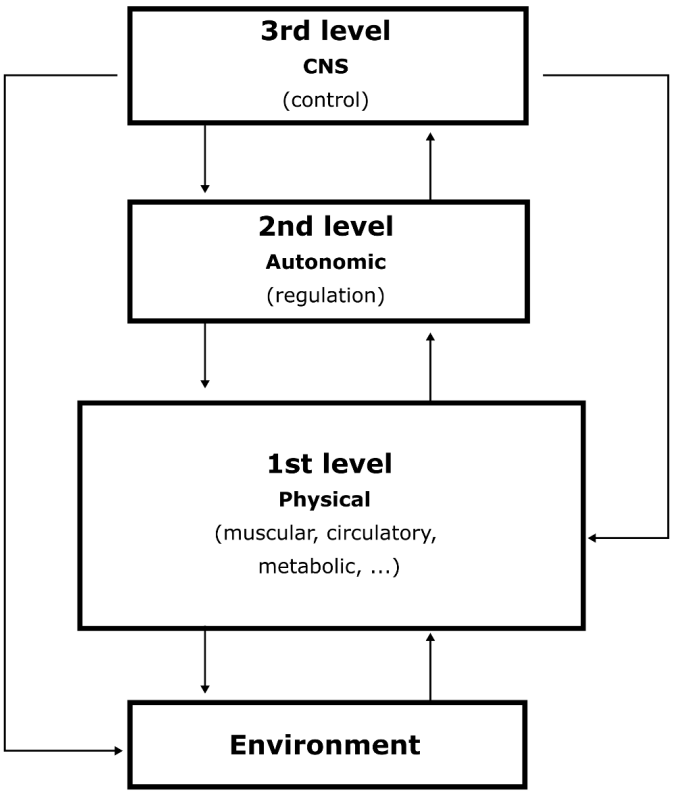

Figure 1: Multilevel regulation sketched from Goodman 1980. CNS= central nervous system

1.2 Thermal homeostasis

As previously mentioned, animals must ensure that their core temperature stays within a certain optimal range for their metabolic processes. A failure in maintaining thermal homeostasis can have severe consequences: from tissue damage to failure of the entire system. It does not come as a surprise that animals have evolved a plethora of different mechanisms to ensure that their body temperature is tightly regulated.

1.2.1 In endotherms

Endotherms, or warm-blooded animals, such as mammals and birds, can exploit both autonomic (involuntary) and behavioral (volitional) measures to maintain their core temperature. For example, mammals, when exposed to intense cold stress, control their core body temperature by, on one hand, promoting sympathetic thermogenesis in the brown adipose tissue (BAT) and, on the other hand, starting involuntary muscle contractions to start thermogenesis through shivering (Nakamura, Nakamura, and Kataoka 2022). The primary neural pathways responsible for coordinating the automatic physiological response to temperature changes in the mammalian brain comprise several hypothalamic and brainstem areas, which include the preoptic area (PoA), the dorsomedial hypothalamus (DMH) and the rostral medullary raphe region (rMR) (Nagashima et al. 2000; Nakamura et al. 2005; DiMicco and Zaretsky 2007) (Figure 2). Information from the skin thermoreceptors are relayed via glutamatergic projections to the PoA (Nakamura, Nakamura, and Kataoka 2022). This region, then, inhibits the sympathoexcitatory neurons in the DMH and rMR, both directly contacting the rMR and indirectly through the DMH. The rMR is the actual premotor center that promotes BAT thermogenesis, cutaneous vasoconstriction and vasodilation, and cardiovascular responses for both heat and cold defensive behaviors (Morrison, Sved, and Passerin 1999; Blessing and Nalivaiko 2001; Cao and Morrison 2003; Nason and Mason 2004; Nakamura and Morrison 2011). Conversely, the DMH facilitates some of those responses, such as BAT thermogenesis and cardiovascular responses but it is not involved in others (e.g. vasoconstriction) (Houtz et al. 2021). Those measures tend to be activated in a hierarchical fashion probably reflecting the difference in energy expenditure for the animal. For example, before promoting sweating and, consequently, water loss, heat stress triggers vasodilation (Costill and Fink 1974).

Figure 2: In mammals the PoA integrates signals from different homeostatic threats

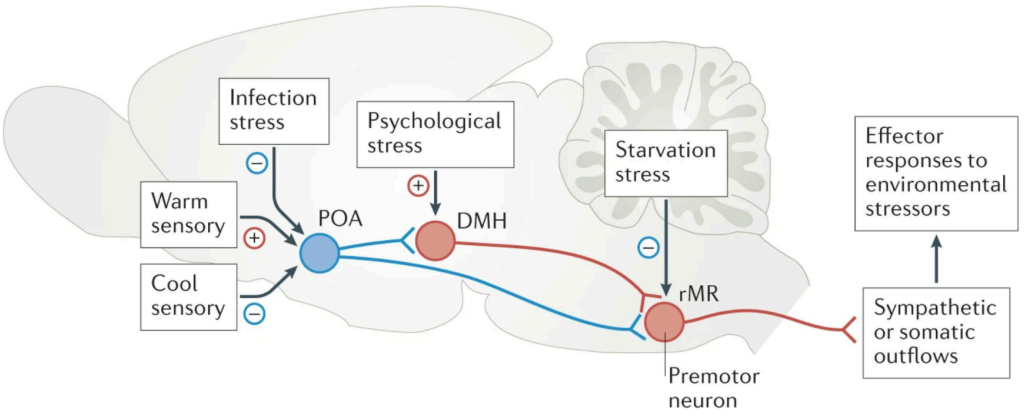

Fig. 2: Diagram illustrating the various inputs to and outputs from the Preoptic Area (PoA), emphasizing its role in thermal regulation and response to diverse physiological stressors. DMH = dorsomedial hypothalamus, rMR = rostral medullary raphe region. From Nakamura, Nakamura and Kataoka 2022.

When these mechanisms are not sufficient to achieve or maintain thermal homeostasis, they can be coupled with voluntary behavioral responses. Whereas physiologic responses are involuntary, thermoregulatory behaviors are flexible, goal-oriented and optimized to reach homeostasis faster (Tan and Knight 2018). Mammals exhibit complex behaviors which include nest or burrow making (Terrien, Perret, and Aujard 2011), social behaviors such as huddling with conspecifics (Batchelder et al. 1983); and, in humans, wearing clothes and turning on air-conditioning. However, the most basic and evolutionary conserved behavioral strategies animals, including endotherms, use are warm and cold-seeking behaviors, in which animals move in their environment to alter the rate of heat loss or absorption (Tan and Knight 2018, Figure 2). The circuit associated with these behavioral responses is still not completely understood. The PoA itself is sufficient but not necessary for operant responses to heat (Gale, Mathews, and Young 1970; Laudenslager 1976; Satinoff 1964; H. J. Carlisle 1966; H. J. Carlisle and Laudenslager 1979) and optogenetic stimulation of different subpopulations in the PoA promote cold-seeking behavior, facilitate postural extension for heat dissipation and inhibit nest building in a cold environment (Tan and Knight 2018). However, the majority of lesions in the PoA leave most of the thermoregulatory voluntary behaviors intact. The following results suggest that the behaviors observed are more of a consequence of the loss in autonomic regulation (Tan and Knight 2018). Furthermore, forebrain ablations have not yet revealed any specific region essential for thermoregulatory behaviors, comparable to the PoA's role in autonomic responses.

Strikingly, the PoA - DMH - rMR pathway is also involved in tracking and orchestrating responses to other homeostatic threats, such as infections and starvation and it interacts with circuits involved in psychological stress (Nakamura, Nakamura, and Kataoka 2022) raising the compelling hypothesis that the PoA acts as a "homeostat". This structure can use a combination of feedback or feedforward mechanisms to ensure that physiological stressors do not push the system away from its optimal range.

1.2.2 In ectotherms

Unlike mammals and birds, the vast majority of animals, such as amphibians, reptiles, fish and most invertebrates, are ectotherms. They do not possess autonomic measures to cope with thermal stress. Therefore, their core temperature closely follows the environmental temperature. To minimize thermal stress they have two main mechanisms in place. On one hand, if temperature fluctuations occur at long timescales (e.g., seasonal), neural networks have evolved to be robust. Consequently, even if different types of ionic channels are affected to different extents by temperature, the overall circuit still manages to function over an extended temperature range (Alonso and Marder 2020). However, when temperature fluctuates rapidly, animals have only one option to prevent serious damage: they must relocate within their habitat to find where, in the surrounding environment, the temperature aligns with their homeostatic setpoint. As a consequence, understanding how an ectotherm achieves thermal homeostasis is a question tightly linked with uncovering how it navigates in its environment.

1.3 The vast array of navigational strategies

Navigation is an extremely complex phenomenon which happens at multiple time scales and couples evolutionary conserved behavioral strategies with more recent mechanisms supporting complex spatial representations. For this reason, Wiener et al. 2011 proposed that navigation can be divided into hierarchically organized building blocks (see Figure 3). Those blocks are not intended to be strictly discrete, neither the framework of the *Navigational Toolbox* suggests animals consciously "select" the level to use, rather it proposes that even complex behaviors and neural representations are synthesized from more elemental processes. Understanding how the lower and fundamental levels work, can help to shed light on what are the most basic transformations that the brain computes.

The first and most fundamental level comprises the *sensorimotor transformations*. The direct input from different sensory modalities such as vision or olfaction is coupled with easily distinguishable behavioral patterns. Importantly, the action is directly linked with the sensory reafference and the animal does not need to remember its past actions or any allocentric cue.

In the second level, animals start combining inputs from different sensory modalities to extract information about position and direction of traveling. A set of representations referred to as *spatial primitives*. Examples of those could be velocity, heading direction or landmark identification.

Finally, in the third level, animals form *spatial constructs* from the *spatial primitives*. For example, velocity and information about the landmarks can be combined to compute current location in relation to the surrounding environment. The animal then has an internal representation of space (i.e. a cognitive map) that can be used to calculate shortcuts.

Already from this distinction, it is clear that animals don't need to have all the tools or all the levels listed in Figure 1 to show navigational behavior. For example, an animal could use only the tools from the *sensorimotor toolbox* when exposed to temperature fluctuations to locate its homeostatic setpoint.

Figure 3: The different levels in the navigational toolbox

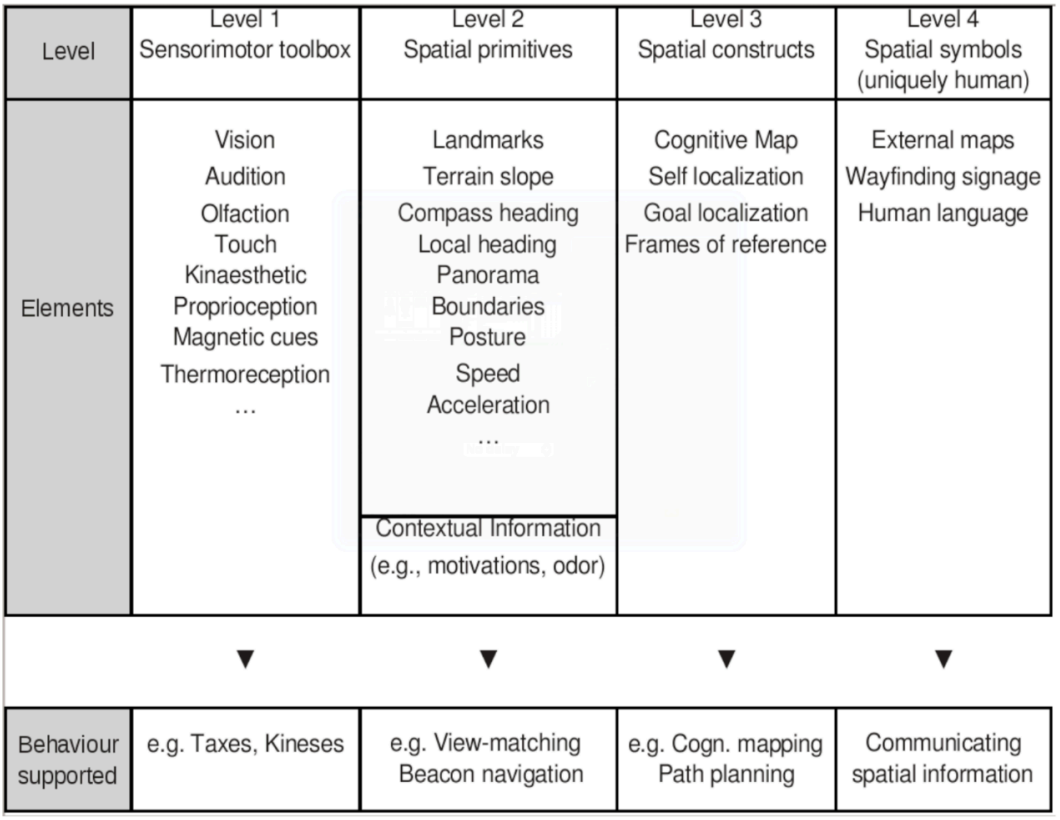

Fig. 3: The Navigational Toolbox from Wiener 2011

1.4 Conceptual relevance: homeostatic navigation

As previously mentioned, there is limited knowledge about the brain regions that support voluntary behavioral strategies (i.e. navigation) in thermoregulation. In the case of endotherms, interpreting the results becomes challenging due to the simultaneous presence of autonomic measures during the manifestation of warm or cold-seeking behavior. Conversely, ectotherms are forced to relocate within their environment whenever they are pushed away from their homeostatic setpoint and this is true not only for temperature but also in presence of other homeostatic threats.

In my work, I decided to investigate the brain regions involved in homeostatic navigation in a small ectotherm. To simplify the problem and focus on its most fundamental and conserved aspect, I chose to concentrate on uncovering the neural substrates of a highly studied navigational strategy. This tactic is expressed when animals navigate spatial gradients of resources and homeostatic threats and it is referred to as **behavioral hysteresis** (Glauser 2013). A concept borrowed from physics and initially used to describe the behavior of ferromagnetic materials in a magnetic field (Bertotti 1998). This strategy is evolutionarily conserved across diverse species and exhibits remarkable robustness in its expression across various sensory modalities.

1.5 The importance of gradient navigation

When thinking about natural environments, one quickly realizes that, with the notable exception of predators, sensory cues signaling the presence of resources and physiological threats are not organized in an all-or-nothing fashion, rather they form spatial gradients. When animals face the fundamental challenge of preserving homeostasis, they have to quickly extract relevant information about the distribution of the resource or the threat at hand to quickly navigate closer to their homeostatic setpoint (Gomez-Marin and Louis 2012).

Even though organisms move in a variety of ways in many different environments and mediums, it is important to remember that their goal, during relocation, is to extract spatially-relevant information, often across different modalities, to instruct a motor output. Although the vast spectrum of sensory inputs and array of behaviors calls for caution in drawing parallelism, one cannot overlook the fact that some processes in gradient navigation may have been conserved during evolution (Wiener et al. 2011).

1.6 Fundamental navigational strategies in gradient climbing

When exposed to a gradient, animals use a plethora of tools to locate the source: visual cues, landmarks and past experience (Gire et al. 2016). However, when they have no prior knowledge about the surrounding environment and they don’t have access to visual cues; the only information available becomes the stimulus intensity detected by the sensors across the animal's body (Gomez-Marin and Louis 2012). Then, organisms need to organize a behavioral strategy which leads to either approach or avoid the stimulus source.

Regardless of the specific movement characteristics, body plan and medium, avoidance is usually achieved through reorientation, while approach is mediated by periods in which the animal keeps its current direction of traveling, with a straight trajectory (Berg and Brown 1972; Berg 2000; Garrity et

al. 2010; Mori, Sasakura, and Kuhara 2007; Linjiao Luo et al. 2010; Glauser 2013; Larsch et al. 2015; Berrigan and Pepin 1995; Gomez-Marin and Louis 2012; Simões et al. 2021; Herrera et al. 2021).

Because the momentary detection of stimulus intensity does not carry any directional information per se (Wechsler and Bhandawat 2023; Le Goc et al. 2021), animals need to have strategies in place to compute if they are moving away or toward the source. For doing so, they can either compare the stimulus intensity at several separate sensors across their bodies or compare stimulus intensity in time during sequential sampling (Gomez-Marin and Louis 2012).

Considering these assumptions, we can delineate two broad scenarios. In the first case, the animal has constant access to sensory cues and therefore can associate the change in stimulus intensity with its own actions, in real time, in a feedback loop. This type of behavioral strategies only require the tools from the *sensorimotor toolbox* where different movements properties such as speed, frequency of movements, amount of reorientation is directly linked to the **change in stimulus intensity**.

In the second scenario access to sensory cues and consequently change in stimulus intensity is intermittent. For example, in the presence of wind or if there are obstacles on the path. In this type of environment, the stimulus is permissive to express certain behavioral patterns, but the execution of said patterns is mostly independent from the stimulus presence (Wechsler and Bhandawat 2023). The animal can use additional cues such as landmarks, or heading direction to know if it is moving in the right direction or leverage a longer working-memory of the stimulus changes and past actions. Those behavioral strategies employ a mixture of tools from the *sensorimotor toolbox* and *spatial primitives* (Wiener et al. 2011).

1.7 Behavioral Hysteresis in gradient navigation across different organisms and sensory modalities

Not to be confused with Hysteria

-Wikipedia

When an animal is moving in a spatial gradient, and cannot directly detect any stimulus intensity difference across its body, it needs to extract this information in time from sequential sampling (Figure 4a). As a result of its own movements, the animal can encounter different stimulus values. I will refer to these as WCxt (Worsening Context) when the animal moves away from its homeostatic setpoint, and ICxt (Improving Context) when it moves closer to its homeostatic goal (Figure 4b).

Importantly, the instantaneous information about the stimulus intensity, even after it is compared to the internal homeostatic setpoint, is not sufficient to determine whether the animal is traveling in the right direction and does not lead to any sort of structured behavioral strategy or navigation (Le Goc et al. 2021, Figure 4c, d). The only way an animal can infer whether it is successfully approaching the setpoint is by comparing the stimulus intensity across (at least two) sequential sampling events. This type of process requires the use of memory (Figure e, f).

The animal stores the information about stimulus intensity acquired over time, computes the derivative to know if it is moving away or toward the homeostatic setpoint and it finally instructs the behavior accordingly. In particular, it reorients more when it detects that the conditions are worsening and keeps the current direction of traveling when the situation is improving and it is approaching its homeostatic goal. Behavioral hysteresis can lead to opposite behavioral outputs for the same absolute stimulus intensity. This behavioral strategy has been extensively described across many different organisms, from unicellular bacteria to mammals, and sensory modalities.

Figure 4: Importance of sensory history in gradient navigation

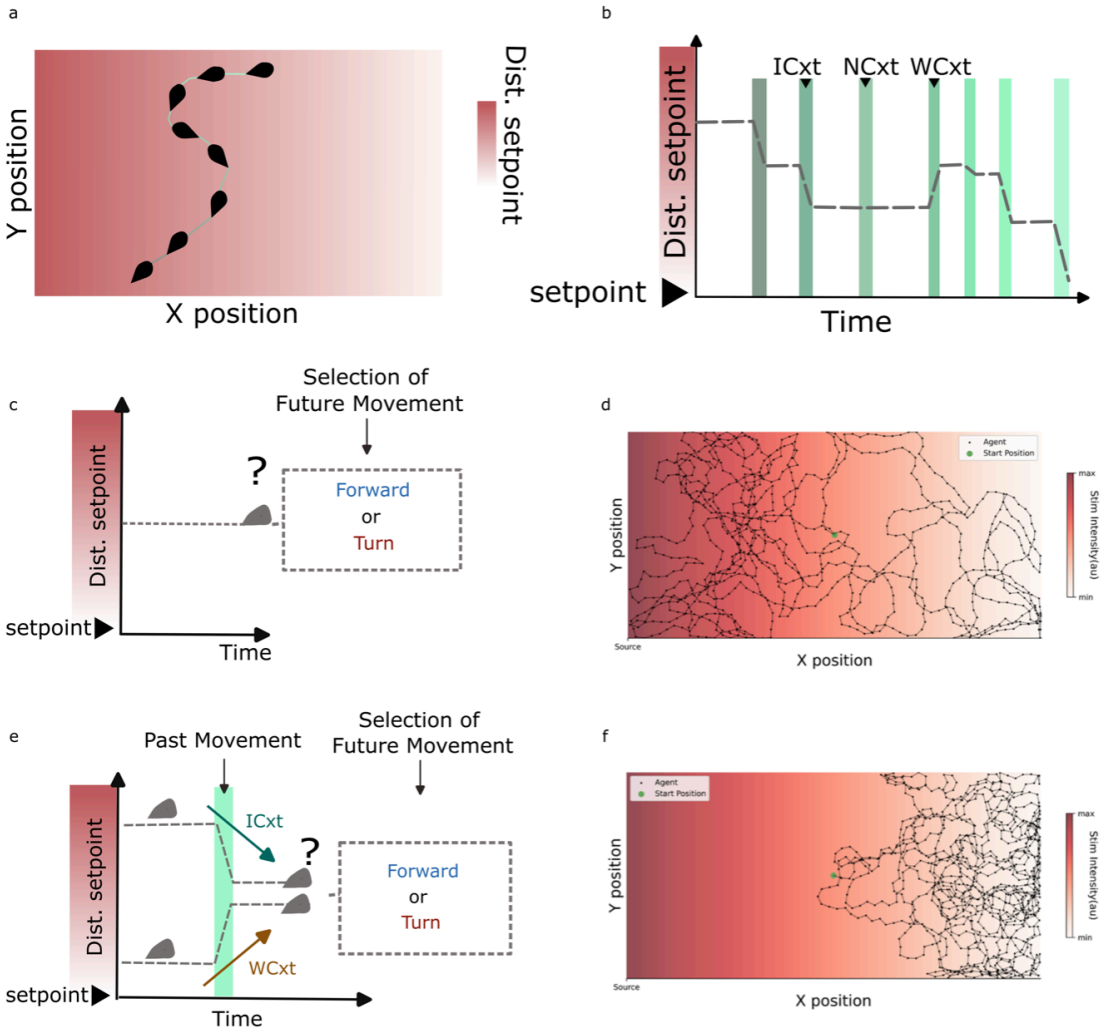

Fig. 4: **a**. Sketch of an example trajectory of an animal navigating in a spatial thermal gradient. The different shades of green represent the progression of time from dark to light green. **b**. Context associated with the change in temperature experienced during a movement. ICxt = Improving Context. The animal moved closer to setpoint. WCxt = Worsening Context. The animal moved further away from the homeostatic setpoint. **c**. The animal has no memory besides the instantenous detection of the stimulus intensity and its behavioral ouput just depends on the distance from the setpoint. **d**. Simulation where the probability of turning is solely influenced by the stimulus intensity. The animal fails to reach its homeostatic setpoint **e**. The animal retains memory of the temperature experienced in the past and computes the derivative with the current measurament to bias its behavior based on context. **f**. Simulation where the amount reorientation is influenced by sensory context. The animal quickly and efficiently finds its homeostatic setpoint.

1.7.1 In *E. coli*

Pioneering work from Howard Berg (Berg and Brown 1972; Berg 2000) showed that the unicellular bacteria E. *coli* navigates up a gradient of a chemoattractant by suppressing the amount of reorientation (i.e. tumbles) when the concentration of the stimulus was increasing. When there is no chemical gradient present, a swimming bacterial cell engages in a three-dimensional random walk. Briefly, the cell punctuates periods of swimming in a straight line with tumbles (Figure 5 top). Before reorienting E. *coli* briefly stops, opens the flagella and then reorients and starts swimming in a random direction (Figure 5 bottom). Turns direction is not correlated over time, meaning that there is no memory of the previous direction the cell sampled. Consequently, each time there is the same stochastic probability that a direction is chosen for a reorientation maneuver (Figure 5 top). Strikingly, Berg also showed that the amount of reorientation E. *coli* exhibits when it is moving away from the source of the chemoattractant is indistinguishable from the spontaneous tumbling rate in isotropic solutions. This rate only diminishes when the cell is moving toward the chemoattractant (Figure 5 top). As a result, runs are prolonged when the cell is heading up the gradient, effectively, producing behavioral hysteresis. He also uncovered the molecular machinery supporting this process. He showed that under isotropic conditions the spontaneous rate of tumbling is set by an intracellular phosphorylation cascade that eventually reverses the rotation of the flagella, causing the cell to reorient in a random direction. Extracellular ligands can bind to chemoreceptors expressed on the membrane and modulate the tumbling rate by reducing the frequency at which this phosphorylation process happens (Berg 2000).

E. coli also has adaptation mechanisms in place which allow the cell to maintain sensitivity over a substantial range of attractant concentrations. In this way, the information used to navigate away or toward the attractant predominantly comes from the changes in solute concentration and not from the overall absolute concentration of the attractant (Falke et al. 1997). Otherwise, the behavioral output would be predominantly dominated by absolute stimulus intensity and its distance from the desired homeostatic goal and, as previously stated, this would not allow for efficient gradient navigation (Le Goc et al. 2021). While less is understood about the mechanisms governing thermotaxis, studies have demonstrated that *E. coli* can navigate thermal gradients using a similar strategy as described for chemotaxis (Demir and Salman 2012). Furthermore, the molecular machinery involved in thermotaxis and chemotaxis exhibits significant redundancy, indicating that the cell employs a single molecular mechanism to regulate its homeostatic needs.

Figure 5: Gradient navigation in *E. coli*

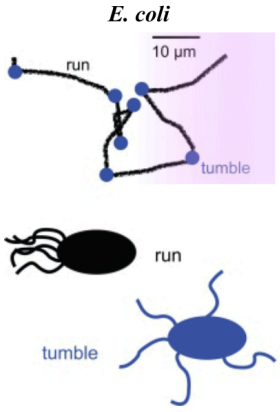

Fig. 5: **Top**: Example trajectory of *E. coli* naviganting a gradient of a chemoattractant. When the concentration increases the cell favors longer runs. **Bottom**: Depiction of the position of the flagella during a run and a tumble. Adapted from Gomez-Marin et al., 2010

1.7.2 In *C. elegans*

Despite having a relatively small central nervous system, with just 302 neurons in the hermaphrodite, *C. elegans* exhibits fairly sophisticated thermosensory behaviors (Glauser 2013). Moreover, this model system leverages powerful genetic tools, fast generation time, the entire wiring diagram reconstructed and a wide range of stereotyped behaviors. It doesn't come as a surprise that *C. elegans* is the most extensively studied model organism for understanding thermotaxis (Hedgecock and Russell 1975; Jurado et al. 2010; Kimura et al. 2004; Mori, Sasakura, and Kuhara 2007; Garrity et al. 2010; Glauser 2013). Generally, when placed on an agar plate, worms lie on either of their sides and move either forward or backward, contracting their muscles along the ventral and dorsal surface (Iino and Yoshida 2009) (Figure 6 bottom). Similarly to *E. coli, C. elegans* moves in the surrounding environment using a random walk, alternating straight runs with turns, where the animal reorients and then selects another random direction (Figure 6 top and bottom). The first interesting observation about *C. elegans* behavior in a thermal gradient is that worms do not have a fixed homeostatic setpoint but they rather choose a temperature they learned to associate with the presence of food when exposed to a static, spatial thermal gradient (I. Aoki and Mori 2015). Hedgecock and Russell in 1975 have shown that *C. elegans* use three main modes of thermotactic behavioral strategies: positive thermotaxis (exhibited below the preferred temperature (Tpref)), negative thermotaxis (exhibited

above Tpref) and isothermal tracking (exhibited in proximity of Tpref). During isothermal tracking, *C. elegans* manage to stay remarkably close to their preferred temperature by orienting perpendicular to the gradient (in both radial and linear gradients) and following isothermal lines for up to 2 minutes while diverging less than 1 mm. Worms exhibit negative and positive thermotaxis, although negative thermotactic behavior is more robust and happens under a broader range of environmental conditions. However, in both cases, similar to *E. coli*, *C. elegans* modulates the probability of performing a reorientation maneuver depending on whether it is moving away or toward its preferred temperature, effectively showing behavioral hysteresis (same as in chemotaxis Figure 6 top). In striking similarity to *E. coli,* the behavior employed by *C. elegans* in the presence of a chemoattractant is exactly the same as in a thermal gradient (Hedgecock and Russell 1975; Iino and Yoshida 2009). Moreover, when the main thermosensory neuron, AFD, is ablated, animals are still able to migrate to cold regions during thermotaxis. AWC neurons, mostly involved in chemotaxis, have been shown to respond to temperature changes as well (Kuhara et al. 2008; Biron et al. 2008). Additionally, AFD has been shown to be involved in hygrotaxis (Russell et al. 2014). Finally, both AFD and AWC project to the same interneuron AIY, therefore suggesting that the neural circuit modulating thermotaxis and chemotaxis is, at least, partially overlapping (I. Aoki and Mori 2015).

Figure 6: Gradient navigation in C. *elegans*

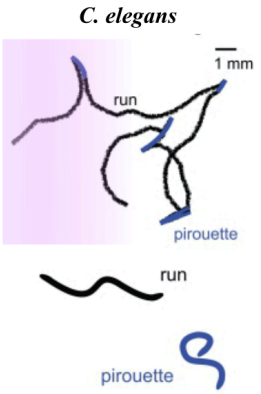

Fig. 6: **Top**: Example trajectory of C.elegans naviganting a gradient of a chemoattractant. When the concentration increases the worm favors longer runs. **Bottom**: Depiction of the body movement during a run and a piroutte. Adapted from Gomez-Marin et al., 2010

1.7.3 In *D. melanogaster*

The fruit fly *D. melanogaster*, an insect about 3 mm long, is one of the most extensively studied animal models in biology. It rose to worldwide significance thanks to the discoveries about the chromosome theory of heredity (Morgan 1910). The array of biochemical, molecular and cellular techniques pioneered in this model organism are impressive (Fernández-Moreno et al. 2007) and in more recent years a monumental effort has reconstructed almost the entire connectome of the fly brain (~100.000 neurons) (Scheffer et al. 2020). Moreover, for what concerns specifically the field of systems neuroscience the array of optogenetic and genetic tools is unparalleled (Venken and Bellen 2005; 2007; Venken, Simpson, and Bellen 2011; Duffy 2002).

The fruit fly life cycle is short, which means that it is very easy to raise a large number of individuals for experiments. The generation time is around 10 days from fertilized egg to eclosed adult, which then lives for 60 to 80 days. Its life cycle can be divided into 4 stages: embryo, larva, pupa and adult (Fernández-Moreno et al. 2007). Temperature sensation is important throughout drosophila development (Tyrrell et al. 2021). While early-stage larvae and adults seek a warm temperature of around 24 degrees, the preferred temperature drops in the late third instar when they are preparing for metamorphosis (Linjiao Luo et al. 2010). Regardless of the specific homeostatic setpoint, drosophila larvae exhibit robust positive and negative thermotaxis (Luo et al. 2010).

Similar to *C. elegans* and *E. coli* the trajectory of the larva can be described as an alternating sequence of runs and turning events. During runs, drosophila larva extends its body with the head aligned with the centerline; the forward movement is driven by a peristaltic rhythm (Berrigan and Pepin 1995). Conversely, during turns, the larva pauses and bends its body, sweeping its head one or more times. The turning event ends when the larva, after pointing the head to a new direction, starts another run (Figure 7a). In a thermal gradient the strategy adopted is exactly the same as in *E. coli* and *C. elegans*. During positive thermotaxis runs last longer when the larva is heading toward its homeostatic setpoint and the probability of reorienting is what drives this increase in runs length (Linjiao Luo et al. 2010). Therefore, the animal exhibits clear behavioral hysteresis. However, there is one notable difference. In *E. coli* and *C. elegans* thermal navigation, the changes in direction between runs are random (Gomez-Marin and Louis 2012). In other words, turn events are only used to regulate run length and, theoretically, random reorientation would produce equal numbers of runs in different directions. In drosophila larva, however, this is not the case. The animal exhibits a clear bias toward its preferred temperature when turning. They also tend to favor small changes in heading when they are already pointed toward their homeostatic setpoint and randomize headings when they happen to be traveling toward more unpleasant temperatures (Figure 7c). This bias is absent during runs. Larvae do not steer toward their preferred temperature when they are performing a run to improve their alignment (Luo et

al., 2010). In this case, turning events become decision points where the animal evaluates if its strategy has been successful or not. Importantly, this behavior, which is mirrored in negative thermotaxis, completely relies on a temporal strategy. The animal infers whether it is succeeding or not to reach its homeostatic setpoint using sequential sampling events and biasing accordingly its runs and turns (Luo et al., 2010).

Even after undergoing metamorphosis, during which most of the larval organs and tissues undergo complete degradation (Fernández-Moreno et al. 2007), adult Drosophila continues to display a pronounced thermal preference for temperatures around 24 °C (Sayeed and Benzer 1996; Simões et al. 2021). Moreover, flies are extremely sensitive to heat and will become quickly incapacitated when exposed to temperatures around 35-37 °C. In the fly nervous system, temperature changes are detected by specific population of hot and cold-activated neurons located in the third segment of the arista (Sayeed and Benzer 1996; Gallio et al. 2011). Those neurons then project to two adjacent glomeruli in the posterior antennal lobe, where activity shows a topographic map for temperature representation (Gallio et al. 2011; Frank et al. 2015). In addition to the cells located in the arista, adult flies have internal heat sensors within the head capsule, the anterior Cells (Simões et al. 2021). Finally, they have multi-modal and mechanical nociceptors distributed across their body (Tracey et al. 2003; Shimono et al. 2009). The projection neurons from the posterior antennal lobe send axons,

among other regions, to the calyx of the mushroom body (MB). This region is capable of undergoing short- and long-term synaptic plasticity and has been historically studied during olfactory choice behaviors (e.g. review Owald and Waddell 2015). Interestingly, the MB is also required for innate temperature preference (S.-T. Hong et al. 2008) and several independent studies have linked dopaminergic neurons (DANs) innervating the MB to heat perception (Bang et al. 2011; Tomchik 2013; Galili et al. 2014). DANs are also thought to acutely modulate the output of the MB during olfactory choice behavior (Cohn, Morantte, and Ruta 2015; Owald et al. 2015; Lewis et al. 2015; Sayin et al. 2019). The convergence of different sensory modalities in the mushroom bodies (MB) and dopaminergic neurons (DANs) brings to mind the partial circuit overlap observed in *C. elegans* neurons involved in chemotaxis and thermotaxis. It suggests the existence of a more abstract representation, specifically in terms of the dynamic changes (i.e. relative valence) of the stimulus rather than its identity (Aso et al. 2014). It is compelling to think that these brain regions have the capacity to encode fluctuations of natural stimuli that are crucial for maintaining homeostasis. In simpler terms, the MB could act as a decision-making center that monitors fluctuations in the environmental temperature and the distance from the homeostatic setpoint and guides its behavior based on the changing nature of the stimulus.

For what concerns the behavior of the adult *D. melanogaster*, there are still several open questions on what is the exact strategy employed by the animal when trying to reach thermal homeostasis. On one

hand, when the fly encounters sharp boundaries in a thermal gradient the difference in temperature experienced across the two antennae is thought to be responsible for driving sharp U-turns (Simões et al. 2021). In this case, the animal would be leveraging an instantaneous spatial comparison across the two sensors and not a sequential sampling of stimulus intensity. However, when flies are starved and an appetitive odor is presented they tend to favor longer runs (Sayin et al. 2018), suggesting that they may also show behavioral hysteresis when navigating a gradient. It is also worth mentioning that numerous studies in the field have documented an intriguing behavior of flies: even under high-temperature conditions, where one might anticipate increased turning behavior, flies persist in maintaining straight trajectories with a consistent heading. Remarkably, this heading is held at an arbitrary angle with respect to an external landmark, such as a bar displayed on a screen. This behavior is thought to support long-term dispersal as it relies on fixed, distant landmarks and is named menotaxis (e.g. (Giraldo et al. 2018; Green et al. 2019; Haberkern et al. 2019; Hulse et al. 2021)). The brain region underpinning this behavior is the fly's central complex. This area has garnered considerable attention in recent years, as it has been proposed to act as the center where the fly's head direction is computed (Seelig and Jayaraman 2015). Neurons in the ellipsoid body, a sub-region of the

fly central complex, are known to be activated by temperature changes (Buhl et al. 2021). The exact circuit carrying temperature information to the fly central complex is yet to be elucidated.

In summary, both the exact behavioral strategy utilized by the fruit fly to achieve thermal homeostasis and the neuronal circuit supporting it remain unknown. An intriguing hypothesis would be that, unlike the other ectotherms discussed so far in this thesis, *D. melanogaster* may employ a combination of tools from the *Navigational Toolbox* when navigating a thermal gradient. Specifically, it might directly associate sensory information with its actions (Level 1), and also use spatial primitives when sensory cues are scarce (Level 2).

Figure 7: Gradient navigation in *D. melanogaster* larvae and adult

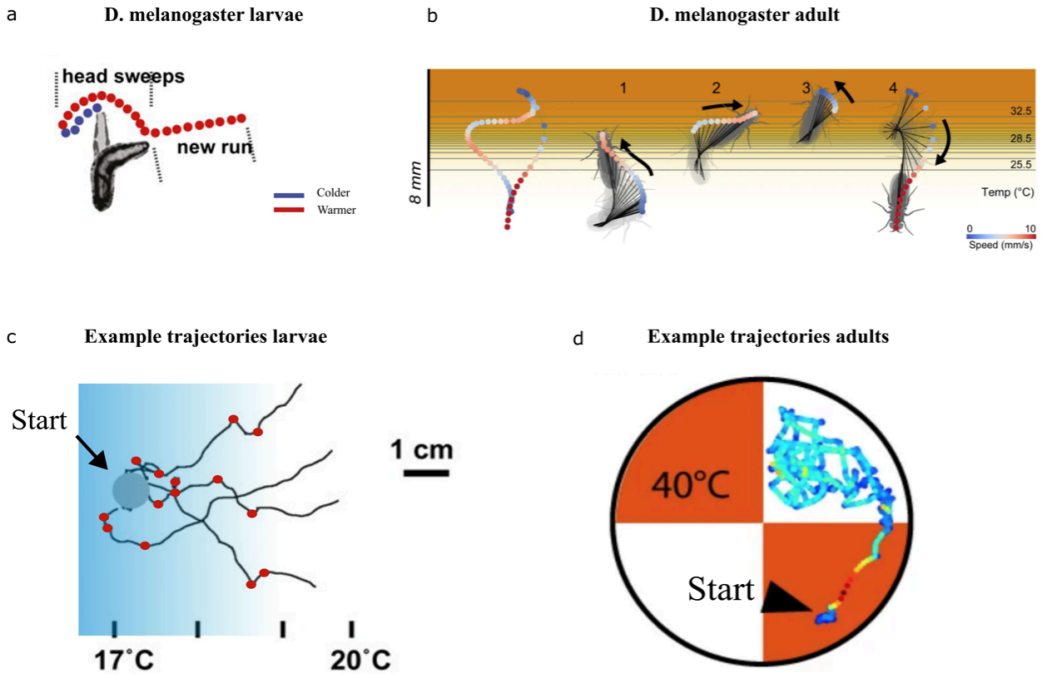

Fig. 7: **a**. Biased reorientation in *D. melanogaster* larvae. Before choosing a new direction larvae cast their head back and forth. Assuming the animal is performing positive thermotaxis and it is isothermally aligned, on one side it will perceive a drop in temperature (blue dots) while on the other side it will experience a rise in temperature (red dots). It will then use this information to select a direction for starting a new run. Adapted from Garrity et al., 2010. **b**. Adult fruitfly rapidly reorient as soon as they perceive an increase in temperature and they tend to increase their speed once they feel the temperature is getting closer to the homeostatic setpoint. Adapted from Simões et al., 2021. **c**. Example trajectories of four larvae in a thermal gradient. Turns are marked in red. When the temperature gets closer to their homeostatic setpoint larvae favor longer runs. Adapted from Garrity et al., 2010. **d**. Example trajectory of an adult fruitfly. Flies avoid hot quadrants. Adapted from Simões et al., 2021

1.7.4 In larval zebrafish

Larval zebrafish (*Danio rerio*), has emerged, in recent years, as a powerful model organism in systems neuroscience. Its well-defined behavioral repertoire and brain transparency render this little fish particularly suitable for investigating the neural circuits underlying behavior.

Very importantly, zebrafish larvae swim in discrete events, alternating between multiple oscillations of the tail and quiescent periods (Portugues and Engert 2011). The discrete nature of fish swims significantly simplifies the process of segmenting their trajectories and defining the relevant movement kinematics. Fish also exhibit a large array of innate behaviors, such as sensory-driven navigation (i.e. phototaxis and chemotaxis) and corrective behaviors such as the optomotor response (OMR) (Orger et al. 2008) and the optokinetic response (OKR) (Easter and Nicola 1997). The well-defined behavioral repertoire is coupled with an impressive array of imaging tools available for recording and manipulating neural activity (Kerr and Denk 2008; Ahrens et al. 2013; Panier et al. 2013; Portugues et al. 2013). Several transgenic lines can be generated either by enhancer trapping (Scott et al. 2007) or by labeling populations expressing particular genetic markers (Suster et al. 2009), allowing for a particular pattern of gene expression in a well-defined neuronal population.
With a number of roughly 100.000 neurons, the zebrafish brain also shares a good level of homology with mammalian brains. The larval zebrafish brain is divided into the forebrain, midbrain and hindbrain. The forebrain (comprising the telencephalon and the diencephalon) contains nuclei analogous to the mammalian olfactory bulb, basal ganglia (Subpallium), amygdala (dorsal Pallium), hippocampus (lateral Pallium), habenula and thalamus (Mueller and Wullimann 2015). The functional role of the activity of these regions is still far from being understood. They have being linked, in adult fish, with abstract cognitive abilities (T. Aoki et al. 2013; Amo et al. 2014a; Cheng, Jesuthasan, and Penney 2014; W.-Y. Chen et al. 2019), sensory-driven navigation (Zhang et al. 2017; Koide, Yabuki, and Yoshihara 2018; Choi et al. 2021; Herrera et al. 2021), memory and associative learning (Palumbo et al. 2020; Cherng et al. 2020; Okamoto et al. 2021). On the other hand, the hindbrain comprising the cerebellum, reticular formation, various clusters of reticulospinal premotor neurons, the interpeduncular nucleus (IPN) and serotonergic nuclei mostly modulates motor activity (Orger et al. 2008; Severi et al. 2014; Dunn et al. 2016; Kawashima et al. 2016; Knogler, Kist, and Portugues 2019) Like mammals, larval zebrafish also have the preoptic area of the hypothalamus (Mueller and Wullimann 2015). The exact function of this brain region remains to be uncovered, but it has been associated with processing homeostatic threats and cues from conspecifics (Wee et al. 2019; Corradi et al. 2022). A potential role in thermal homeostasis is yet to be investigated.

Larval zebrafish move away and toward small molecules and robustly perform phototaxis (X. Chen and Engert 2014; Zhang et al. 2017; Koide, Yabuki, and Yoshihara 2018; Choi et al. 2021; Herrera et

al. 2021). Strikingly, a recent study described that when fish navigate in a salinity gradient, they move towards less saline water. This is not surprising, as animals' internal ionic content is tightly regulated. What is interesting, though, is the behavioral strategy employed by larval zebrafish to achieve ion homeostasis. Fish increase their reorientation maneuvers in saltier conditions and perform forward swims upon detecting a decrease in salinity. The study also showed that this behavior is driven by perceived changes in salinity, rather than by the absolute solute concentration in the water (Herrera et al. 2021). These results support the hypothesis that larval zebrafish, similarly to *C. elegans* and drosophila larvae, exhibit behavioral hysteresis when navigating spatial gradients. Yet, it remains to be determined whether fish employ similar behavioral strategies when navigating thermal gradients, and whether such a strategy is universally applicable across diverse homeostatic challenges. Compared to other sensory modalities, very little is known about the circuit supporting thermal navigation. The only evidence comes from two studies where it has been shown that fish integrate temperature information in a 400 millisecond window preceding a swimming event (Haesemeyer et al. 2015). The articles also reported that when temperature dropped, larvae were biased towards performing more extended and forward-directed swims (Haesemeyer et al. 2015). This finding suggests that larval zebrafish may show behavioral hysteresis when trying to maintain thermal homeostasis, similarly to what has been observed in the salinity gradient. They also identified the neural circuit processing fast temperature changes (Haesemeyer et al. 2018a). The authors found temperature-related responses in the trigeminal ganglia neurons and in their target region, rhombomere 5 and 6. These findings partially addressed the question of where temperature is sensed in the brain, but a lot remains to be uncovered downstream from the sensory processing regions. It is also particularly interesting to speculate what the function of the preoptic area of the hypothalamus, which orchestrates the autonomic response in mammals (Nakamura, Nakamura, and Kataoka 2022) to thermal stress, may be in an ectotherm like larval zebrafish.

Figure 8: Gradient navigation in larval zebrafish

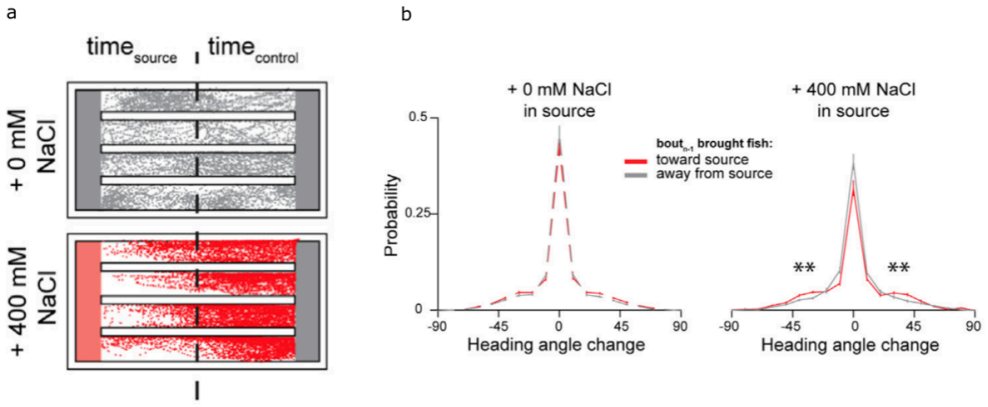

Fig. 8: **a**. Trajectories from zebrafish larvae when 0 mM (top) or 400 mM (bottom) were added to an agarose pad on one side of the arean. **b**. Average turn angle when fish were swimming away or toward the high salinity area. Fish upregulate the amount of reorientation when moving toward the salty pad. Adapted from Herrera et al., 2021.

1.8 Thesis objectives

This study aims to investigate the fundamental components of the behavioral strategy underpinning homeostatic navigation in a small ectothermic vertebrate and the brain regions supporting it. Temperature is the primary focus of this work, serving as a prototypical example of an environmental factor that profoundly affects the physiological processes of all organisms. Addressing these questions using an ectotherm is particularly insightful, as these organisms lack the ability to use internal homeostatic mechanisms to handle thermal stress. Consequently, they often move within their environment to find a temperature that aligns with their homeostatic needs, allowing us to interpret their "beliefs" about their current thermal condition from their behavior. I argue that this phenomenon is applicable to all homeostatic threats, not just temperature. Despite extensive research into the behavioral strategies and brain regions involved in navigation or homeostasis (e.g. Wiener et al. 2011; Nakamura, Nakamura, and Kataoka 2022), the interaction between these two processes and how the nervous system supports homeostatic navigation remains to be adequately addressed. It is also an open question whether the brain areas that regulate temperature homeostasis in endotherms also support homeostatic navigation in ectothermic organisms. To attempt to answer some of these questions, I have decided to utilize the well-defined behavioral repertoire of larval zebrafish, its vertebrate brain and, more importantly, its optical accessibility.

For this purpose, I initially designed several behavioral setups aiming to replicate the environmental statistics an animal would encounter while freely moving. Specifically, I set up a rectangular arena where a linear thermal gradient was established to determine the animals' preferred temperature and overall behavioral strategy. A smaller square arena where the temperature was homogeneously changed across the entire surface was used to investigate whether the behavioral strategy was entirely driven by temporal cues. Lastly, I developed a preparation for head-restrained animals, suitable for fast whole-brain imaging under a lightsheet microscope (Ahrens et al. 2013; Panier et al. 2013), where pulses of water at varying temperatures could be easily delivered.

The rationale was that these setups could help to uncover how the fish reaches and remains around its homeostatic setpoint, as well as to identify the neural circuit supporting homeostatic navigation in a thermal gradient. Using the same setups, I also aimed to confirm the observations reported in salt gradients and conduct fast whole-brain imaging while independently altering both the temperature and the salinity in the same fish.

Furthermore, I decided to examine whether evolutionarily distant animals, living in entirely different mediums and moving in dissimilar ways, would employ the same fundamental behavioral strategy when trying to achieve thermal homeostasis. To test this, I planned to expose the adult fruitfly to the

same spatial thermal gradient in the same arena where I tested larval zebrafish. I also tested *D. melanogaster* in the small square arena to confirm that the behavioral output was primarily modulated by temporal cues. Additionally, I developed a head-embedded preparation for the adult fruitfly that would allow for fast whole-brain lightsheet imaging while dynamically changing the temperature in the surrounding environment, similar to the method used in Gallio et al., 2011. The main hypothesis was that the primary behavioral strategy employed by fish, and, to some extent, by the fruitfly, is to upregulate the number of reorientation maneuvers when they are moving away from their homeostatic setpoint and to promote straighter trajectories when they approach their preferred temperature. This behavioral effect would be entirely driven by changes in temperature over time - the derivative - and not by the absolute temperature experienced.

From the imaging experiments conducted under the lightsheet microscope, I expected to identify the neural circuit tracking various features of the temperature stimulus. Among the different brain regions I was particularly interested in investigating a potential role of the PoA and dHb in homeostatic navigation, also by leveraging different types of acute and chronic manipulations.

In conclusion, I propose that the framework of homeostatic navigation in small ectotherms is a powerful tool for addressing fundamental questions such as:

- How did different brain regions evolve to satisfy the specific homeostatic needs of various species?
- To what extent is the behavioral strategy used by ectotherms in thermoregulation generalizable across other homeostatic threats?

This framework can also provide insight into whether there is functional convergence in brain regions from evolutionarily distant animals that share similar behavioral strategies when performing homeostatic navigation.

2. Material and Methods

2.1 Zebrafish husbandry

All procedures related to animal handling were conducted following protocols approved by the Technische Universität München and the Regierung von Oberbayern. Adult zebrafish (Danio rerio) from Tüpfel long fin (TL) strain were kept at 27,5-28°C on a 14/10 light cycle, and hosted in a fish facility that provided full recirculation of water with carbon-, bio- and UV filtering and a daily exchange of 12% of water. Water pH was kept at 7,0-7,5 with a 20 g/liter buffer and conductivity maintained at 750-800 μS using 100g/liter. Fish were hosted in 3,5 liter tanks in groups of 10 to 17 animals and fed the adults with Gemma micron 300 (Skretting USA) and live food (Artemia salina) twice per day and fed the larvae with Sera micron Nature (Sera) and ST-1 (Aquaschwarz) three times a day.

All experiments were conducted on 5-8 dpf larvae of yet undetermined sex. The week before the experiment, one male and one female or three male and three female animals were left breeding overnight in a Sloping Breeding Tank or breeding tank (Tecniplast). The day after, eggs were collected in the morning, rinsed with water from the facility water system, and then kept in groups of 20-40 in 90 cm Petri dishes filled with Danieau solution 0.3x (17.4 mM NaCl, 0.21 mM KCl, 0.12 mM MgSO4, 0.18 mM Ca(NO3)2, 1.5 mM HEPES, reagents from Sigma-Aldrich) until hatching and in water from the fish facility afterwards. Larvae were kept in an incubator at 28,5°C and a 14/10 hour light/dark cycle, and their solution was changed daily. At 4 or 5 dpf, animals were lightly anesthetized with Tricaine 440 mesylate (Sigma-Aldrich) and screened for fluorescence under an epifluorescent microscope. Animals positive for GCaMP6s and mCherry fluorescence were selected for the imaging experiments.

2.2 Transgenic fish

The Tuepfel long-fin (TL) wild-type strain was used for freely swimming behavioral experiments. The nacre (mitfa−/−, lacking melanophores) transgenic zebrafish lines Tg(elavl3:GCaMP6s+/+), labeling all the neurons, and Tg(16715:GAL4VP16);Tg(UAS:NTR-mCherry)), labeling the dorsal part of the Habenula, were used respectively for functional imaging experiments and chemogenetic ablations.

2.3 Flies husbandry and transgenic line

Drosophila melanogaster stocks were raised on a standard cornmeal medium (composed of 1170 g agar, 10 kg corn flour, 1 kg soya flour, 1850 g brewers' yeast, 4 kg diamalt, 4 kg sugar beet syrup, 250 g methyl paraben, and 1 L 10% phosphoric acid) at 25°C in a 60% humidified incubator with a 12-hour light-dark cycle. Experimental flies were collected immediately after hatching, sorted on CO2 fly pads, and tested at 4-8 days. It is important to note that all experiments were conducted using female flies that had not mated (virgin flies). The transgenic line used for testing *in vivo* lightsheet imaging in the fruitfly was generated in the Grunwald Kadow Lab. Briefly, to enable imaging of both PPL1 and PAM DANs, two transgenic driver lines were combined. TH-Gal4 (PPL) driver and 58E02-Gal4 (PAM) driver, on the third chromosome. The resulting line, carrying the recombination, was then crossed with the UAS-GCaMP6f reporter line to facilitate *in vivo* imaging. For all the behavior experiments *Canton-S* flies were used.

2.4 Experimental Setups

2.4.1 Freely swimming rectangular arena (large arena)

The custom-made arena (Figure 9) consists in a rectangular pool (200 × 40 × 3.5 mm3) made of aluminum for homogenous heat dispersal. The surface of the plate is taped, before each batch of experiments, with white tape (Tesa) to increase contrast and allow online tracking of fish or flies. At both ends of the arena two Peltier modules (digikey, TEC-40-39-127) were fixed with thermal tape or thermal glue (Conrad Electronic). The arena is placed on a metal block which dissipates heat from the Peltier elements and whose temperature is constantly monitored (RS Components, Nr. 706-2743). The temperature is constantly monitored at both ends of the pool with waterproof thermocouples type Pt100 (RS Components, Nr.762-1134). Temperature was controlled by two independent TEC controllers (Meerstetter, TEC-1091). After about 5 min, the temperature of the water at both sides of the pool reaches the target temperatures (25 °C and 33°C), which then remains constant over time. Water level is usually between 3-4 mm. Freely swimming larvae are monitored using a Ximea camera (MQ022MG-CM) at 110 fps, coupled with a macrolens (Navitar). The whole apparatus is placed in a light-tight box, illuminated with a homogeneous IR light emitted by a LED panel (Wilktop) placed on both sides, above the arena, spanning the entire small side of the setup.

Figure 9: Spatial gradient setup

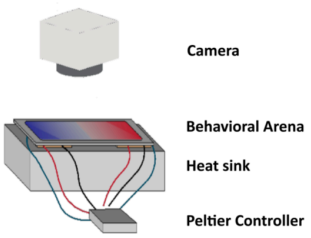

Fig. 9: Schematic of the rig used to establish a spatial thermal gradient.

2.4.2 Freely swimming square arena (small arena)

The arena consists of a square pool (40 × 40mm) made of aluminum filled to a depth of 3-4 mm (Figure 10). A single 36 W Peltier element (50 x 50 x 3.5 mm) (Namvo) is sandwiched between the heat sink and the arena, and fixed with thermal tape (Conrad Electronic). Temperature is, therefore, changed homogeneously in the entire volume of water (water level 3-4 mm). The Peltier is driven by a single TEC controller (Meerstetter, TEC-1091) and temperature is constantly monitored with a Pt100 thermocouple placed in the center of the arena (RS components, Nr. 891-9145). Homogeneous illumination is provided from the side using IR light emitted by LED stripes (Solarox). Fish are tracked at 150 fps with a Ximea camera (MQ013MG-ON), coupled with a lens (Edmund Optics).

Figure 10: Temporal gradient setup

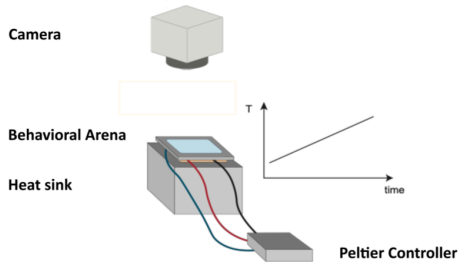

Fig. 10: Schematic of the rig used to establish a temporal thermal gradient.

2.4.3 Perfusion system for head-embedded preparation under lightsheet microscope

The head of the tethered fish is targeted with a constant flow at a rate of 1.5 ml min−1 of filtered fish water delivered through a needle (19 gauge) placed in front of the fish at an angle of 20-30° via a gravity-based 4-channels perfusion system. The needle is connected to an in-line solution heater/cooler (Warner Instruments, SC-20) to precisely regulate the temperature. Excess heat produced by the SC-20 Peltier is dissipated through a liquid cooling system (Koolance, Cat. EXT-1055). Water is constantly removed from the chamber to avoid overflowing using a small peristaltic pump controlled with an Arduino. The procedure ensures no changes in the water level (important for functional imaging purposes) and doesn't affect the behavior of the fish. The desired temperature is set through a single channel temperature controller (Warner Instruments, Cl−100) externally triggered by the computer handling the behavior protocol through a LabJack series U3-LV (LabJack). The controller also allows reading online the temperature inside the Heater/Cooler element and inside the chamber with a thermocouple which was placed immediately in front of the needle. For salt experiments, I kept the temperature of the water flowing in the chamber at room temperature and I switched selectively between only fish water and fish water + increased salinity (40 mM NaCl added to fish water). The switch is mediated by solenoid valves pinching the tubing and whose state is controlled by a ValveLink 8.2 perfusion controller (Automate Scientific) timed with the behavior protocol through an Arduino 1 (Arduino). A perfusion pencil tip combining 4 tubes into a single tip

(AutoMate Scientific, 04-08-250) placed between the solenoid valves and the inline heater/cooler (switched off for this particular experiment) ensures rapid liquid volume exchange. The setup was adapted from (Herrera et al. 2021, Figure 2a).

2.4.4 Embedded (tethered) preparation for fish

For lightsheet experiments 6-8 dpf fish are placed in 2.2% low-melting point agarose (Thermofisher) in a chamber optimized for our lightsheet microscope.

The chamber is filled with filtered fish water and agarose is removed along the optic path of the lateral and frontal laser beams (to prevent scattering), around the tail of the animal, to enable movements of the tail and around the mouth and nose. After embedding, fish are left recovering overnight before the imaging session. Before starting the imaging, light tapping on the side of the chamber is used to select the most active fish for the experiment.

The tail of the fish was tracked using an infrared source (RS Components) illuminating the larva from above. A camera (Ximea) was focused on the fish from below and through the transparent bottom of the lightsheet chamber and acquired frames at 400 Hz. Tail movements were tracked online using Stytra (Štih et al. 2019).

2.4.5 Embedded (tethered) preparation for fly

To develop a preparation in fly for fast whole-brain imaging I adapted the design of our fish chambers. I inserted a fly in a pipette tip, to which I gently removed the last part so that just the head could protrude. Then I applied dental glue (Permaplast LH Flow) around the neck of the drosophila to seal the head from the rest of the body and prevent abrupt movements and I UV curated it (SuperLite 300). Then, the entire pipette tip was positioned in a hole at the center of the chamber so that the fly head would be at the same level of the fish once it is embedded. At this point I filled the entire chamber with saline solution and I removed the cuticle on the top of the head and around an eye while leaving untouched the antennae. Then I changed the temperature in the water by adding cold water with a pipette tip (Figure 11).

Figure 11: Preparation for whole-brain imaging in *D. melanogaster*

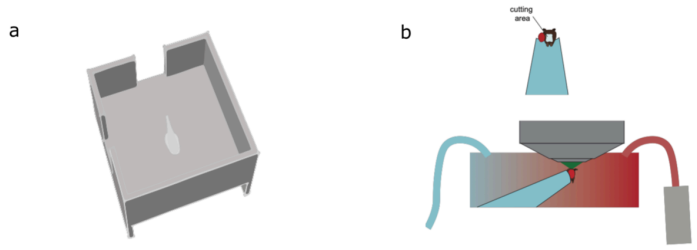

Fig. 11: **a**. Sketch of the view from the top of the lightsheet preparation in *D. melanogaster*. **b** Sketch of the view from the side of the drosophila head, microscope and inlet and outlet for temperature control.

2.5 Behavioral Experiments

All the experiments where behavior was recorded were run from 10.00 h to 20.00 h. Since all experiments were carried out in darkness, I removed the fish and flies from the incubator at least 2 hours before testing them and I always made sure that the overall room temperature was never below 23 °C.

2.5.1 Spatial gradient in the large arena for multiple animals

For controlling the thermal gradient stability, on top of having the temperature constantly monitored at both ends of the pool by waterproof thermocouples, I divided the chamber into 10 bins of 2 cm each and I measured the temperature in each bin with a digital thermometer at the beginning and at the end of the day to check for gradient stability. A cohort of 12 fish or 12 flies was placed in the arena and left to habituate for 20 minutes at a constant temperature of 25 °C, then a gradient along the long side was established for 30 minutes. The temperature range for these experiments was 20-35 °C . The warmer size was randomized across experiments.

2.5.2 Spatial gradient in the large arena for individual fish

Individual fish were transferred to the arena and their behavior was monitored in the gradient for 15 minutes. Larvae were placed in the pool after the target temperatures (25 °C and 33°C) were reached. The warmer side was randomized across experiments. For an example shape of the gradient see Figure 12.

Figure 12: Gradient shape in spatial gradient setup

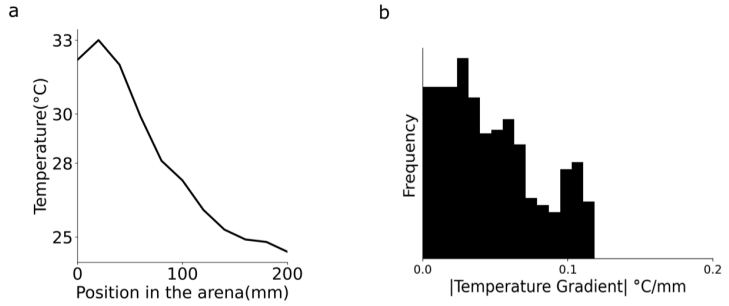

Fig. 12: **a.** Example measurament of the gradient shape in the spatial gradient setup. **b.** Histogram of temperature gradient along the arena x -axis.

2.5.3 Long temporal gradient in the small arena and for head-restrained preparation in fish

This protocol was presented to both head-restrained larvae under the lightsheet microscope and freely swimming larvae in the small square arena. The experiments lasted a total of 63 minutes. The temperature was changed in the whole arena from 24 °C to 30 °C and then back to 24 °C with 2 °C steps lasting 2 minutes each. Each fish was presented with three repetitions of this ramp stimulus. At the end and at the beginning of each ramp the fish had 5 minutes where the temperature was kept constant at 24 °C. The temperature was monitored online (Figure 13).

Figure 13: Thermal ramp for head-embedded and freely swimming fish

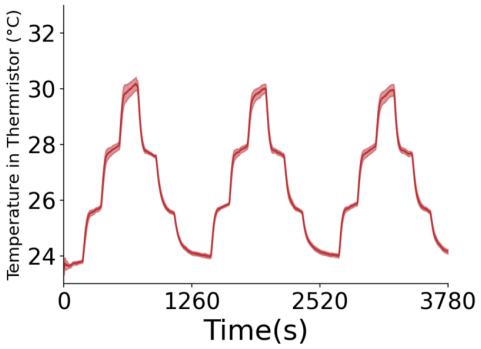

Fig. 13: Thermal ramp. Calibration was carried out in real time in the water

2.5.4 Temporal gradient in the small arena for flies

An individual fly was transferred to a small square arena and subjected to temperature ramps. In the first ramp, the temperature ranged from 24 °C to 33 °C, with a 3 °C change every 600 seconds. In the second ramp, the temperature also changed by 3 °C, but every 70 seconds. Both protocols included a pause at the beginning and end, with a 5-minute pause for the long ramp (Figure 14 left) and a 125-second pause for the short ramp (Figure 14 right).

Figure 14: Thermal ramp for *D. melanogaster*

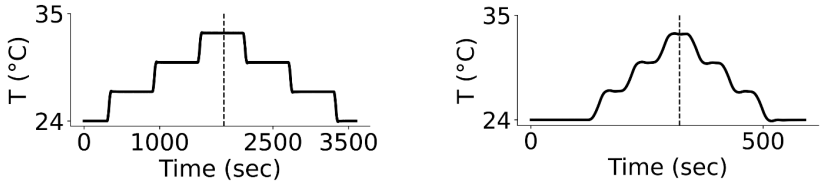

Fig. 14: Stimulus protocol for thermal ramp in *D. melanogaster*

2.5.5 Multimodal short temporal gradient for head-restrained preparation

Each head-restrained larval zebrafish I tested with this protocol was presented with a salt followed by a temperature session or vice versa. Before starting the experiment, fish were placed under the microscope with the laser on and fish water flowing for five minutes to let them habituate. The protocol comprised 5 repetitions of the same stimulus block. Each stimulus block lasted 480 s. The fish stayed at baseline (room temperature and fish water flowing at low rate) for the first 40 s, then there was an increase in temperature (or in salinity) lasting for 40 s, finally there was a 90 s pause to let temperature (or salinity) go back to baseline before the second part of the stimulus. The second part started with another 50 s at 27 °C (or 40 s + 10 s pause of salt + fish water), followed by another 40 s at 29 °C (or another 40 s of increase in salinity). The block ended with 140 s of pause. The length of the pulses and pauses was carefully chosen to obtain the same stimulus profile across modalities and to not have an accumulation of temperature and salinity in the chamber over time. To this end, I measured the conductance in water with an Arduino and I matched the amplitude of changes in salinity from baseline to what I recorded with the thermocouple in the chamber. Randomization of double and single pulses was not possible due to accumulation phenomena in the case of two double pulses coming one after the other (Figure 15).

Figure 15: A multimodal virtual gradient assay

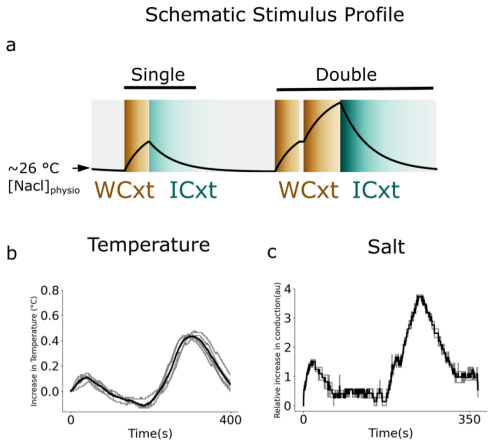

Fig. 15: **a**. Protocol used for the lightsheet experiments. **b** Calibrations for temperature stimulus in an example trial. **c**. calibrations for salt stimulus in an example trial.

2.5.6 Salt experiments in freely-swimming fish

For these experiments the same large arena employed for the spatial thermal gradient was used. As in Herrera et al., 2021 two agarose pads (4% low melting point agarose (Invitrogen)) were, first, poured into silicon casts and then cut out and added to the arena. To make the ionic solution the salt (400mM) was added to the water before pouring the agarose.

2.6 Data analysis and Statistics

All analyses were performed using Python 3.8 and relevant Python libraries for scientific computing, like numpy (Harris et al. 2020), scipy (Virtanen et al. 2020) and scikit-learn (Pedregosa et al. 2012). Dataframes and dataframe manipulations were performed with pandas library (Reback et al. 2020).

The figures were produced using matplotlib (Hunter 2007). For statistical analysis, unless otherwise stated, I used the non-parametric Mann-Whitney U test for unpaired comparisons (*mannwhitneyu* from *scipy*).

In all the figures:

n.s.: not significant, p-value > 0.05

*: p-value 0.05-0.01

**: p-value 0.01-0.001

***: p-value < 0.001

2.6.1 Behavior

2.6.1.1 Tracking and general preprocessing

For both WT freely swimming and head-restrained experiments the relevant parameters were tracked online using Stytra (Štih et al. 2019). For each experiment metadata with all the relevant information were saved in the same folder of the behavior and the stimulus file. For WT flies, an ellipse was fitted to the fly's body, and from there, the heading and angle of turn were computed and saved for further analysis. Most of behavioral preprocessing (like extraction of swim events) was performed using the python package Bouter (Štih, Vilim et al. 2022). Briefly, swim events were segmented putting a threshold on the velocity of the centroid. I, then, calculated the angle turned as the difference in heading between the beginning and the end of a swim.

For experiments with nacre (mitfa−/−) transparent fish I recorded an .mp4 video, extracted fish centroid with Deeplabcut (Mathis et al. 2018; Nath et al. 2019), and then preprocessed with custom-made scripts. In particular, I segmented swim events using velocity of the centroid (1mm/s for swim onset) and extracted angle turned by fitting a linear vector using xy trajectories before and after a bout and measuring the signed angle between them.

For head-restrained experiments, I computed the standard deviation of the tail angle trace in a rolling window of 50 ms. Then, using a threshold of 0.1, I found swims onset. The sum of the tail angle during the first 70 ms of a swim has been shown to approximate well the angle turned by a freely swimming fish (Huang et al. 2013; Dragomir, Štih, and Portugues 2020) and was therefore used to define angle turned during swims.

I set a threshold of ± 0.52 radians (30 degrees) and I respectively classified swim events (both for freely-swimming and head-restrained experiments) as right, left and forward swims. By convention, the negative sign of angle turned is toward the left.

2.6.1.2 Path straightness index in drosophila

The straightness index of a trajectory was calculated in a rolling window by dividing the displacement between the initial and final positions by the total path length, representing the sum of distances

between consecutive positions. Trajectory chunks where the velocity was above 50 mm/s were discarded from further analysis.

2.6.1.3 Extraction of relevant behavioral parameters for large arena experiment

I flipped horizontally the trajectories when the warm side was on the right. Therefore, by convention, the unpleasant stimulus is always on the left. To express the coordinates of the fish in terms of the temperature experienced I quadratically interpolated temperature calibrations taken every 2 cm in the arena before and after each batch of experiments.

Since all experimental conditions except for the WT preferred a higher temperature, I decided to express the currently experienced temperature as a function of the absolute distance from the fish setpoint. This setpoint was separately computed for WT, chemogenetic experiments and 2-photon ablation experiments. As shown by Figure 41, no difference in setpoint was found between experimental and control groups, indicating that this shift in setpoint is independent from the region ablated.

The point of the analysis was to see whether fish behavior was modulated by sensory history and previous motor choices. To this end, I computed, for each bout, the following parameters:

- Angle turned during the swim event (see previous paragraph).
- Experienced temperature before and after swim
- Difference in temperature brought by the previous swim (swim-1), if the interswim interval was ≤2 seconds. In the work, I refer to this variable as sensory context.
- Difference in temperature brought by the second-to-last swim (swim-2), if the interbout interval between bout-1 and bout-2 was ≤2 seconds. In the work, I refer to this variable as past sensory context.

Sensory context and past sensory context were further classified in WCxt , ICxt and NCxt . For such classification, I used a conservative threshold of 0.13°C, which I posit to be the thermal sensitivity in the temporal domain (Stevens and Choo 1998; Paricio-Montesinos et al. 2020). Fish that swam less than 1/3 Hz during an experiment were excluded from further analysis. Strikingly, an important index to quantify behavioral hysteresis, presented later in the thesis (see Chapter 3.3), was not affected by the threshold used to define the NCxt (Figure 16).

Figure 16: Threshold for NCxt

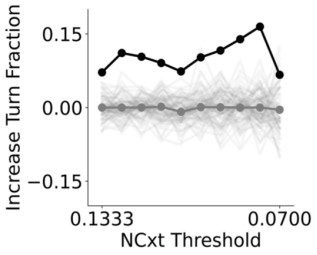

Fig. 16: Increase of turn fraction for the WCxt→NCxt condition by changing the threshold used to define a NCxt

2.6.1.4 Increase in turn fraction index

To assess whether a fish would be more prone to turn when it experienced a WCxt I took all the swim events happening at least 1 °C away from setpoint and I looked at the fraction of turns happening in a WCxt and in an ICxt. Then, I took the difference between the two contexts.

In this analysis, I did not use the swim events in a NCxt. However, given the shape of our arena and gradient, it was common for the fish to use more than one movement to reverse a WCxt in an ICxt or vice versa, therefore going through movements during which the temperature didn't change. Despite this, fish still proved efficient homeostatic navigation. To account for this, I repeated the previous analysis, but this time, I selected bouts when the sensory context was NCxt but past sensory context was either WCxt or ICxt.

2.6.1.5 Motor correlation index

In order to investigate if fish strengthen directional correlation during WCxt I selected all swims during such sensory context and further selected swims that were preceded by a turn (either left or right). Finally, I computed the theta swim normalized by the direction of the previous turn (I flipped the sign of current swim if the previous turn was toward the left), such that if the sign is positive it means that fish moved ipsilateral respect to previous direction, contralateral otherwise.

2.6.1.6 U-maneuvers

In order to extract U-maneuvers, I selected sequences of six consecutive swims and computed the absolute amount of reorientation. If this number exceeded 100°, that sequence was considered a U-maneuver. I further selected U-maneuvers where the first swim was in a WCxt. Finally, I averaged the ΔTemperature experienced during each swim in the sequence. Is important to notice that the selection of U-maneuvers is agnostic with respect to the ΔTemperature experienced by the animal.

2.6.1.7 Increase in turn fraction and motor correlation in open-loop head-restrained and freely swimming (small arena)

In these experiments, I tested whether the direction of change (WCxt vs ICxt) was enough to modulate the reorientation probability and directional correlation even if the fish had no control over the experienced temperature change. For data analysis, I considered two main parts: when the temperature was moving away from 24 °C (24 °C to 28 °C = WCxt) and when it was moving towards 24 °C (28 °C to 24 °C = ICxt). I excluded the step at 30 °C from the analysis. I next computed the increase in turn fraction and motor correlation in the same way as it was done for the big arena experiment (see Increase in turn fraction index and Motor correlation index).

2.6.1.8 Coefficient of dispersion

To test whether ablated fish were less able to stay around their setpoint the coefficient of dispersion was calculated:

$$CoD = \left(\sum_{i}^{N} |x_i - x_m|\right) / \left(N x_m\right)$$

Where x_i is the median temperature experienced during the last 600 seconds of the experiment, x_m is the median across the group population and N is the total number of fish in that group.

2.7 Lightsheet functional imaging

2.7.1 Lightsheet microscope

For our experiments I used a custom-build microscope with two excitation scanning arms placed at 90° from each other. A laser beam coming from a 473 nm laser source (Cobolt) is split and directed into the two arms. In both arms, the laser beam gets expanded by a telescope before being focused through a glass coverslip on the fish. By scanning at 800 Hz the beam on the horizontal plane I generated the excitation lightsheet. The brain of the fish is targeted from the side and from the front

giving access to the entire brain at a single-cell resolution. The emitted fluorescence was collected through a water immersion objective (Olympus, Japan), mounted on a piezo (Piezosystem Jena, Germany) and focused on a camera (Orca Flash v4.0, Hamamatsu Photonics K.K., Japan) with a tube lens (Thorlabs, USA). For further details refer to (Markov et al. 2021). The piezo, galvanometric mirrors and the triggering of the camera were controlled by Sashimi (Štih et al. 2022). a custom-written python software developed in the lab. The lightsheets and the collection objective were synchronously oscillating along the vertical axis with a frequency of 2.0 Hz, covering in depth around 250 µm. Frames were acquired at equally spaced intervals along the volume with a spacing of 9.66 µm.

2.7.2 Lightsheet data analysis

2.7.2.1 Lightsheet imaging data preprocessing

Data was saved in hdf5 format. To preprocess functional imaging data I used the package fimpy (https://github.com/portugueslab/fimpy). For alignment (*function align_volumes_with_filtering*) and ROI extraction (function *correlation_map* and *grow_rois*), I used a similar pipeline used in (Markov et al. 2021) (see "Whole-brain functional imaging data analysis"). Since planes were spaced by ~10 µm, ROIs detected across planes were not merged. Once the ROIs were identified, I generated an ID ROI stack: a matrix with the same shape of the lightsheet data where to each pixel was assigned a scalar value corresponding to the ID of a single ROI. After ROI detection I removed spurious ROIs detected outside the brain by manually drawing a mask. I further removed all ROIs detected in the olfactory epithelium since it was imaged only in a fraction of fish and it was prone to many movement artifacts. Alignment was performed independently for both temperature and salt session while ROI extraction only for temperature. After alignment, I additionally computed an anatomical stack by averaging fluorescence throughout the experiment for both sessions (anatomical stack, Figure 16a).

2.7.2.2 ROI segmentation across sessions

Registration across sessions was performed by finding an affine transformation matrix semi-manually. This was done by finding ~15 corresponding single isolated neuronal nuclei in the temperature (used as reference) and the salt session anatomies and computing a least-squares fit of a 12-parameter affine transform matrix (e.g. Figure 17 b). Once found, I applied the inverse transformation (from the temperature to the salt session space) to the ID ROI stack computed in the temperature session in order to extract fluorescence activity from the same neuron in the salt session.

Figure 17: Pipeline for ROI segmentation across sessions

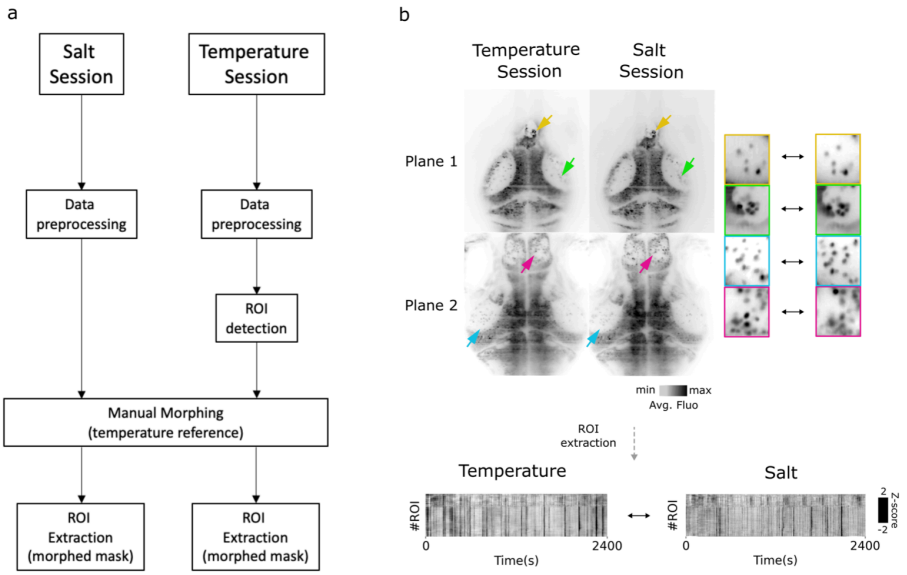

Fig. 17: **a**. Flowchart of the pipeline for ROIs extraction across sessions. **b** Two examples planes in the temperature and salt session. Yellow, green, cyan and purple arrows point to four different pattern of neurons visible in both sessions (zoomed in version shown on the right). **Bottom**: raw activity of 10% of neurons, randomly selected, in the two sessions. Nurons were arranged following the rostro-caudal axis.

2.7.2.3 Anatomical Registration and region segmentation

Image registration was performed using the free Computational Morphometry Toolkit (CMTK - http://www.nitrc.org/projects/cmtk) (Rohlfing and Maurer 2003). First, I choose one of the anatomical stacks as the initial reference brain, and non-affine volume transformations were computed to align each fish's anatomical stack to this reference stack using the affine and warp functions (Severi et al. 2014). After this step, I averaged all the aligned anatomical stack from all fish in order to obtain an intermediate reference stack. I finally repeated the fish-wise alignment on the intermediate reference stack. These transformations were then used to transform individual ROIs from each fish into the frame of reference of the final reference brain, allowing us to compare the anatomical location of ROIs from different fish. Finally, I built an internal atlas by manually defining anatomical regions using clear anatomical landmarks and by looking at the Max Planck Zebrafish Brain Atlas (https://mapzebrain.org) (Kunst et al. 2019).

2.7.2.4 Describing temperature sensory responses

Raw traces were first smoothed with a median filter of size 1.5s (function *medfilt*). Then, I cropped all traces from the beginning to the end of each trial (single + double pulse), z-scored each of them, and performed an average response per each ROI (Trial trigger average or TTA). In addition, I computed the average correlation (reliability index) of the responses across all individual trials (Prat et al. 2022). With the reliability index, I was able to quantify the responsiveness of each ROI to the temperature stimulation independently from each specific response profile. I classified each ROIs as "reliable" if the aforementioned index was higher than 0.3 and further analyzed only this subset of ROIs. This procedure allowed us to keep only neurons reliable across trials. In order to further screen for neuronal responses that were also reliable across animals, I cross-correlated (Pearson correlation) each TTA with all the TTAs of all the other fish and kept only neurons with a coefficient higher than 0.65 with at least one TTA of all the rest of the fish. At the end, I pooled together all the TTAs that passed these screenings. I then performed PCA and projected each TTA on the first two PCs (cumulative explained variance 65%) (Figure 18a) so that each point in the principal component space was a TTA. Finally, I performed k-means clustering and I set the number of clusters (k parameter) to 3. This number was chosen by looking at the Davies Bouldin score (*davies_bouldin_score*) (Figure 18b); lower values of this score indicate better clustering. Clustering quality was also checked by repeating the procedure with different centroids initializations. Regional percentages of different clusters were computed using the internal atlas.

Figure 18: Explained variance and clusterabilityfor temperature responses

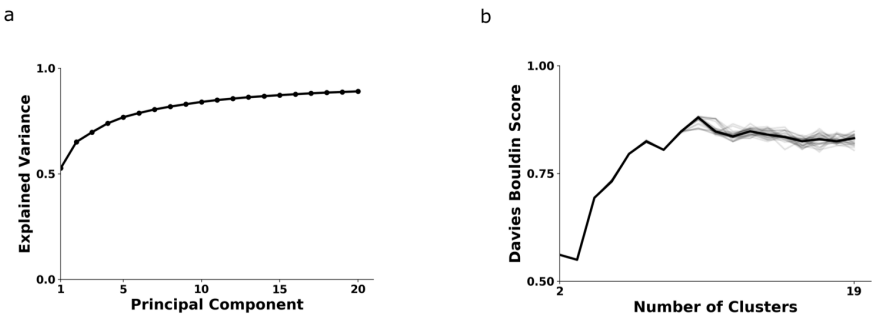

Fig. 18: **a**. Normalized explained variance for the PCA analysis. **b** Davies-Bouldin score for different number of clusters during k-means clustering. Lower values indicate better clusterability with that number of clusters.

2.7.2.5 Visualization of whole brain maps

In order to generate whole brain maps displayed in the current work I used either a scatter plot or a density map. For the scatter plot (Figure 31a), color of each dot (representing a ROI) was decided based on cluster identity while transparency was proportional to the local density within a sphere of 30 µm radius. For the density maps (Figure 32a, 33c, 35b, c), I initialized a zero array with the same size of our internal reference brain (see "Anatomical Registration and region segmentation"). I then increased by one (+1) pixel value corresponding to a spherical region of 15 µm around each selected ROI. For the visualization, I used a sum projection along the three main anatomical axes.

2.7.2.6 Multimodal Neurons

In order to find multimodal neurons, I first selected all ROIs that reliably responded during both temperature and salt session (threshold: 0.3). Anatomical distribution of these ROIs is shown in Figure 35b. I then cross-correlated (Spearman correlation) the TTA of the two sessions and, for each ROI, generated a null-distribution by repeating the cross-correlation with circular-shuffled versions of the TTAs. Using the real correlation and the null-distribution I computed a p-value for each ROI. I considered a ROI multimodal if such correlation was higher than 0.3 and the p-value lower than 0.025 (Figure 19). I, then, applied a spatial constraint on the generated density maps shown in Figure 35b, c such that I show only regions with an overlap of at least 5 and 10 ROIs respectively.

Figure 19: Correlation values of multimodal neurons

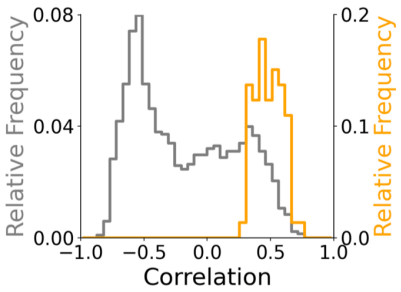

Fig. 19: **a**. Distribution of correlation coefficients of ROIs with p-values > 0.025 in gray and p-values < 0.025 in orange.

2.7.2.7 Swim triggered analysis

The analysis aimed to identify neurons whose fluorescence increased after a swim event. First, I selected swim events temporally spaced 2 seconds from the preceding and 10 seconds from the next. Then I split swims according to the angle turned in order to classify them as left, right or forward swims. For each fish, the number of bout per each category was at least 3. I then cropped each ROI around swim onset (from -2 to +10s from bout onset). For each ROI, I computed 3 reliability indexes, one for each swim category. I used the 90th percentile of the distribution created by taking the maximum value among the three reliability indexes of all ROIs in order to find a global threshold, within fish, used to define if a ROI was motor responding and specific to one of the three swim categories. In particular, a ROI in order to be selected needed to have one of the three reliability indexes higher than the global threshold and the other two lower than that one so that each neurons was univocally classified as either left, right or forward tuned. For the map shown in Figure 33c I, then, pooled all the left-right and forward ROIs coming from all fish and computed the density map as described in Visualization of whole brain maps. Percentage of motor ROIs was computed using the internal atlas.

Analysis shown in Figure 33a, b aimed to identify different calcium dynamics upon swim turn onset. In order to do that, I pooled together left- and right- tuned neurons and flipped the x coordinates of

right- tuned ones. Finally, I sorted turn trigger averages according to timing of peak activity and averaged using temporal bins of 0.5-2.5seconds, 2.5-4 seconds, 4-5.5 and 5.5-10.5 seconds.

2.8 Neuron manipulations

2.8.1 Chemogenetic Ablations

To perform targeted ablation of Hb, I employed the Ntr/NFP pharmaco-genetic approach (Bergemann et al. 2018; Corradi et al. 2022). Animals expressing nitroreductase (Ntr) in a cell population of interest were treated with prodrug Nifurpirinol (NFP). Ntr converts NFP into a cytotoxic DNA cross-linking agent leading to death of cells of interest. Nirfurpirinol is, like Metronidazole (MTZ), another nitroaromatic antibiotic and it has been shown to reliably trigger cell-ablation at concentrations 2000 fold-lower than MTZ (Bergemann et al. 2018). I used the line Tg(16715:Gal4v16); Tg(UAS:Ntr-mCherry), which restricts expression in the dorsal Hb (Figure 20a) and I crossed it with TL wild-type fish. Fish were screened with an upright fluorescence dissecting microscope (Leica, M165 FC) for red fluorescence, at 4 dpf. mCherry-positive Tg(16715:Gal4v16); Tg(UAS:Ntr-mCherry +/-) fish were tested at 5dpf in the freely swimming rectangular arena (Genetic control). In the evening, 5dpf mCherry-positive Tg(16715:Gal4v16); Tg(UAS:Ntr-mCherry +/-) fish and mCherry-negative Tg(16715:Gal4v16); Tg(UAS:Ntr-mCherry -/-) (Treatment control) were taken from their Petri dish minimizing the amount of water transferred and placed into a new 9 cm Petri dish filled with 40 ml of 0.2% DMSO (Dimethyl sulfoxide) to increase tissue permeability, 5 µM Nifurpirinol (diluted 1:500 from stock 2.5 mM) and fish water. Solution preparation and fish transfer happened in darkness. Larvae were then placed in the incubator at 28 °C for 16 h in a black box to prevent the inactivation of the drug. The next morning fish were rinsed 3 times to completely remove the NFP and DMSO and were left to recover for one day in fresh fish water.

Positive Hb fish treated with NFP (Experimental group) and negative Hb fish treated with NFP (Treatment control) were then tested at 7 dpf in the freely swimming rectangular arena. After the experiment fish were inspected individually under the fluorescence dissecting microscope to ensure absence of mCherry fluorescence.

The efficiency of Hb ablations was further evaluated by randomly selecting, each time I ran experiments on a different batch of fish, 5-6 mCherry-positive nacre (mitfa−/−) several larvae. Those animals were imaged under a confocal microscope (Olympus FV1000) before ablations at 5 dpf and then after ablation at 6 dpf and again at 7 dpf (see Supplementary Figure 6 b). The rationale of the last step at 7 dpf was to confirm that the process of ablation keeps progressing up to 48 h after treatment with NFP (Figure 20b).

Figure 20: Hb ablations

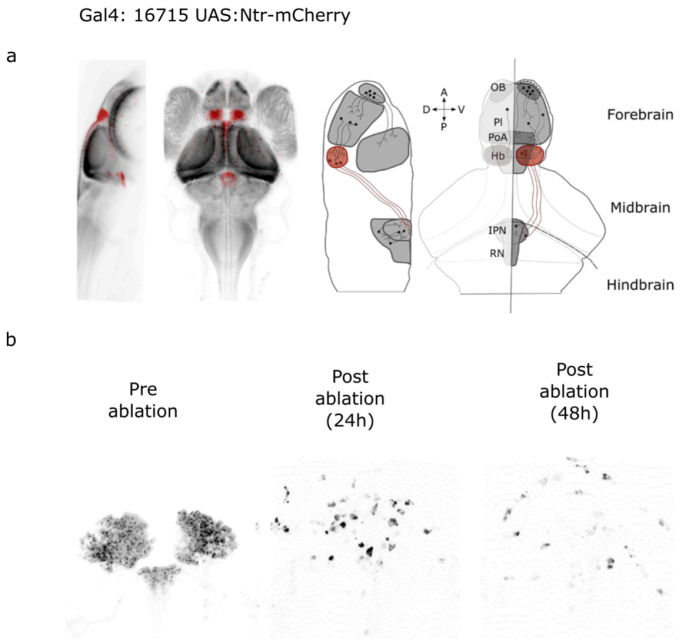

Fig. 20: **a**. **Left**: Anatomy of the reference brain (gray) and the line Gal4:16715 UAS:Ntr-mCherry (courtesy of Florian Engert and Martin Haesemeyer (red) used for chemogenetic ablations. **Right**: Sketch of the relevant connections. **b** Confocal anatomy of the Hb acquired before, 24 hours and 48 hours after treatment.

2.8.2 Laser-mediated cell ablations

At 5 dpf Tg(elavl3:GCaMP6s+/+) (mitfa−/−) fish were mounted in 1.5 % agarose in fish water, anesthetized with 1x Tricaine (168 mg/L) directly added to fish water and placed under a custom-made 2-photon microscope. For the microscope design and details refer to (Petrucco et al. 2023). To test the involvement of the PoA in thermal navigation I set to bilaterally ablate this structure (Figure 21a). The PoA was identified based on its anatomical location and clear anatomical landmarks. Before the experiment, I acquired for each fish a 100 µm stack of the areas I intended to target (Figure 21b). Then I used galvo scanning to focus 800 nm on a small group of cells at either side of the midline. The laser power was set to its maximum on the software, which resulted in 130 mW power measured at the objective back aperture. I developed a protocol where I targeted the cells for 200 ms with a 500 ms of interval repeated three times. A Python script automatically controlled both the shutter and exposure time. Neurons were considered successfully ablated when the fluorescence sharply increased and the nuclei looked irregular and fragmented (Figure 21b). At this

point, I took another anatomical image to monitor the localization and extent of the ablation. If the fluorescence of the neurons didn't increase or the damage exceeded the size of the region targeted the fish was not used for subsequent experiments. In control fish, I applied the same protocol to the Optic Tectum (OT). The OT was the only brain region that did not reliably or strongly respond to my temperature stimulus (Figure 31a). Successfully ablated fish were freed from agarose, and returned to a petri dish with fresh fish water and provided with Sera Micron (Sera). Fish were tested 24-48 hours later at 7 dpf. For some fish an additional anatomical stack was acquired after 48 hours to further monitor the scars.

Figure 21: PoA ablations

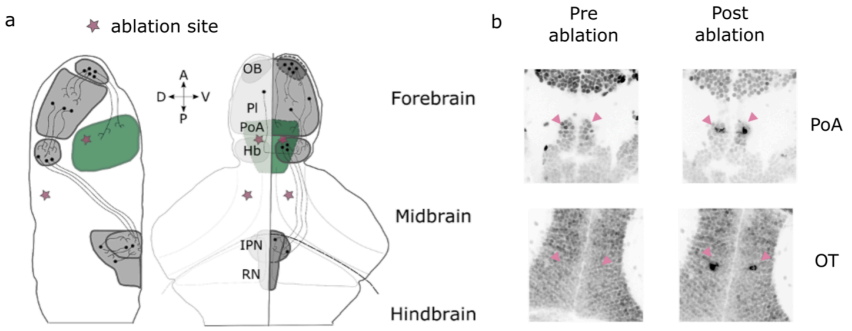

Fig. 21: **a**. Sketch of the circuit. In green the PoA. Pink stars show the targeted sites. **b** Anatomy before and after laser ablations in the PoA and in the OT.

2.8.3 Fluoxetine Treatment

Zebrafish larvae were subjected to treatment with 1.5 mM fluoxetine hydrochloride (Sigma-Aldrich), which was dissolved in fish water. The treatment started 4 to 6 hours prior to behavioral experiments. It should be noted that the drug was not present in the medium during the actual execution of the experiments.

2.9 Simulations

In the simulation, fish could engage in two types of movement: straight swims or turns. The change in heading angle during these movements was modeled using a Gaussian distribution for straight swims and two lognormal distributions for turns (left and right). The fish selected the angle from one of the two main distributions (forward and turns distribution) according to a probability decided based on the

virtual stimulus and the sensorimotor algorithm in place. As the fish moved through the simulated environment, they encountered temperature changes. These changes were represented by a linear temperature gradient increasing from right to left. After each movement, the distribution of potential reorientation for the next movement was updated based on either the absolute temperature encountered or the change in temperature from the last movement. In the first case, increase in temperature value increased the probability of the turn distribution being selected increased. For the second, the probability of the turning distribution being selected increased by 0.05 if the previous turn led to a worsening of conditions (similarly to our behavioral findings).

3. Thermal homeostasis in larval zebrafish: behavioral principles

The focus of this chapter is describing the behavioral aspects of how larval zebrafish regulate their body temperature in the presence of spatial and temporal thermal gradients.

3.1 Fish successfully regulate their body temperature in a spatial thermal gradient

To begin with, I verified that larval zebrafish are capable of modulating their body temperature through navigation within a shallow thermal gradient, without needing additional sensory information. To this end, I designed a rectangular arena, measuring 20 x 4 cm and heated a 4 x 4 cm square area at one end to a temperature of 33 °C (Material and Methods, Figure 9). In this way, a linear thermal gradient was established along the longest side, with an increase of 0.04 °C per mm (Material and Methods, Figure 12a). In this controlled environment, the highest temperature change experienced by a fish across its body would be around 0.02 °C (Material and Methods, Figure 12b). I, then, monitored individual zebrafish larvae, between 5 and 7 dpf, for a period of 15 minutes (Material and Methods, Spatial gradient in the large arena for individual fish). I observed that, by the end of the experiment, zebrafish larvae consistently avoided the warmer end of the arena (Figure 22a, top and bottom panel). Following an initial exploratory phase of about 260 seconds (Figure 22c), the fish rapidly exhibited a clear preference for a temperature of approximately 25.3 °C (Figure 22a bottom right). I posit this temperature to represent their homeostatic setpoint, or the temperature at which their body works most efficiently. Conversely, control fish that didn't experience any gradient did not show any spatial preference (Figure 22b top and bottom panel).

Figure 22: Larval zebrafish maintain homeostasis in a linear thermal gradient

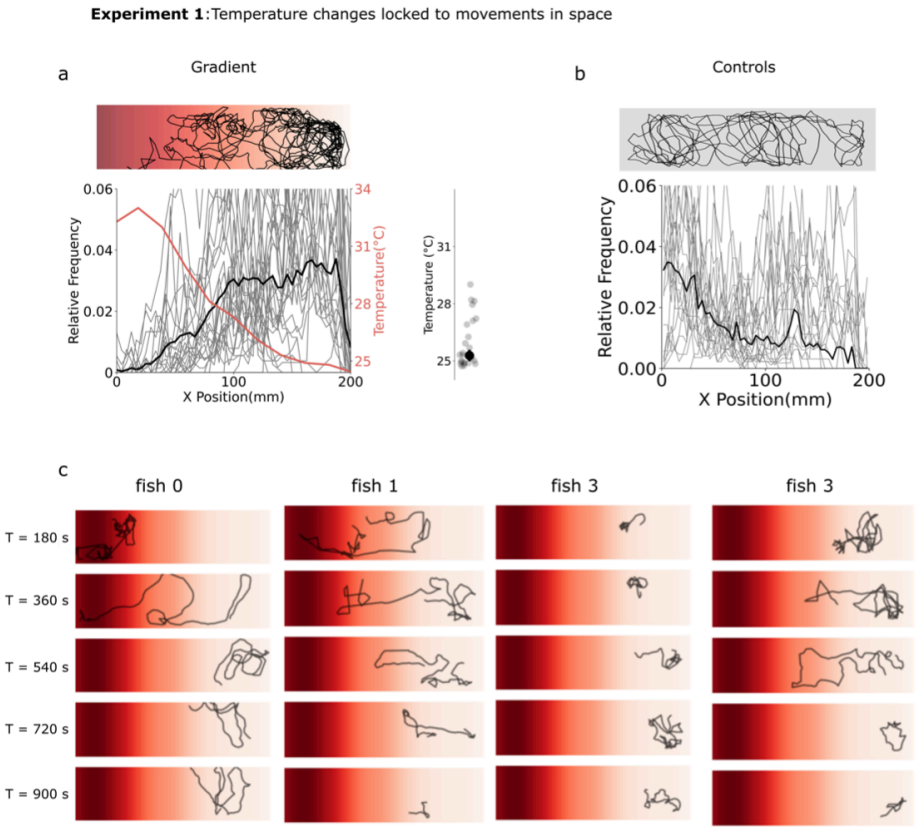

Fig. 22: **a.** Top: example trajectories of 3 fish for the entire duration of the experiment (15 min). Actual temperature measured in the water is pictured with different shades of red. The highest temperature (33°C) is represented on the left by the dark red. Bottom: Histogram of animals' x-position in the arena (n=26, gray traces), median of the population (black trace) and temperature measurement (red trace). Bottom right: preferred temperature 25.3 °C. Black dot is the median of the population and the grey dots are individual fish. **b.** Top: example trajectories of 3 fish at room temperature with no gradient, monitored for 15 min. Bottom: Histogram of animals' x-position in the arena (n=23, gray traces), median of the population (black trace). **c.** Example trajectories of 4 selectedfish. Trajectories has been split in 3 -minutes bins to show the temporal progression of their search for the homeostatic setpoint.

Next, I calculated the temperature experienced by the fish, derived from their positions in the arena (Material and Methods, Extraction of relevant behavioral parameters for large arena experiment) to see what are the driving behavioral mechanisms in homeostatic navigation.

3.2 Fish leverage behavioral hysteresis to regulate their body temperature

While the difference between the current and an animal's preferred temperature is the fundamental drive for homeostatic navigation, this information alone cannot instruct a directed behavior (Le Goc et al. 2021; Herrera et al. 2021). I propose that, similarly to other types of taxis (Berg 2000; Gomez-Marin and Louis 2012; Linjiao Luo et al. 2014; Larsch et al. 2015; Oteiza et al. 2017; Zhang et al. 2017; Herrera et al. 2021) and as already discussed, the simplest directional cue is given by the temporal changes in temperature due to an animal's self-relocation (i.e. behavioral hysteresis, Garrity et al. 2010; Glauser 2013) (see Figure 4 e, f). It remained to be tested whether fish would use a non-directional 'tumble and run' strategy as used by bacteria and *C.elegans* to improve their environmental conditions (Berg and Brown 1972; Hedgecock and Russell 1975; Berg 2000; Linjiao Luo et al. 2014; Mori, Sasakura, and Kuhara 2007; Glauser 2013) or a more structured strategy as in drosophila larvae (Berrigan and Pepin 1995; Garrity et al. 2010; Gomez-Marin and Louis 2012); especially in light of previous reports describing directional persistence in the turning behavior of larval zebrafish (Robson 2013; Dunn et al. 2016). To investigate whether fish would, in the first place, exhibit behavioral hysteresis I categorized each movement as a forward swim or a turn (Material and Methods, Tracking and general preprocessing). Then, I took advantage of the fact that larval zebrafish move in discrete swimming events at an approximate rate of 1 Hz (Budick and O'Malley 2000). Therefore, context evaluation should occur at the end of each swimming event. Thus, temperatures experienced at previous movements contextualize the one perceived during the current swim and provide a basic notion of a worsening or improving context, possibly driving an opposite behavioral output, such as increased turning probability versus straight runs (Figure 23a top and bottom panel). I defined three scenarios. Improving context (ICxt) when the temperature change was toward the fish's setpoint regardless of the absolute temperature experienced, worsening context (WCxt) when the fish moved away from the setpoint, and no context (NCxt) for an isothermal movement. For fish to show behavioral hysteresis a WCxt should increase the reorientation probability to change the fish's direction of travel. Conversely, an ICxt, meaning getting closer to the homeostatic setpoint, should result in turning suppression to maintain the current direction (Figure 23b).

Figure 23: Algorithmic implementation of behavioral hysteresis in larval zebrafish

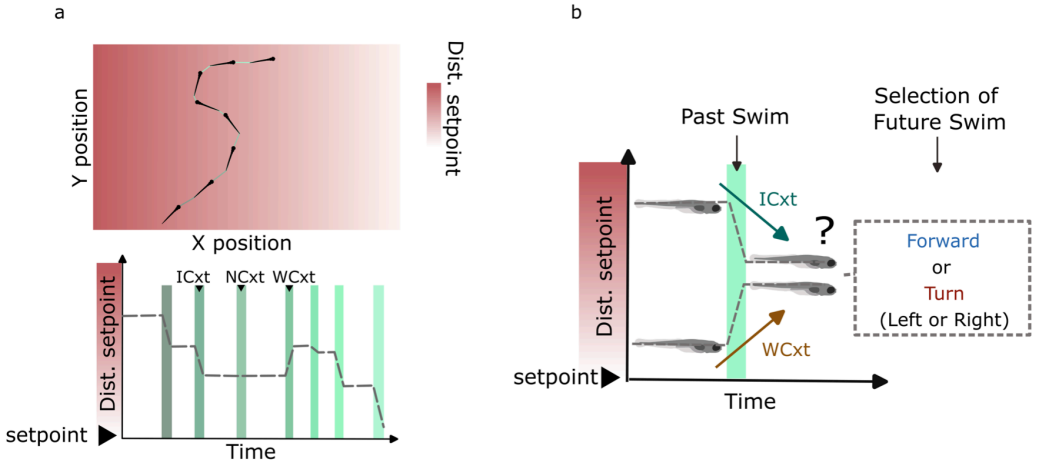

Fig. 23: **a.**Top: Sketch of an example trajectory. Bottom: change of temperature perceived over time for each swim event in the top sketch. Time is coded by the shades of green (from dark to light green). Arrows on top point to a movement in a ICxt (improving context), NCxt (no context) and a WCxt (worsening context), respectively. **b.** Sketch of information available to the fish for behavioral choice using the sensory context provided by the previous swim.

Figure 24 shows an example of a fish moving in the arena along with all the relevant stimulus and behavioral variables I extracted from the trajectory. In the close-up of a behavioral sequence (Figure 24 right), I analyzed several periods where the animal experienced the same temperature but in two different contexts (orange arrow for WCxt and blue arrow for ICxt). In the WCxt (orange arrow), the reorientation probability was highly modulated by the sensory context (improving vs. worsening), such that turning frequency increases. Furthermore, as shown in the bottom panel, fish tend to concatenate turns in the same direction where right turns are followed by additional right turns and vice versa.

Figure 24: Summary of the relevant stimulus and behavioral variables

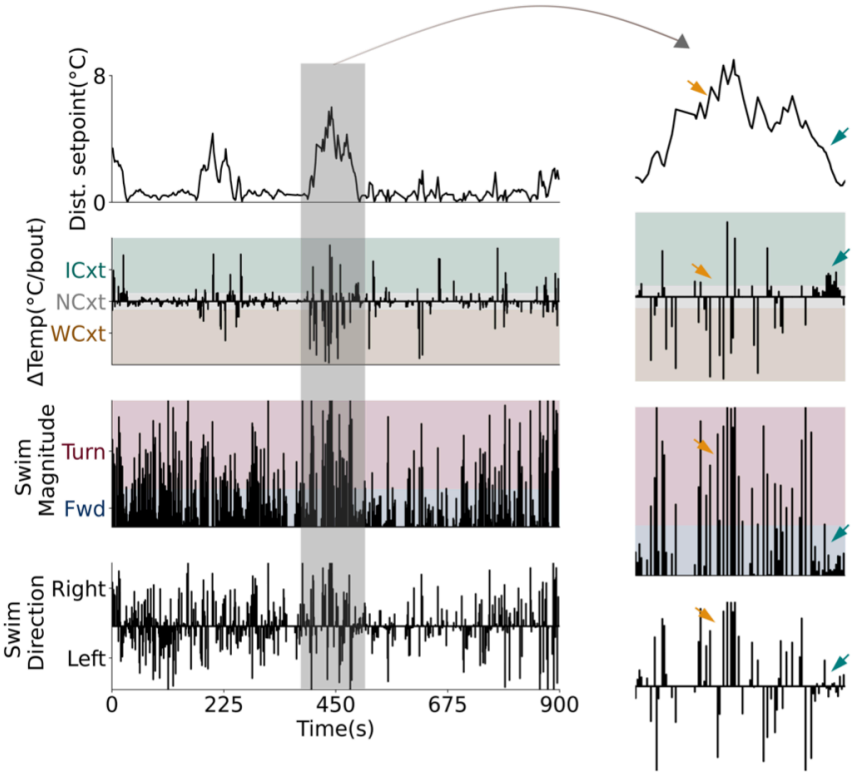

Fig. 24: Summary of all the stimulus and behavioral variables used in this study for a representative individual fish. On the left: the entire duration of the experiment. On the right: close up of the trajectory and the relevant variables highlighted in the grey box. The four graphs show: (i) temperature experienced by an example fish, (ii) ΔTemperature (difference in temperature between current and last movement) experienced [color coding represents: worsening of conditions (in brown, away from physiological setpoint), improvement (in turquoise, toward physiological setpoint) or no change (in gray)], (iii) the absolute value of reorientation for each swim [color coding represents: turn (in red, when reorientation is higher than 30 degrees), or forward (in blue, when reorientation is lower than 30 degrees)] and (iv) the direction of turns, either left or right.

To further quantify, for all the tested fish, whether they would actually turn more in a WCxt I defined as the minimal block the difference in temperature perceived during the last movement. By plotting the relative distribution of the absolute angle turned for all fish for WCxt and ICxt (Figure 25a) I confirmed that larval zebrafish show behavioral hysteresis. I have also established a simple index that will be used for all subsequent analyses to quantify the extent to which sensory context modulates the probability of reorientation. Briefly, I computed the difference between the turn fraction during WCxt and the turn fraction during ICxt. Again, a significant difference in turning behavior between contexts was observed (Figure 25b). I also noticed, as previously observed, that the direction of turning was not stochastically decided during each movement (Robson 2013; Dunn et al. 2016). In fact, when I quantified swim direction with respect to the previous turn event for the WCxt scenario I observed a high correlation. This result suggested that a form of memory is used by the fish to persist in the previously chosen direction (Figure 25 c) (Robson 2013; Dunn et al. 2016). Moreover, this observation strongly hints at the fact the fish is using a more complex strategy than *E.coli* and *C. elegans*.

Figure 25: Behavioral hysteresis and directional persistence are leveraged to achieve thermoregulation

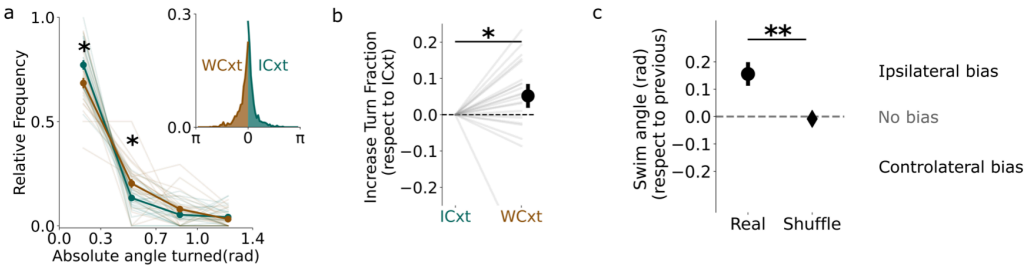

Fig. 25: **a.** Relative distribution of the absolute angle turned when fish experienced a WCxt or an ICxt (mean ± standard error of the mean, Mann-Whitney non parametric test with Bonferroni correction for multiple comparisons). **b.** Normalized increase in turn fraction depending on sensory context (median ± standard error of the median, Mann-Whitney non parametric test). **c.** Direction of swim during WCxt according to the direction of the previous swim (mean ± standard error of the mean, Mann-Whitney non parametric test). Positive values imply that the swim tends to be in the same direction as the previous one. Diamond on the right is a shuffle obtained by assigning the sign for each value randomly. n.s.: not significant, p-value > 0.05, *: p-value 0.05-0.01, **: p-value 0.01-0.001 ,***: p-value < 0.001

3.3 Fish exploit a directional strategy by combining a sensory and motor working memory in a thermal gradient

The hypothesis that larval zebrafish was in fact employing a more structured strategy where a directional component was present was further supported by noticing that, due to the shape of the temperature gradient (Figure 12), it was improbable for the fish to move in a single movement from a WCxt to an ICxt (Figure 26a and figure 26b right). Consequently, such transitions usually took several swim events, where many of those movements did not provide any useful information about the change in temperature (i.e. isothermal, NCxt, Figure 26b left).

I hypothesized that fish were using a longer sensory memory that would help taking into account intermittent sensory cues and combining them with previous motor choices to persist in the behavioral program.

I was able to confirm that fish still exhibit behavioral hysteresis when their last movement was isothermal (Figure 26c). Moreover, fish kept reorienting by performing ipsilateral turns persisting in the chosen direction even without sensory cues (Figure 27 b left). In this way, the reorientation sequences produced U-shaped trajectories (U-maneuvers) commonly ending with the fish facing in the opposite direction, toward the preferred temperature (Figure 26d).

Figure 26: In presence of intermittent sensory cues larval zebrafish use a short-term working memory

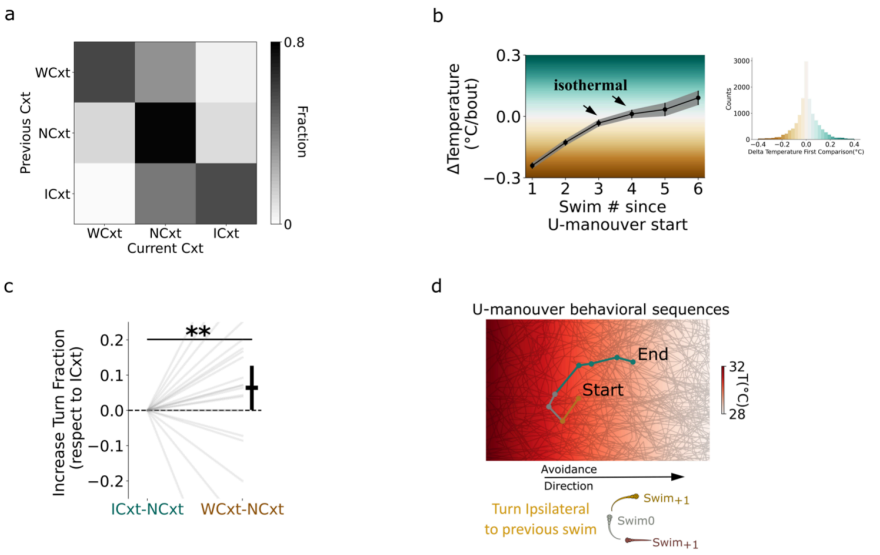

Fig. 26: **a.** Mean transition matrix for sensory context across fish population. **b.** Left: Difference in temperature experienced by fish during the execution of U-maneuvers, starting from in a WCxt (mean ± standard error of the mean). Right: Histogram depicting the difference in temeprature experienced between the beginning and the end of each swim event. **c.** Increase in turn fraction when previous swim did not carry directional cues (NCxt) but the second to last was either a WCxt or a ICxt (median ± standard error of the median, Mann-Whitney non parametric test) **d.** Top: example U–maneuver performed during experiment 1. Bottom: sketch of a U-maneuver. n.s.: not significant, p-value > 0.05, *: p-value 0.05-0.01, **: p-value 0.01-0.001 ,***: p-value < 0.001

3.4 Behavioral hysteresis and direction persistence are robust when the rate of change of the stimulus is varied

Lastly, I tested the robustness of behavioral hysteresis by exploring its response to different timescales of stimulus change. The objective was to investigate whether the observed behavioral pattern remains consistent regardless of variations in the speed or duration of temperature changes. To this end, I challenged the fish with a step-like ramp ranging from 24 °C to 30 °C (Figure 27a bottom and b top). Every two minutes, the temperature changed in the whole arena by 2 °C (see Material and Methods, Long temporal gradient in the small arena and for head-restrained preparation in fish). For these experiments, I developed a square-shaped, smaller arena, which allowed the temperature to change

homogeneously on the entire surface (Figure 10, see Material and Methods). The fish was, just as before, able to swim freely.

Similar to the experiments in the large rectangular arena, the analysis of the turn fraction (Figure 27a top for all fish, Figure 27b for median, Figure 27c, Material and Methods, Increase in turn fraction and motor correlation in open-loop head-restrained and freely swimming (small arena)) revealed that behavioral hysteresis was preserved, with more reorientation maneuvers when the temperature was moving away from the preferred setpoint. Furthermore, the analysis of swim direction during the WCxt epoch confirmed the high correlation in time of turning direction (Figure 27d). This result highlights the robustness and replicability of the fish's behavioral strategy across different setups and conditions.

Figure 27: Externally controlled temperature changes still trigger behavioral hysteresis and direction persistence

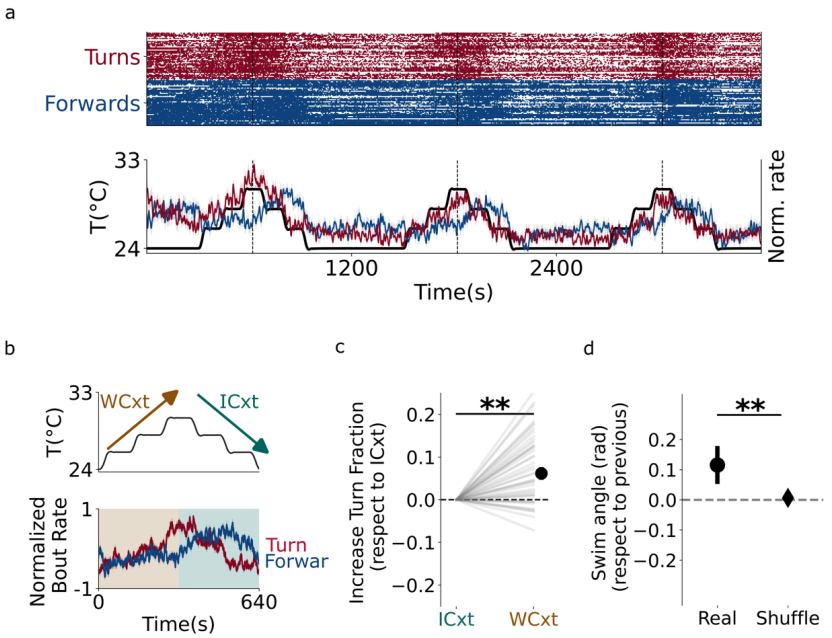

Fig. 27: **a.** Top: all the individual turns (red) and forward movements (blue) performed by n=40 fish for th eentire duration of the experiment. Bottom: Normalized turning (red) and forward (blue) rate overlayed on the stimulus trace. **b.** Top: stimulus protocol for temporal gradient experiment. Bottom: average normalized turning rate (red) and forward swim rate (blue) for n= 40 fish. **c.** Increase in turning fraction depending on sensory context for temporal gradient experiment, similar to 25b (median ± standard error of the median, Mann-Whitney non parametric test). **d.** Turn correlation upon WCxt, similar to 25c (mean ± standard error of the mean, Mann-Whitney non parametric test). n.s.: not significant, p-value > 0.05, *: p-value 0.05-0.01, **: p-value 0.01-0.001 ,***: p-value < 0.001

3.5 Summary: behavioral principles in thermoregulation

To summarize the behavioral observations, I have confirmed that larval zebrafish exhibit behavioral hysteresis when exposed to a thermal gradient, regardless of the environmental statistics. When moving away from the homeostatic setpoint, the probability of turning increases, while moving towards the preferred temperature promotes forward movements. This behavioral strategy is similar to what has been observed in other organisms. However, in contrast to *E. coli* and *C. elegans*, my research showed that larval zebrafish display turn persistence by continuously steering in the same direction, even in the absence of sensory cues. This behavior allows them to execute coherent steering maneuvers.

4. Whole-brain imaging in larval zebrafish

The central focus of this chapter is the comprehensive whole-brain imaging analysis carried out in larval zebrafish as they navigated a virtual thermal gradient. The average recording comprised half of the total number of neurons in the larval zebrafish brain, offering insights into their activity alongside behavioral observations. The main objective was to characterize distinct response patterns to different features of the stimulus. Specifically, I wanted to identify neurons that effectively tracked the dynamic changes of the stimulus over time. This type of response could play a crucial role in driving behavioral hysteresis.

4.1 Behavioral hysteresis in head-restrained preparation in larval zebrafish

Before analyzing the neuronal activity, I conducted experiments to investigate behavioral hysteresis in a head-restrained preparation. To precisely control the fish's temperature during imaging, a small tube was positioned near the fish's head. This setup facilitated a constant water flow, which could be heated or cooled upstream of the tube using a Peltier element (detailed in the Material and Methods section, *Perfusion system for head-embedded preparation under lightsheet microscope*). Following the same stimulus protocol as described in Chapter 3.4 (Figure 28a, b), I observed a similar modulation of the reorientation probability (Figure 28c) and directional correlation for WCxt (Figure 28d), replicating the findings from my freely swimming experiments (see Figure 27 and Figure 28).

Figure 28: Behavioral hysteresis in a head-restrained preparation for whole-brain imaging

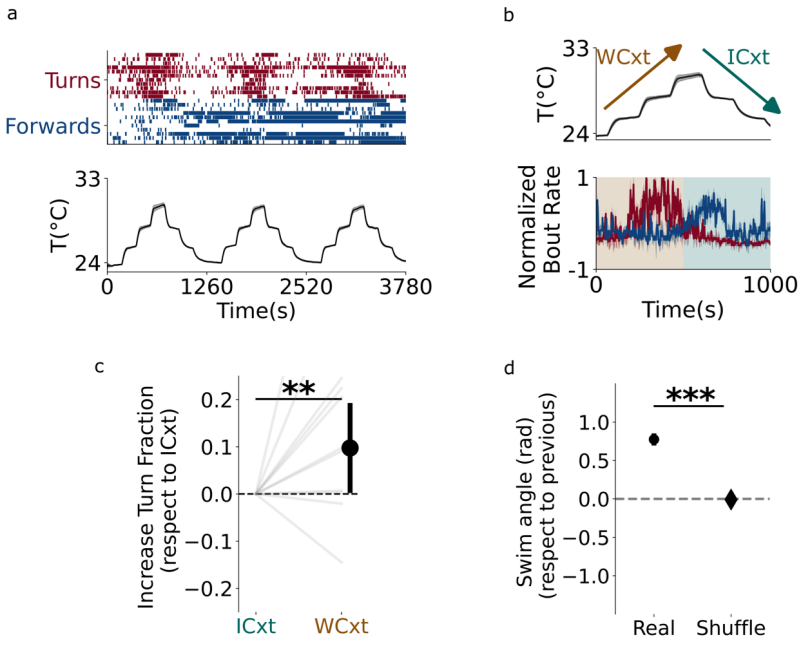

Fig. 28: **a.** Top: all the individual turns (red) and forward movements (blue) performed by n=11 fish for the entire duration of the experiment. Bottom: Stimulus trace. **b.** Top: stimulus protocol for temporal gradient experiment. Bottom: average normalized turning rate (red) and forward swim rate (blue) for n= 11 fish. **c.** Increase in turn fraction depending on sensory context for head-fixed experiments (median ± standard error of median, Mann-Whitney non parametric test). **d.** Turn correlation upon WCxt (mean ± standard error of mean, Mann-Whitney nonparametric test). n.s.: not significant, p-value > 0.05, *: p-value 0.05-0.01, **: p-value 0.01-0.001 ,***: p-value < 0.001

While this protocol elicited a strong and clear behavioral modulation, I recognized that the relatively long duration of each trial used above (~20 minutes) was not optimal for an imaging experiment where a large number of repetitions and a stable preparation are beneficial. Therefore, I devised a shorter protocol with 5 repetitions of a shorter stimulus block (Figure 15). In each block, the fish experienced an increase of +0.25°C away from room temperature (~26°C) before the temperature was brought back to baseline (single pulse). Then the increase was repeated, but this time the temperature was subsequently further increased to ~26.5°C (double pulse) (Figure 15a). The rationale behind this protocol is to present the fish with a slightly unpleasant situation which can then either improve (single pulse, ICxt) or get worse (double pulse, WCxt), thus mimicking a naturally occurring scenario

that the fish encounters while swimming freely. While this protocol is designed for imaging purposes and elicited a far less strong response in terms of behavior, I was still able to observe an increase in forward movements during an improvement and more turning behavior during a worsening pulse (data shown in Chapter 5.2).

4.2 Responses profile to temperature stimulus

To identify neurons reliably responding to different stimulus features in a virtual gradient navigation assay I employed an unbiased approach to analyze the whole-brain datasets acquired with a lightsheet microscope. For each neuron I computed a reliability index across trials and across individuals (Material and Methods, Describing temperature sensory responses), I selected only "reliable neurons" using a fixed standard threshold criterion for all fish and computed the trial trigger average (TTA) for all included neurons. To see which features of the stimulus were primarily modulating neural activity I performed a principal component analysis (PCA) over time on the neuronal responses. Neural activity appeared to be mostly modulated by stimulus intensity and context (Figure 29a). A PCA on neural responses highlighted the most prominent type of responses. In Figure 29b I projected the TTAs on a 2D space (cumulative variance explained 65% variability, Figure 18a) and finally clustered them using the k-means clustering algorithm (k=3, Figure 29c). The number of clusters was decided based on the Davies-Bouldin score (see Material and Methods and Figure 18b). The three clusters corresponded to three populations of neurons: a population that responded to the stimulus profile (type I), a population that responded with a longer rise constant (type II) and a population that tracked the stimulus change (type III) (Figure 29c). Activity in the latter was bidirectionally modulated (see Figure 29c), with a reduction from baseline fluorescence during temperature increase (WCxt) and an increase in fluorescence during temperature decreases (ICxt).

Figure 29: Reliable tracking of stimulus features in larval zebrafish brain

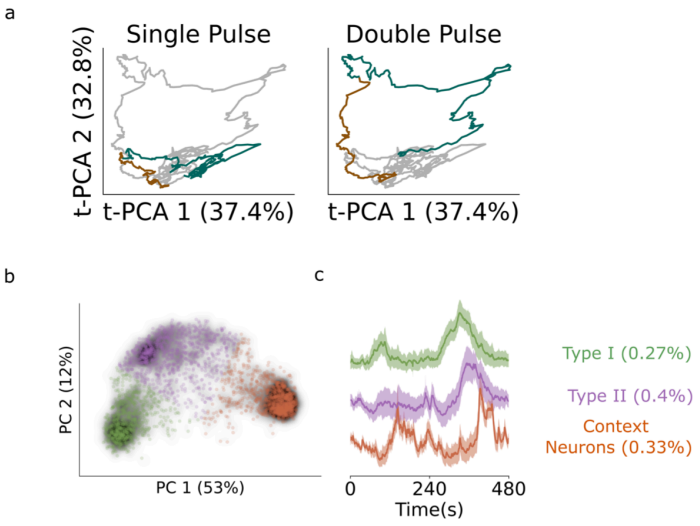

Fig. 29: **a.** Temporal trajectories in PC space of the neuronal activity of reliable neurons, color-coded based on stimulus context (orange WCxt, blue ICxt). **b.** Projection onto PC space of all reliable neurons color-coded according to their cluster identity. **c.** Mean activity of each cluster (mean ± standard error of mean) and fraction of cells per group (tot n= 3270).

4.3 Context neurons are not modulated by stimulus intensity

When I computed the difference in fluorescence intensity peaks between the single and double pulse within the stimulus block (Figure 30a) I found that the activity in type I and type II neurons scaled with absolute temperature, while that of type III neurons showed minor modulation, suggesting that responses of this cluster did not scale with stimulus intensity (Figure 30b, see also raw traces in Figure 30c, black and orange arrows). Moreover, as shown by the raw traces in Figure 30c, these responses do not arise from an averaging artifact or motor activity. They are already visible within individual fish at the single trial level and are dissociated from purely motor-related activity. Neurons of type III are well-suited to inform the fish on whether the context is worsening or improving (context neurons).

Figure 30: Context neurons are not modulated by absolute stimulus intensity

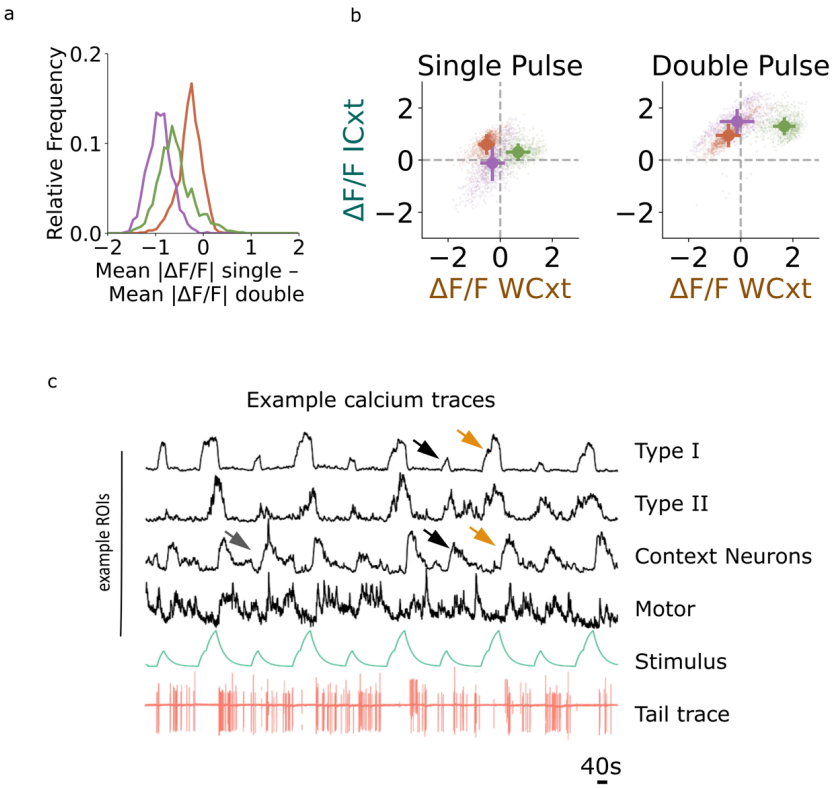

Fig. 30: **a.** Relative frequency distribution of the difference in meanfluorescence change during the single and double pulse stimulation for each cluster. Negative valuesimply that the fluorescence increased with increasing absolute temperature. **b.** Scatter plot of the average deviation from baseline fluorescence during single (on the left) and double pulse (on the right) split bysensory context (WCxt and ICxt) for the neurons in the three clusters (mean ± standard error of mean). **c.** Example raw traces from the three clusters and one motor ROI (all in black), the approximate stimulus profile (green)and the tail trace showing behavior (pink). Black and yellow arrow point to responses to single and double pulse in Type 1 and Context Neurons respectively.

4.4 Functional groups are organized in a gradient along the rostro-caudal axis

Importantly, the three clusters were organized in a functional gradient following the rostro-caudal axis of the fish brain (Figure 31a). In particular, by looking at the proportion of different ROIs types (Figure 31b) it clearly emerged that Type I and II neurons were enriched in rostral regions like the Olfactory Bulb (OB), Pallium (Pa) and right Habenula (rHb) while context neurons were found in other regions like the Preoptic Area (PoA), anterior Hindbrain (aHb), Interpeduncular Nucleus (IPN), and Superior Raphe (RN). Most of the aforementioned regions are known to be strongly connected (I. Bianco and Wilson 2009; I. H. Bianco et al. 2008; Miyasaka et al. 2014; Jetti, Vendrell-Llopis, and Yaksi 2014; Turner et al. 2016; Bartoszek et al. 2021) and in Figure 31c I have highlighted the relevant connections across brain regions. The next obvious step was to find out which of these regions were mostly sensory and which ones were also responding to motor activity.

Figure 31: Functional clusters are organized in a gradient along the rostro-caudal axis

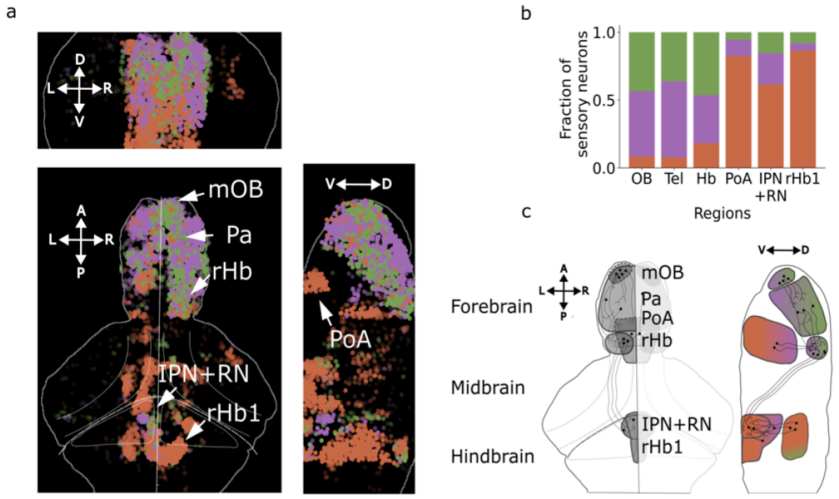

Fig. 31: **a.** Anatomical distribution of reliable ROIs according to cluster identity. Difference panels depict different projections. mOB: medial Olfactory Bulb, Pa: Pallium, rHb: right Habenula, PoA: PreopticArea, IPN+RN: Interpeduncular Nucleus and Raphe Nucleus, rHb1: Rhombomere 1. **b.** Proportion of ROIs from thedifferent clusters for different anatomical regions. OB: Olfactory Bulb, Tel: Telencephalon(Pallium+Subpallium), Hb: Habenula (Left + Right Habenula), PoA: Preoptic Area, IPN+RN (Interpeduncular Nucleus + Median Raphe + Dorsal Raphe), rHb1 (Rhombomere 1). **c.** Sketch ofhypothesized synaptic connections based on activity maps and literature.

4.5 Pre-Motor Areas

In order to identify putative pre-motor areas that could be informed by sensory history-detecting neurons, I searched for neurons that were reliably activated by either forward or directional swims (Figure 32a and Material and Methods, Swim triggered analysis). In line with other reports (Ahrens et al. 2012; Severi et al. 2014; Kist and Portugues 2019; Dragomir, Štih, and Portugues 2020; Markov et al. 2021), I observed neural correlates of motor activity around the nucleus of the medial longitudinal fasciculus (nMLF) and hindbrain regions. I also examined the localization of motor-related signals in brain regions that were previously identified as crucial for tracking stimulus features. I noticed that regions with a higher number of context neurons tended to also have more motor correlates (Figure 32b). This activity, locked to swimming events, could be directly instructive or could represent a short-term memory trace of what the animal did in the immediate past. This latter representation could provide a motor context required for the U-shaped behavioral sequences that I observed in the freely moving experiments (see Figure 26d).

Figure 32: Brain regions enriched with context neurons also present a high fraction of motor correlates

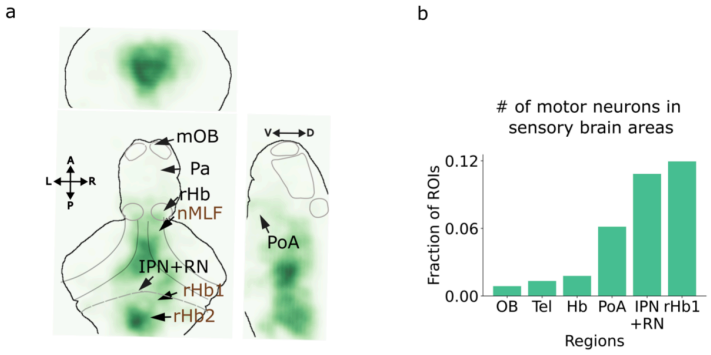

Fig. 32: **a.** Anatomical density distribution of motor triggered ROIs. Selected cells can be either forward, left or right-swim tuned **b.** Fraction of motor-triggered ROIs for each sensory identified region.

I reasoned that a potential neural substrate for such motor memory should lag with respect to a canonical premotor neuron and display more persistent activity. In order to find any temporal

progression of neural activity following a turn I clustered turn responding neurons depending on the timing of their peak activity (Figure 33a) and then computed the average activity in each cluster (Figure 33b and Material and Methods, Swim triggered analysis). As shown by the anatomical maps of the different timing clusters (Figure 33c), turn-related activity elicited a temporal progression of different neuronal populations. Fast neurons are localized contralateral with respect to turn direction and in a diffuse area of rhombomere II while slow neurons are ipsilateral and localized in a small medial region of the aHb .

Figure 33: Direction-selective neurons with slow dynamics are localized in a small medial region of the aHb

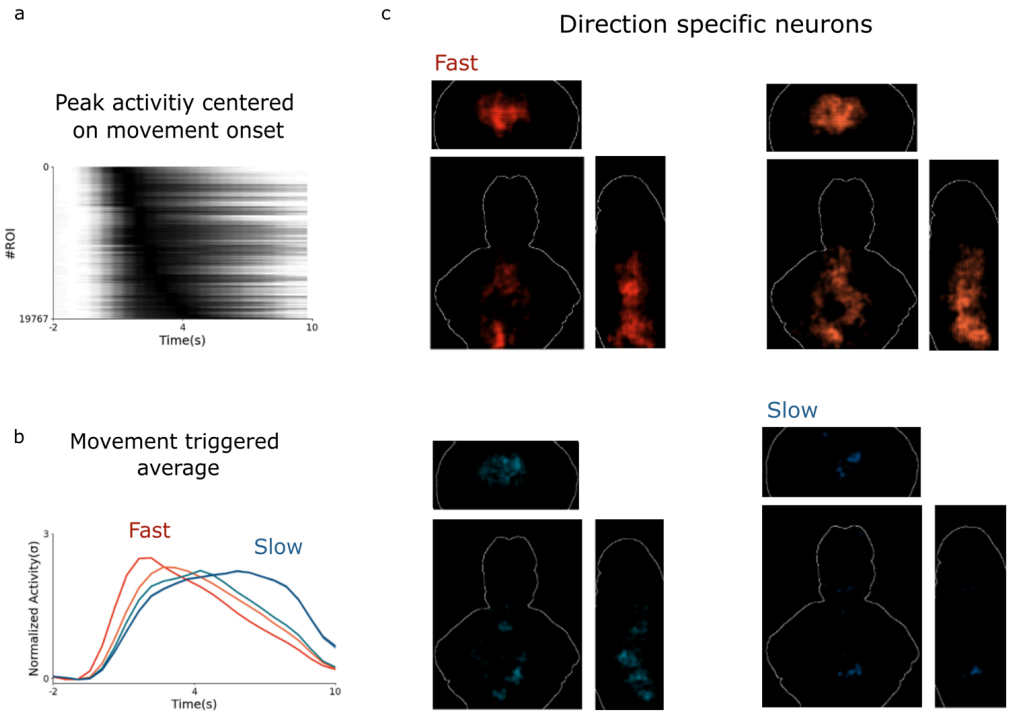

Fig. 33: **a.** Trial turn average for all turn-tuned ROIs. **b.** Mean activity for different lags **c.** Anatomical density distributionfor motor ROIs responding with different lags. From left to right: distribution of ROIs with increasing lag. Color coding in thes ame as in Figure b

4.6 Summary: neural responses to temperature follow a functional and anatomical gradient in larval zebrafish brain

In summary, my whole-brain analysis confirmed that temperature is sensed by neurons located in the olfactory system, probably among other regions that were not imaged in this study such as the trigeminal ganglion (Haesemeyer et al. 2018a). This information is then broadcast to hypothalamic regions such as the PoA and from there to the dHb-IPN-RN system. The PoA was particularly enriched in temperature-specific context cells, suggesting a role in thermoregulation, just as in mammals. Regarding the dHb-IPN RN system, the situation is more complex. Although responses in the dHb are mainly sensory, responses in the IPN, the main target of the dHb, were enriched in context and motor-modulated cells. The Hb is also known to receive direct input from the Pa and the PoA. Finally, the Hb was also particularly enriched with neurons that generalized across modalities. Overall, suggesting that both the PoA and the Hb could be involved in conveying the sensory context during homeostatic navigation.

5. Similarities across homeostatic threats

In Chapter 1 I have provided evidence that behavioral hysteresis is a strategy that biological systems use across many different types of gradients, not just temperature. In (Herrera et al. 2021) it has been shown that larval zebrafish navigate in a salinity gradient with a very similar strategy to what I have described in Chapter 3. Moreover, the rHb emerged in several studies as a strongly multisensory region (Dreosti et al. 2014; Haesemeyer et al. 2018a; Fore et al. 2020). Thus, I asked whether the fish brain encodes a representation of the stimulus history that generalizes across different sensory modalities, regardless of the stimulus identity.

5.1 Fish navigate in a salinity gradient showing behavioral hysteresis

I first replicated the experiments as in (Herrera et al. 2021), where I let individual fish swim for 15 minutes in a salinity gradient obtained by placing an agarose pad with NaCl mixed inside on one end of the arena and an agarose pad with no NaCl on the other side.

Based on these experiments, I could conclude that even taking into account the differences across homeostatic threats in reaction time and strength of the behavioral response, animals robustly rely on the interplay between turns and forward movements (Figure 34a, b, c) to locate their homeostatic setpoint. Even when the change in stimulus intensity over time was extremely subtle - as in the virtual gradient navigation assay I devised for whole-brain imaging (Figure 15) - fish exhibited behavioral hysteresis (Figure 34d).

Figure 34: Larval zebrafish maintain homeostasis in different type of gradients

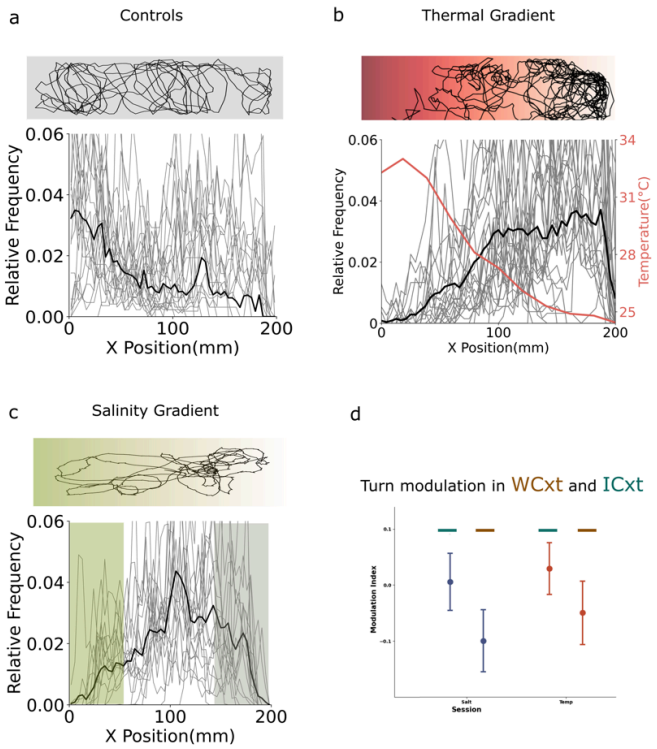

Fig. 34: **a.** Top: example trajectories of 3 fish at room temperature with no gradient, monitored for 15 min. Bottom: Histogram of animals' x-position in the arena (n=23, gray traces), median of the population (black trace). **b.** Top: example trajectories of 3 fish for the entire duration of the experiment (15 min). Actual temperature measured in the water is pictured with different shades of red. The highest temperature (33°C) is represented on the left by the dark red. Bottom: Histogram of animals' x-position in the arena (n=26, gray traces), median of the population (black trace) and temperature measurement (red trace). **c.** Top: example trajectories of 3 fish monitored for 15 minutes in a salinity gradient. The salty pad is depicted in gree. Bottom: Histogram of animals x position in the arena (n= 30, grey traces are the individual fish, black trace is the median of the population). **d.** N = 5, Modulation index of turning behavior as the difference of turns performed in the ICxt and in the WCxt. Values below zero mean more turning, values above zero more forward movements. Median and sem are displayed. First dot for each modality (displayed on the x axis) shows the modulation index for the ICxt in the single pulse. The second dot shows the modulation index for the WCxt in the double pulse.

5.2 Multimodal neurons

I then, decided to test the hypothesis that sensory modalities sharing a homeostatic value would converge onto the same circuit by keeping track of the relative changes in stimulus intensity over time (i.e. relative valence) to activate the same premotor areas and instruct behavior.

To this end, I recorded the brain activity during transient increases in salinity (salt session), which can be equally threatening to the animal's physiology. Importantly, the stimulus profile of the salt session session matched the one in the temperature session (Figure 15), to properly compare brain responses independent of sensory modality. In addition, I carefully matched single neuron identity across the three sessions (Figure 17, see Material and Methods, ROI segmentation across sessions) and extracted their fluorescence throughout (Figure 17). For each fish I extracted 44,772 ± 7,090 (mean ± std.) ROIs spanning the forebrain, midbrain, and parts of the hindbrain until the rhombomere II. Then, I selected neurons that reliably responded to both sessions (Figure 35a). Several brain regions had neurons responding during the two sessions (Figure 35b). However, to specifically identify multimodal neurons with similar stimulus response profiles across modalities I cross-correlated the trial triggered averages (TTAs) of reliable neurons in all the sessions and then computed a p-value based on circular shift shuffle versions of such traces (see Material and Methods). I finally selected neurons with significant p-value ($p<0.025$, Figure 35a and Figure 19) and correlation higher than 0.3 (Figure 36a, b). These neurons were anatomically restricted to the medial nucleus of the right dHb (Figure 35c mr-dHb), medial Olfactory Bulb (mOB) and a small cluster of the medial Pallium (mPa).

Figure 35: Different homeostatic threats converge onto the same circuit

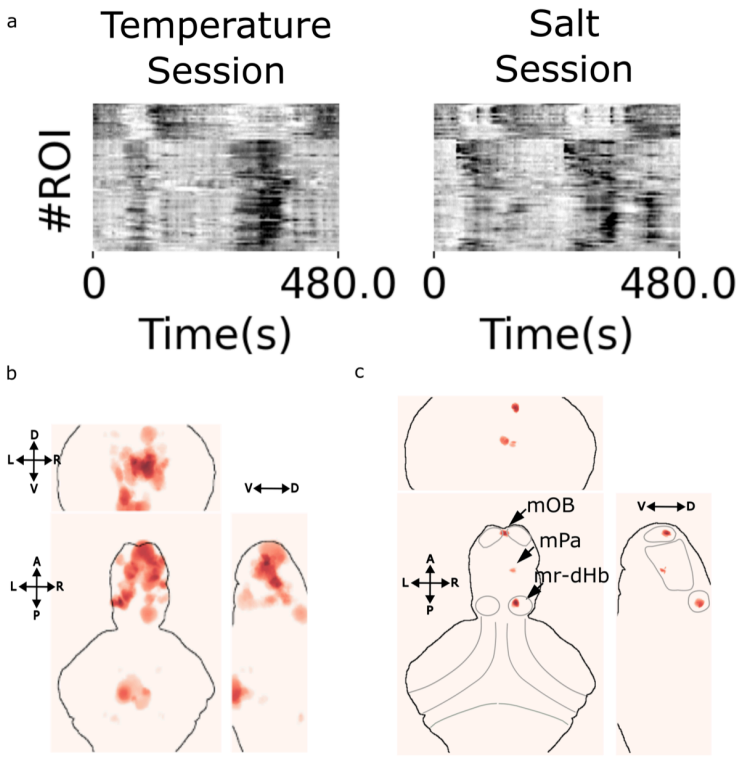

Fig. 35: **a.** Trial trigger average of all multimodal neurons found during temperature (left) and salt (right) sessions. The identity of the neurons was preserved. **b.** Anatomical density distribution of neurons reliability responding during both temperature and salt session before the p-value based filtering. **c.** Anatomical density distribution of multimodal neurons mOB: medial Olfactory Bulb, mPa: medial Pallium, mr-dHb: medial nucleus of the right dorsal Habenula.

Raw activity and mean activity (Figure 36a, b) of the responses in the mOB, mPa and rHB showed that neurons in these regions responded with remarkably similar responses to both temperature and salt sessions. Keeping track of the absolute stimulus intensity and the context (Figure 36a, b).

Figure 36: A small population of dHb, mOB and mPa neurons respond similarly to temperature and salinity changes

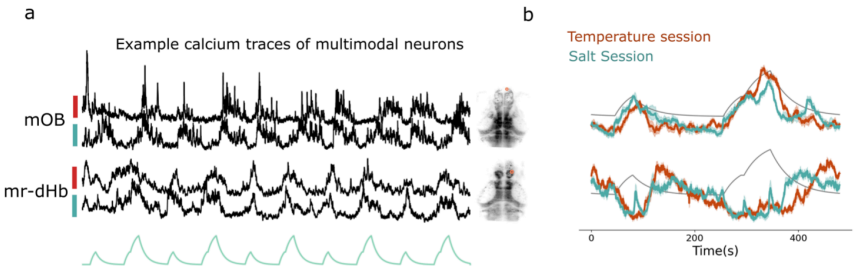

Fig. 36: **a.** Raw activity of two examplemultimodal neurons (one from the olfactory bulb and one from the habenula) in black for both the730 temperature and the salt session. **b.** Mean of the multimodal neuron clusters (k=2, mean ± standard error of the mean).

5.4 Summary: a generalist circuit for relative valence processing across homeostatic threats

In summary, in line with previous reports (Dreosti et al. 2014; Haesemeyer et al. 2018a; Fore et al. 2020), I have shown in this chapter that there is a circuit spanning the mOB, mPa and dorsal rHB which responds to relative valence regardless of stimulus identity. It is important to point out that the neurons highlighted in this pathway are activated **with similar dynamics** by both salinity and temperature changes while more brain areas are recruited by both stimuli without showing the same activation profile. In particular, there was activation of regions downstream of the Hb such as the IPN and the RN, to both salinity and temperature changes. Those findings suggest that there is an abstract representation of stimulus relative valence regardless of stimulus identity broadcasted by the Hb. However, this representation then diverges again in premotor areas downstream of the Hb, where, one can speculate, the final motor output needs to be adjusted in a modality-specific manner.

6. The PoA and the dHb jointly support homeostatic navigation

In my whole-brain screen (Chapter 4), I presented the PoA and dHb-IPN-RN pathways as potential candidates for influencing homeostatic navigation. On one hand, there was the PoA's role in thermoregulation in endotherms and its projections to the Hb and, on the other hand, the right dHb emerged as a multimodal region. To causally investigate their involvement in thermoregulation, I performed ablations of the PoA and dHb and evaluated the fish's behavior in the spatial gradient arena.

6.1 The PoA controls reorientation probability

Bilateral ablations of the PoA, as functionally identified in my previous lightsheet experiments, were conducted using a Ti-Sapphire laser at 5 dpf (Figure 21, see Laser-mediated cell ablations). As a control group, I targeted a portion of the medial Optic Tectum (OT), as this region showed minimal activation in response to temperature stimuli (n=20 for both groups, see Material and Methods). Following the ablation procedure, the fish were allowed to recover for 40-48 hours and then tested at 7 dpf (Figure 21). The ablation of the PoA led to a higher coefficient of dispersion in the thermal gradient at the end of the experiment, indicating a difficulty in maintaining proximity to their homeostatic setpoint (Figure 37a). To test my hypothesis, I calculated the same increase in turn fraction as used for wild-type fish. The results revealed a significant impairment in the modulation of reorientation probability based on sensory history (ICxt vs. WCxt) compared to the control group upon PoA ablation (Figure 37b). This lack of modulation was also evident in the reduced turn fraction throughout the experiment compared to controls (Figure 37c). Importantly, the directional persistence during U-maneuvers - when the fish experienced a WCxt - was impaired (Figure 37d). These findings suggest a critical involvement of the PoA in driving reorientation behavior and facilitating navigation towards the homeostatic setpoint.

Figure 37: PoA ablations suppress turning behavior when conditions are worsening

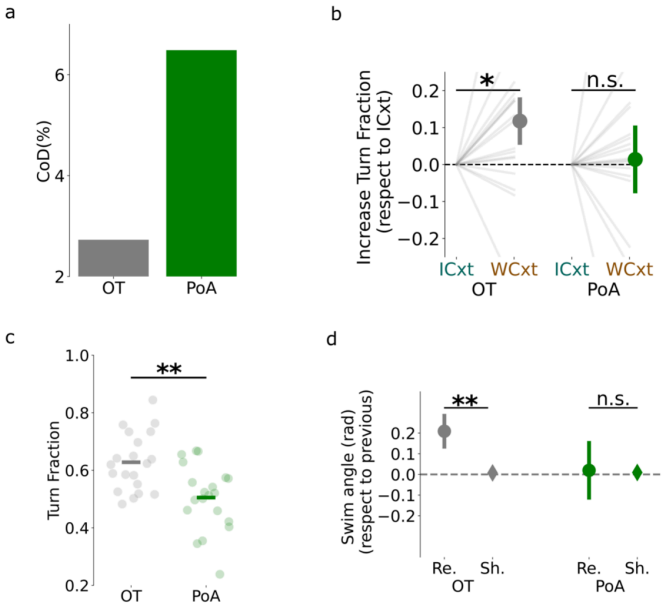

Fig. 37: **a.** Coefficient of Dispersion for control group (light gray), ablation group (green). **b.** Increase in turn fraction depending on sensory context. Left: control OT ablation, right: PoA ablation. (median ± standard error of the median, Mann-Whitney non parametric test). **c.** Median turn fraction computed throughout the entire experiment (median ± standard error of the median, Mann-Whitney non parametric test). **d.** Turn correlation upon WCxt for the control and ablation groups (mean ± standard error of the mean, Mann-Whitney non parametric test). n.s.: not significant, p-value > 0.05, *: p-value 0.05-0.01, **: p-value 0.01-0.001 ,***: p-value < 0.001

6.2 The dHb-IPN pathway combines a longer sensory memory with a motor memory

I next used the transgenic Tg(Gal4:16715; UAS:Ntr-mCherry) line to selectively ablate the dHb at 5 dpf using a chemogenetic approach (see Material and Methods, Chemogenetic Ablations). This

transgenic line restricts the expression of Nitroreductase (Ntr) to the dHb region (Figure 20a). As control groups, I included a genetic control and a treatment control (n=25, 23, and 14 for the genetic control, treatment control, and ablation group, respectively, see Material and Methods, Chemogenetic Ablations). In a similar fashion to the PoA ablations, the dHb-ablated fish exhibited a higher group dispersion coefficient compared to controls (Figure 38a). However, surprisingly, ablated fish still showed behavioral hysteresis (Figure 38b).

Nonetheless, when I investigated their ability to utilize a short-term working memory in the absence of sensory cues during the last movement (e.g., WCxt→NCxt or ICxt→NCxt), the increase in reorientation probability was lost in the ablated group (Figure 38c).

Figure 38: Hb ablations impair sensory memory when fish is challenged with intermittent sensory cues

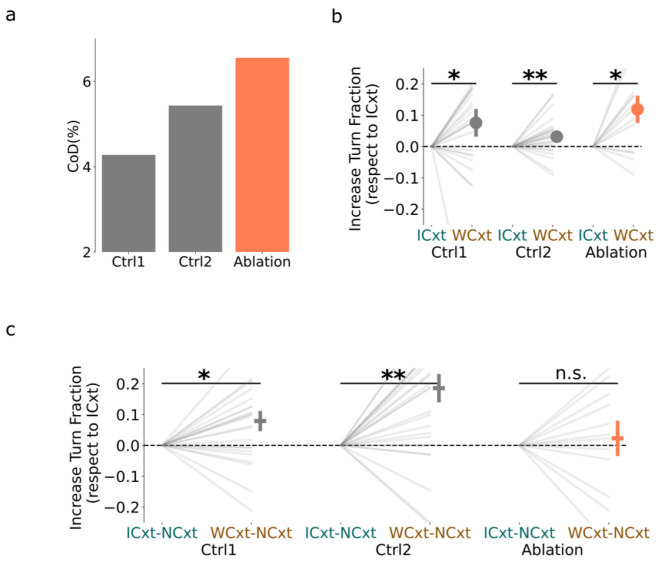

Fig. 38: **a.** Coefficient of Dispersion for control groups (light gray), ablation group (coral). **b.** Increase in turn fraction depending on sensory context. Genetic control, Treatment control and Hb ablation. (median ± standard error of the median, Mann-Whitney non parametric test). **c.** Increase turn fraction when last bout brought a NCxt (median ± standard error of the median, Mann-Whitney non parametric test). n.s.: not significant, p-value > 0.05, *: p-value 0.05-0.01, **: p-value 0.01-0.001 ,***: p-value < 0.001

Interestingly, I also observed a general increase in reorientation maneuvers in the ablated group (Figure 39a) regardless of the context the animal was currently in. These reorientation maneuvers, similar to the PoA ablations, were completely uncorrelated. Consequently, fish did not exhibit any

direction persistence and U-maneuvers were impaired in the ablated group compared to controls (Figure 39b). Suggesting that even if these animals reorient more in a WCxt, they do so by leveraging a strategy that has lost any type of structure and resembles what has been described in *C. elegans* or *E. coli*.

Figure 39: Hb ablations impair the directional component of homeostatic navigation

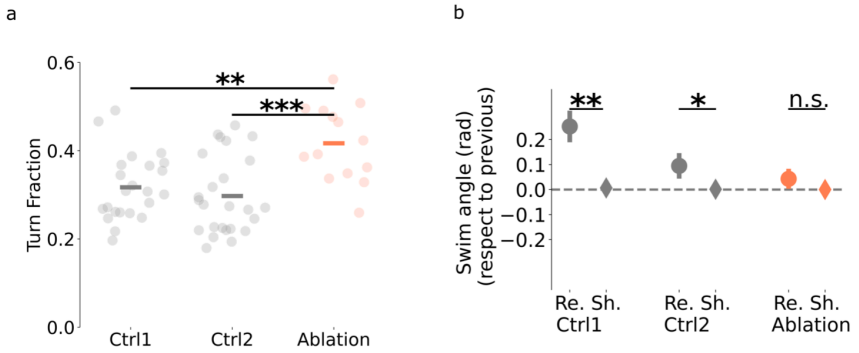

Fig. 39: **a.** Turn fraction computed throughout the entire experiment (median, Mann-Whitney non parametric test). **b.** Turn correlation upon WCxt for the two controls and the ablation group (mean ± standard error of the mean, Mann-Whitney non parametric test). n.s.: not significant, p-value > 0.05, *: p-value 0.05-0.01, **: p-value 0.01-0.001 ,***: p-value < 0.001

6.3 Serotonin manipulation impairs larval zebrafish ability to localize its homeostatic setpoint

The RN is the ultimate output of the Hb-IPN pathway and it has been implicated in temperature perception and homeostatic setpoint regulation in other model organisms (Sheard and Aghajanian 1967; Li et al. 2013; Inoue, Yamashita, and Agata 2014; Tan and Knight 2018; Nakamura, Nakamura, and Kataoka 2022). In my case I indeed noticed that fish treated with fluoxetine (for protocol see Material and Methods, Fluoxetine Treatment) were unable to converge into a particular position in the arena (for example see Figure 40a). When I looked at different characteristics of their behavior I noticed that they reacted less than a WT to the absolute stimulus intensity (Figure 40b) and they also exhibited less behavioral hysteresis (Figure 40c). Finally, instead of concatenating movements in the

same direction fish were more prone to constantly switching direction during U-maneuvers (Figure 40d). Effectively losing direction persistence.

Figure 40: Manipulation of serotonin affects different aspects of thermoregulation

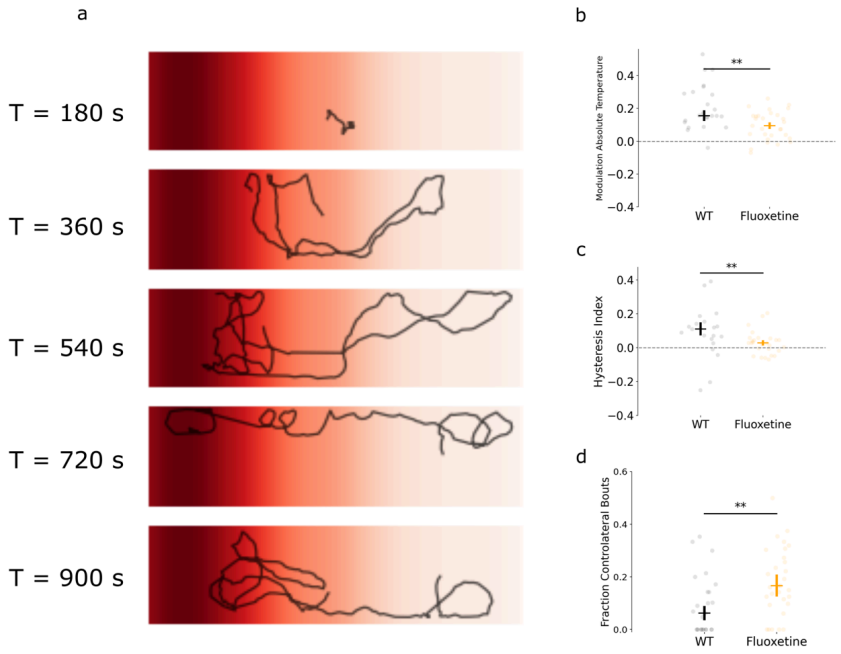

Fig. 40: **a.** Example trajectory of a fish treated with fluoxetine divided in 3 min bins**. b.** Difference in number of turns perfomed above and below 2.5 °C above the homeostatic setpoint for WT in black and fluoxetine treated fish in yellow (mean ± standard error of the mean, Mann-Whitney non parametric test). **c.** Relative increse in number of turns upon WCxt in WT in black and fluoxetine in yellow (mean ± standard error of the mean, Mann-Whitney non parametric test). **d.** Fraction of turns in the opposite direction of the one just performed in a WCxt. WT in black and fluoxetine treated in yellow. (mean ± standard error of the mean, Mann-Whitney non parametric test) n.s.: not significant, p-value > 0.05, *: p-value 0.05-0.01, **: p-value 0.01-0.001 ,***: p-value < 0.001

6.4 Neuronal manipulations increase the homeostatic setpoint

As a final finding I noticed that every time fish experienced a chemogenetic or laser manipulation, their homeostatic setpoint would shift toward warmer temperatures (Figure 41). The animals were healthy and the change was present in both the experimental and the controls groups (Figure 41b, c). All the analysis were carried out normalizing by the preferred temperature of the controls and experimental group in a certain experiment (see Material and Methods, Extraction of relevant

behavioral parameters for large arena experiment). However, it is interesting to speculate whether this mechanism could be reminiscent of a “behavioral fever”.

Figure 41: Neuronal manipulations induce a shift in the homeostatic setpoint

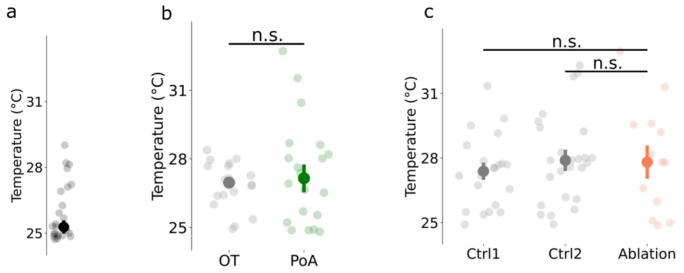

Fig. 41: **a.** Preferred temperature for WT fish **b.**Preferred temperature for the control and the experimental group (green). c. Preferred temperature for the two controls and the ablation group (mean ± standard error of the mean, Mann-Whitney non parametric test). n.s.: not significant, p-value > 0.05, *: p-value 0.05-0.01, **: p-value 0.01-0.001 ,***: p-value < 0.001

6.5 Summary: In homeostatic navigation the PoA controls the reorientation drive and the dHb-IPN-RN pathway orchestrates the directional component

These findings validate the results obtained through calcium imaging and provide further insights into the role of the PoA and the dHb in homeostatic navigation. Both regions contribute to this process in a coordinated manner. The PoA assesses the distance from the setpoint before and after a swimming event and initiates reorientation when the fish is in a WCxt. It also relays this information to the dHb.

On the other hand, the dHb utilizes inputs from the PoA to generate consistent steering trajectories, facilitated by a working memory of the sensory history. This working memory becomes particularly crucial in shallow temperature gradients where individual movements may not significantly alter the perceived environmental temperature. Consequently, the dHb enables the fish to navigate directionally even in the absence of continuous new information following each movement.

Finally, serotonin plays a role as well in shaping gradient navigation and driving thermoregulation. However, in contrast to the PoA and the dHb, serotonin affects multiple components of homeostatic navigation from stimulus sensitivity to final motor output, raising the compelling hypothesis that this neuromodulator may act as a global signal, triggering the animal to switch between behavioral states such as exploration/exploitation.

7. Thermoregulation in larval zebrafish and the fruitfly

The last part of my work was focused on the effort of building rigs that would allow for the systematic investigation of thermoregulation across evolutionarily distant organisms to try to highlight fundamental patterns in the behavioral strategies employed (e.g. behavioral hysteresis).

To this end, I built behavioral arenas where both model organisms would be challenged by the same environmental conditions. The 20 x 4 cm rectangular arena (Figure 9) where I controlled the temperature at each side, was used, with a lid, to also test thermal preference and navigation in the fruitfly. I also used the squared small arena (Figure 10) to test the timescales at which sensory history would trigger behavioral hysteresis in fly and fish. Finally, I established a preparation for whole-brain imaging under the lightsheet microscope that could be used for chronic imaging in fly.

7.1 Both fish and flies use behavioral hysteresis to control their body temperature

I first tested groups of 12 individuals for both fly and fish (Material and Methods, Spatial gradient in the large arena for multiple animals) in the spatial arena to investigate the homeostatic setpoint of both model organisms.

Both fish and flies controlled their body temperature by navigating the provided thermal gradient in darkness. They both didn't rely on visual cues or sufficiently steep temperature differences across the length of their body, but they still managed to locate the temperature that matched their homeostatic setpoint (Figure 42).

By the end of a 30 minute experiment (see Materials and Methods, Spatial gradient in the large arena for multiple animals), where animals had an habituation and a gradient period, I found that both fish and flies were robustly avoiding the hot side (Figure 42)**.** Particularly, I observed that, already, after 10 minutes both organisms would gather respectively ~25.3 °C and ~23 °C, which I posit to be their homeostatic setpoint (Figure 42).

Figure 42: Larval zebrafish and the fruitfly maintain homeostasis in a linear shallow thermal gradient by quickly finding the homeostatic setpoint

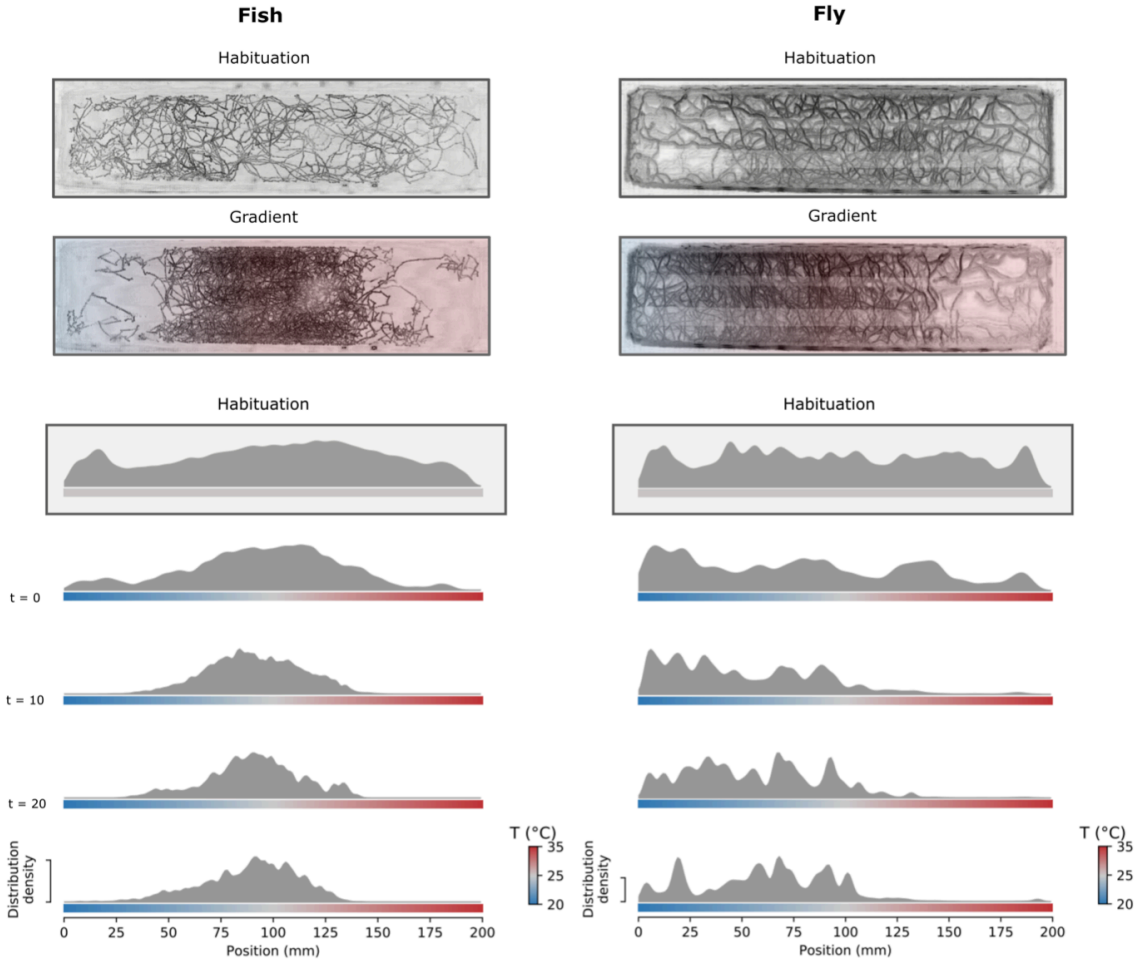

Figure 42: **Top**: example trajectories of a cohort of 12 fish (left) and 12 flies (right) for the habituation period (20 min) and gradient period (30 minutes). The temperature measured in the water is pictured with different shades of red and blue. The highest temperature (35°C) is represented on the right by the dark red. The lowest temperature (20 °C) is in blue. **Bottom**: Density distribution on the x-position in the arena (n=12, 4 cohorts for both flies and fish)

Next I was interested in investigating whether both fish and fly would increase their amount or reorientation maneuvers when the temperature was externally changed as in Chapter 3.4. I was indeed able to confirm that they both showed behavioral hysteresis (Figure 43).

Figure 43: Larval zebrafish and flies show behavioral hysteresis when they are pushed away from their homeostatic setpoint

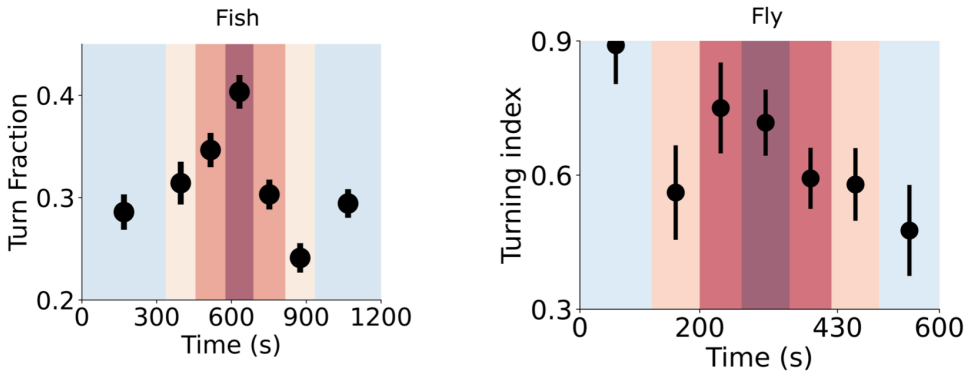

Figure 43: **Left**: In fish. Turn fraction according to temperature experienced and sensory context. Color-coded was decided according to the temperature delivered. The median +- the standard error of the median are depicted.
Right: same plot

7.2 Lightsheet imaging in D. melanogaster

To identify brain areas involved in the sensing of temperature changes I wanted to achieve fast whole-brain imaging in vivo for both fish and fly. I decided to use lightsheet microscopy over two-photon scanning microscopy, as it has the advantage of being faster and, therefore, better suited for probing neural responses simultaneously across different brain regions.

The standard preparation is to embed the fish in low-melting temperature agarose solution in a square chamber filled with embryo medium. The chamber is then placed on a transparent holder, which allows behavioral tracking. Both sides of the specimen chamber along the illumination path consist of glass coverslips. Actually, the lightsheet poses a major challenge decoupling the illuminating

objectives from the recording one, forcing the experimenter to remove, in the non-optically-transparent fly, additional cuticle to grant optical access to the brain. To my knowledge, very few studies have successfully performed in vivo imaging in the adult fly using a lightsheet microscope (Liang, Holy, and Taghert 2016).

In developing our preparation in adult fly, I decided to adapt our fish chamber design, profiting from the knowledge that in temperature studies it is common to have the fly's head immersed in water (Frank et al. 2015). Therefore, after inserting a pipette tip in the floor of the imaging chamber, the fly's head was partially extruded from the pipette using a small piece of paper and then the neck was glued to the head of the fly to both reduce movements and seal the tip, leaving the rest of the body dry (Figure 44a). The entire chamber was then filled with saline solution. I did not change either the position or the shape of the holder, thus allowing the use of the same microscopy setup for both preparations. With this type of solution I recorded for up to two hours and one of the specimens was still alive five hours post surgery.

In Figure 44 b is shown neuronal activity in response to cold water in different parts of the Mushroom Body (MB).

Figure 44: Chronic lightsheet imaging in the fruitlfy

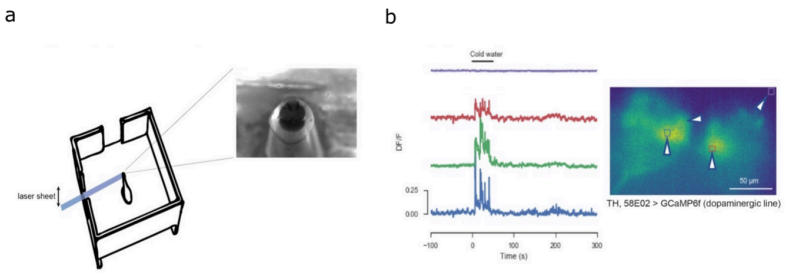

Figure 44: Lightsheet imaging in adult flies. **a**. Schematic showing the custom made 3D printed chamber and the plastic pipette used to holdand immobilize the fly. Upper-right image shows a close-up of fly preparation. The chamber has two slits on adjacent sides that get covered with glass cover slides to allow the two laser beams to scan the fly brain. **b**. Anatomy of a single plane (out of 6) that was imagedat four brains per second while presenting cold water. The hand-picked regions of interest (ROIs) show temperature related responses.

7.3 Summary thermoregulation in fly and fish

In conclusion I have demonstrated that it is possible to address the same questions about thermoregulation in evolutionary distant model organisms by developing an array of different behavioral and imaging preparations. Moreover, I have also provided evidence that behavioral hysteresis is truly one of the most fundamental behavioral strategies in gradient navigation across different modalities and taxa.

8. Discussion

8.1 Overview

In this thesis, I described how larval zebrafish, a small ectotherm, achieve thermal homeostasis by identifying its preferred temperature in the surrounding environment. In a shallow thermal gradient, fish utilize the memory of the experienced temperature changes over time to compute whether they are successfully getting closer to their homeostatic setpoint. Simply put, when they detect a worsening of conditions, they increase the number of reorientation maneuvers to change their heading direction, while they maintain the current direction of travel when an improvement is detected. My results provide further evidence that larval zebrafish leverage behavioral hysteresis during homeostatic navigation and align with observations in a plethora of different model organisms across many sensory modalities. I also uncovered a directional component of this behavior where the fish concatenates several movements in the same direction to produce coherent trajectories. I also confirmed that fish employ the same approach in a salinity gradient, which speaks in favor of a common behavioral strategy employed by animals to cope with homeostatic threats.

Through a whole-brain calcium imaging screen, I was able to identify a brain-wide circuit that reliably responded to different stimulus features in a virtual-gradient navigation assay. I, then, investigated the potential involvement in homeostatic navigation of brain regions tracking, specifically, temperature changes. I found evidence for an evolutionarily conserved role of the Preoptic Area (PoA) across vertebrates. Furthermore, my findings suggest that the dorsal Habenula (dHb) supports the PoA during navigation by retaining memory of experienced temperature changes for several seconds, even in absence of immediate sensory cues. It also combines this memory with a motor memory of the fish's past actions to direct coherent trajectories. In line with other studies, I, additionally, propose that the dHb's and its downstream regions are critical players for multimodal integration, in particular for computing a more abstract representation of the relative stimulus valence and for selecting the appropriate behavioral strategy.

Finally, I examined thermal homeostasis in the fruitfly, specifically focusing on building behavioral setups and on designing a head-restrained preparation for fast whole-brain imaging that would allow for the same stimulus to be delivered, in the same way, in both drosophila and fish. In the end, I succeeded in having the same environmental conditions in both model organisms. In alignment with the initial hypothesis that behavioral hysteresis is a fundamental aspect of animal navigation, I provide

evidence that *D. melanogaster*, similarly to larval zebrafish, increases the amount of turning when navigating away from its homeostatic setpoint and maintains its current direction of travel when approaching its preferred temperature.

8.2 Behavioral strategies in homeostatic navigation

8.2.1 The homeostatic setpoint

Both fish and flies were fast in relocating once they got pushed away from their homeostatic setpoint, quickly finding their preferred homeostatic range within five minutes from the beginning of the experiment (Figure 42). Interestingly, I noticed that flies had a broader distribution around the setpoint compared to fish, suggesting that either they are more temperature-tolerant or that the setpoint can vary among individuals. This phenomenon could be attributed to the distinct rearing conditions for flies. They are typically bred at either 18 °C for stock maintenance or at 25 °C for experimental purposes and faster development (Mołoń et al. 2020). This exposure to two distinct temperature regimes might confer a greater thermal adaptability, promoting tolerance to a broader range of temperatures. Especially, in comparison to other organisms raised in more stable thermal environments such as larval zebrafish.

Interestingly, even though minor changes in rearing temperature (approximately 2-3 °C, data not shown) didn't impact the homeostatic setpoint of larval zebrafish, a shift towards higher temperatures was observed when the fish were subjected to manipulations (Figure 41). This phenomenon could potentially represent a type of defense mechanism resembling a fever, but this interpretation remains speculative at this stage. Importantly, despite these changes in temperature preference, the fish were healthy and swimming for the entire duration of the experimental procedures and were euthanized several days later.

Moving forward, it would be intriguing to investigate whether systematically rearing fish and flies at various temperatures would indeed influence their homeostatic setpoints. A potential coupling with food availability, another environmental factor known to significantly shape the thermal preferences of both endotherms and ectotherms, could also be examined (Hedgecock and Russell 1975; Umezaki et al. 2018; Nakamura, Nakamura, and Kataoka 2022). Finally, another fascinating approach would be to induce a 'behavioral fever' through infection, subsequently observing any potential shifts in the homeostatic setpoint.

Finally, a recent article has indicated that larval zebrafish do not maintain a pre-set homeostatic equilibrium when exposed to NaCl. Instead, fish instinctively migrate towards less saline waters,

potentially leading to harmful conditions if entirely deionized water were naturally available (Herrera et al. 2021). This presents the fascinating question of how this behavior influences the fish's sensitivity to salt as compared to temperature and what variations may exist at the level of the neural implementation.

8.2.2 Behavioral hysteresis: The basic building block of homeostatic navigation

As hypothesized from previously published papers across many different model organisms, the driving force behind homeostatic navigation, in absence of visual cues and previous knowledge of the environment, is the change over time of the stimulus intensity (i.e. the derivative). Fish and flies use this information to bias the behavior accordingly (Figure 43). They increase their probability of turning when they experience a WCxt and favor straighter trajectories in ICxt. In other words, they reorient more or less depending on whether they are moving toward or away from their homeostatic setpoint. This behavioral approach fully depends on the temporal structure of the stimulus, as clearly shown by the findings in the temporal gradient (Figure 43). These results further corroborate the hypothesis that behavioral hysteresis is probably the most conserved behavioral strategies in gradient navigation across the animal kingdom, specifically when animals do not have access to visual cues. I propose that the primary evolutionary drive for developing such a straightforward and reliable strategy was to aid organisms in regulating their homeostatic needs, particularly in the absence of internal homeostatic mechanisms (Figure 45 (i)).

At the same time, my results also uncovered an additional layer in larval zebrafish homeostatic navigation. Specifically, the fish doesn't randomly pick a new direction of traveling after a turn as it happens in *E. coli* and in *C. elegans* but keeps concatenating turns in the same direction, particularly when thermal conditions are worsening. This phenomenon has already been independently observed before (Robson 2013; Dunn et al. 2016). Importantly, this is different from what drosophila larvae do when they bias their run toward the side where they detect a more favorable environment after head-casting (Garrity et al. 2010; Gomez-Marin and Louis 2012). From my preliminary result fish are not taking spatial measurements of stimulus intensity but they rather reinforce successful actions. Moreover, they can couple this memory of past actions with a sensory memory in the order of several seconds that can account for intermittent sensory cues. In a virtual phototaxis assay conducted by (X. Chen and Engert 2014), fish were observed to navigate inside an arbitrarily defined circle. Light conditions were manipulated so that light was turned on when the fish were inside the circle and off when they crossed the invisible boundary. This observed behavior suggested that fish could be storing information about their orientation relative to the boundary or retaining memory of their past actions and the time needed for the environment to improve. Regardless of the specific strategy employed these results suggest that fish could also be leveraging *spatial primitives* (Figure 45 (ii)).

Figure 45: Behavioral principles in larval zebrafish homeostatic navigation

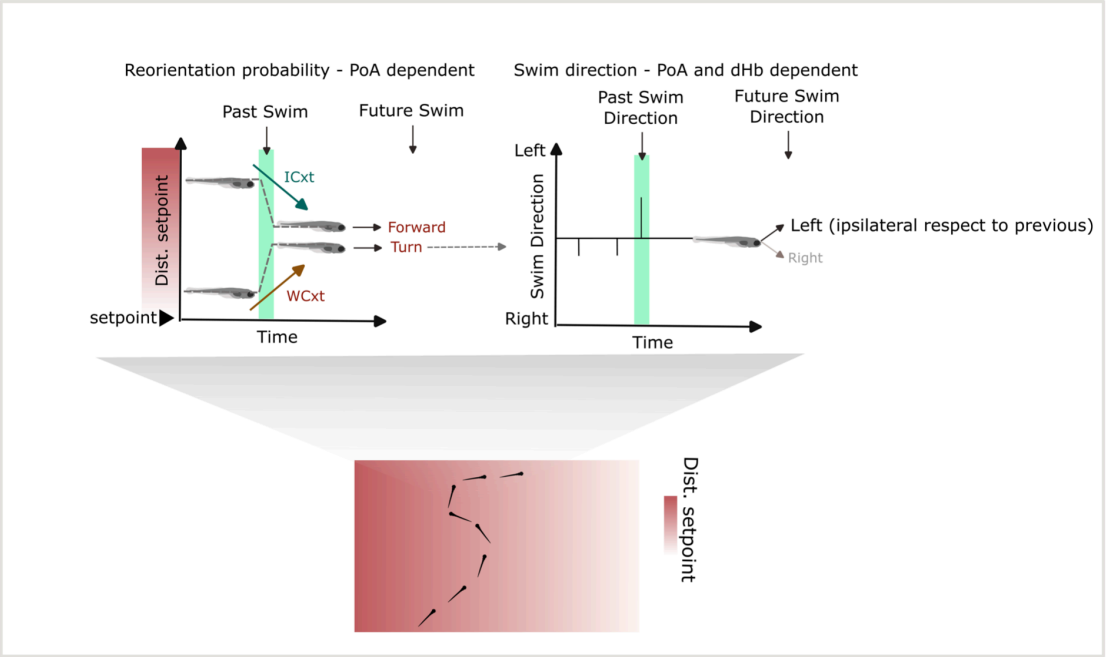

Figure 45: Summary of the behavioral principles underlying homeostatic navigation in larval zebrafish uncovered by this study. Fish behavior has two components: (i) an increase in turning (reorientation probability) when experiencing a WCxt (being pushed away from the homeostatic setpoint) and (ii) turning in a persistent direction during a WCxt. The first strategy is PoA dependent whereas the second depends on both the PoA and the dHb

8.3 A brain-wide circuit for processing homeostatic threats

Utilizing whole-brain functional imaging, I was able to identify specific brain regions that responded to temperature changes during an open-loop virtual gradient assay (Figure 15, Material and Methods, Multimodal short temporal gradient for head-restrained preparation). From my recordings I identified three primary types of temperature responses. Type I and type II neurons displayed a response to the stimulus profile, though their dynamics varied. In contrast, Type III neurons, which I designate as context neurons, tracked the changes in the stimulus. These context neurons demonstrated bidirectional modulation, showing a reduction from the baseline during WCxt and an increase in activity during ICxt, with their activity remaining unaffected by stimulus intensity.

I also noticed a functional gradient along the rostro-caudal anatomical axis. Primarily, Type I and II neurons were situated in the fish's forebrain. Regions like the medial olfactory Bulb (mOB) and the Pallium (Pa) comprised almost exclusively of Type I and Type II cells. The right Habenula (rHb), however, presented a mix of Type I, II, and context neurons. On the other hand, with the notable exception of the Preoptic Area (PoA), context neurons were primarily found in the midbrain and hindbrain of the fish, including regions such as the anterior hindbrain (aHb), the Interpeduncular Nucleus (IPN), and Raphe Nuclei (RN).

Interestingly, most of the regions identified are strongly interconnected (Figure 46). For instance, neurons in the mOB send their projections to both the Pa and the rHb, often through the collaterals of the same neuron (Miyasaka et al. 2014; Jetti, Vendrell-Llopis, and Yaksi 2014). Neurons in the medial portion of the Pa project to the rHb (I. H. Bianco et al. 2008; I. Bianco and Wilson 2009; Bartoszek et al. 2021), together with the PoA (Turner et al. 2016). The Hb is, then, well known to send glutamatergic input to the IPN through the Fasciculus Retroflexus (I. H. Bianco et al. 2008; I. Bianco and Wilson 2009). In particular, neurons in the rHb selectively project to the ventral portion of the IPN with axons wrapping around this structure. Finally, the IPN is a GABAergic nucleus projecting to RN and receiving inputs from the aHB (I. H. Bianco et al. 2008; Petrucco et al. 2023). Strikingly, the RN sends axons to more caudal rhombomeres as well as feedback projections back to forebrain regions such as the OB and Pa (McLean and Fetcho 2004). I, therefore, suggest that these regions are part of a brain-wide network supporting homeostatic navigation.

Figure 46: The circuit supporting homeostatic navigation

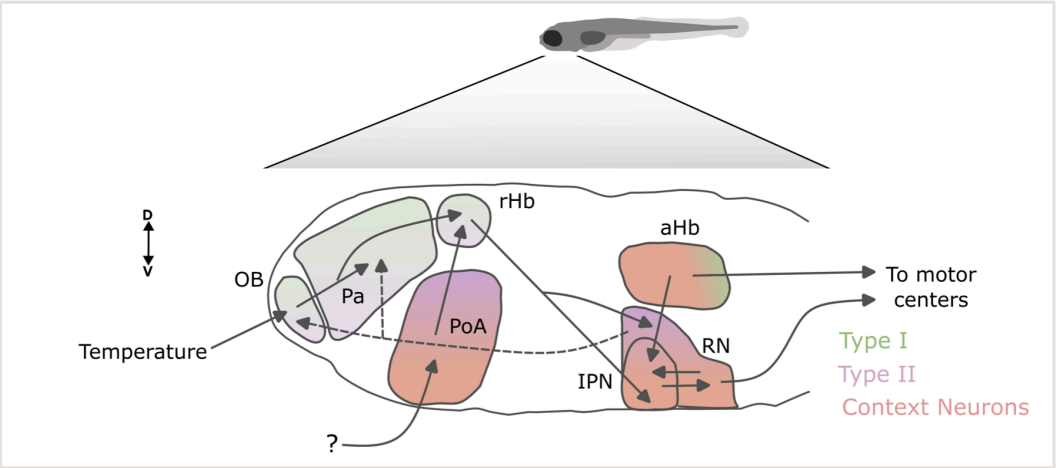

Figure 46: Neural circuitry involved in homeostatic navigation. Neurons representing the three main stimulus features are marked with different colors and the anatomical shading shows the fraction of response types in each region.

8.4 The OB-Pallium-rdHb pathway

Although previous studies have highlighted the trigeminal ganglia as the main entry-point for temperature sensation in the larval zebrafish brain (Haesemeyer et al. 2018), I found that the responses to absolute stimulus intensity, which were most likely to be from primary sensory neurons, were in the mOB (Figure 31a). Moreover, when I looked for multimodal responses to salt and temperature three small areas in the mOB, the mPa and the right dHb, respectively, were selectively highlighted. I speculate that different sensory modalities have converged onto a single navigation circuit to instruct a shared behavioral strategy. From an evolutionary point of view homeostatic navigation could be a result of an ancient chemotaxis navigation circuit being repurposed for other sensory modalities. This circuit, when connected to the PoA, gained the capability to juxtapose external data with an internal homeostatic setpoint. In essence, a basic module is used regardless of the stimulus identity and then evolution facilitates connections to new sensory modalities and brain regions. Afterall, temperature sensing in olfactory circuits has been found in other animals (Kludt et al. 2015; Kuhara et al. 2008; Biron et al. 2008) and in larval zebrafish the activation of olfactory regions has been reported upon exposure to salt (Herrera et al. 2021), changes in pH (Lovett-Barron et al. 2020), food (Dreosti et al. 2014) and carbon dioxide (Koide, Yabuki, and Yoshihara 2018). It would be interesting, in the future, to test for the distribution of receptors sensitive to temperature and

odors in the OB and olfactory epithelium. A previous study has reported the presence of TRPV1 ortholog in the trigeminal ganglia and lateral line but the location and function of additional receptors has not yet been tested (Gau et al. 2013).

The mOB is, additionally, known to send projections and influence the activity of the dHb both directly and indirectly through the Pa (Miyasaka et al. 2009; Kermen et al. 2013; Miyasaka et al. 2014; Jetti, Vendrell-Llopis, and Yaksi 2014). The mOB receives cholinergic inputs through the terminal nerve ganglion and centrifugal projections from the telencephalon (Kermen et al. 2013). Importantly, it also receives serotonergic inputs, as in mammals, from the raphe nuclei (Lillesaar et al. 2009; Kermen et al. 2013).

Together with the mOB and the dHb I also saw wide-spread activation of the Pa during the presentation of the thermal stimuli. Notably, I also observed multimodal activity in a small region of the mPa, a region thought to be the homologous in mammals of the amygdala (Wullimann and Mueller 2004; T. Aoki et al. 2013; Bartoszek et al. 2021). It has been reported that activity in the dHb is highly correlated with the activity in the mPa at resting state, and this network is modulated by external inputs coming from the OB, dampening their synchronous, spontaneous activity (Bartoszek et al. 2021). It is still unclear why this mechanism is in place, but with the present thesis, I have shown that this circuit generalizes across different sensory modalities.

8.5 The preoptic area as a homeostat in ectotherms

I investigated the potential role of the Preoptic Area (PoA) in thermoregulation in larval zebrafish, inspired by its critical role in maintaining stable body temperature in mammals (for a review see (Nakamura, Nakamura, and Kataoka 2022)) and its enrichment in context neurons (Figure 31a, b). Through bilateral ablation of the PoA, I observed a deficit in the test group's ability to reach thermal homeostasis, as they failed to adjust their reorientation probability based on sensory context compared to the control group (Figure 37).

The anatomy of the PoA in larval zebrafish is less understood compared to the dHb pathway (mOB-rHb-IPN-RN). It is known that the main targets of the OB are the rHb, Pa, Posterior Tuberculum and the Ventral Nucleus of the Ventral Telencephalon (Miyasaka et al. 2014), it still remains to be elucidated whether the PoA receives temperature information from the OB, Pa, or other structures such as the terminal nerve (I. Bianco and Wilson 2009), trigeminal, or dorsal root ganglion (Haesemeyer et al. 2018a).

These findings align with previous studies in larval zebrafish suggesting an involvement of the PoA in detecting temperature changes (Haesemeyer et al. 2018a) and responding to various physiological stressors in larval zebrafish (Wee et al. 2019; Lovett-Barron et al. 2020; Corradi et al. 2022). It also supports the idea that the PoA serves an evolutionarily conserved function in regulating body temperature across vertebrates (Figure 47). At the same time, my results expand upon these findings by proposing a role of the PoA in thermoregulation by evaluating the moment-to-moment sensory history in relation to the homeostatic setpoint and transmitting this information to the dHb to persist in the chosen motor program and achieve temperature homeostasis. The PoA acts similarly to a thermostat, using a feedback control mechanism. The specific mechanisms through which the PoA adapts to the physiology and nervous systems of different organisms remain to be understood. In mammals, which possess both autonomic and volitional strategies to cope with thermal stress, the PoA integrates peripheral and central temperature information to enhance thermogenesis and physical activity (Zhao et al. 2017; Tan and Knight 2018; Nakamura, Nakamura, and Kataoka 2022). In contrast, my findings provide evidence that the PoA in larval zebrafish directly triggers active navigation as an efficient homeostatic control mechanism in an organism lacking internal homeostatic mechanisms. These findings contribute to the growing understanding that the PoA, and the hypothalamus more broadly, can influence behavior at faster timescales than previously recognized (Lin et al. 2011; Lee et al. 2014; Füzesi et al. 2016; Barrios et al. 2020).

Further investigations could explore whether specific cell subtypes within the PoA are specifically involved in thermal navigation, similar to the findings in nocifensive behavior (Corradi et al. 2022), and elucidate the interplay between the PoA and the Hb-IPN-RN pathway.

Figure 47: The PoA as a "homeostat"

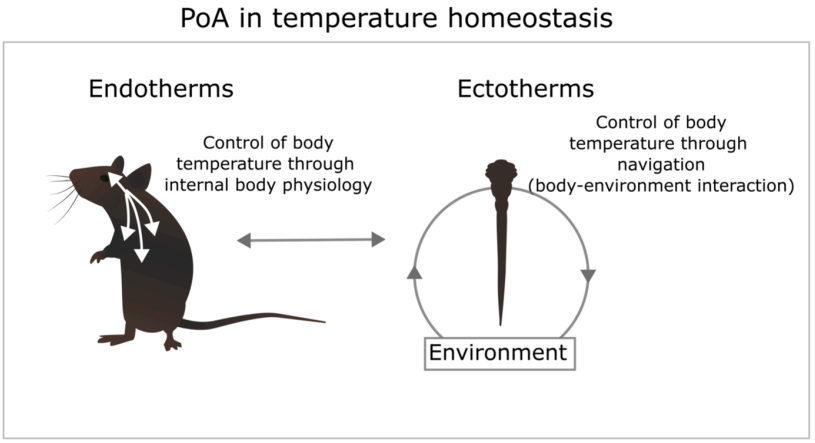

Figure 47: Comparison of the role of the PoA in endotherms vs ectotherms

8.6 The dorsal habenula as a hub for multimodal processing and storage of working memory in homeostatic navigation

In my imaging experiments, the right dorsal Hb (rdHb), along with a small region in the medial mOB and mPa, responded reliably to both increases in temperature and salinity with similar response profiles. These results align with previous reports highlighting the dHb's contribution to various sensory-driven navigation behaviors (Dreosti et al. 2014; Krishnan et al. 2014; Zhang et al. 2017; W.-Y. Chen et al. 2019; Choi et al. 2021). It is suggested that the dHb may provide a general estimate of environmental context to facilitate appropriate behavioral responses. The dHb was also the first station in the aforementioned pathway to exhibit context neurons and showed no modulation due to motor activity.

Contrary to my expectations, the ablation of the dHb did not impair the modulation of reorientation probability based on sensory context (i.e., ICxt and WCxt). However, the coherence in turn direction during WCxt was abolished. Additionally, I observed an impairment in short-term working memory.

These findings indicate that the dHb integrates contextual information over a longer timescale than a single movement and plays a role in the directional component of homeostatic navigation (i.e., left vs. right).

8.5.1 The Hb as an evolutionary conserved brain structure for processing aversive stimuli

In mammals the habenula is divided, by gene expression profiles and connectivity, in a lateral and a medial part. In more basal vertebrates such as fish, the same distinctive profiles define a dorsal and a ventral Hb (Namboodiri, Rodriguez-Romaguera, and Stuber 2016; Okamoto et al. 2021). Based on their efferent targets and transcriptome the dHb and vHb in fish correspond to the medial and lateral Hb in mammals respectively (Okamoto et al. 2021). The habenula is an interesting region for several reasons. First, it has connections with both the dopaminergic and serotonergic systems in mammals (Namboodiri, Rodriguez-Romaguera, and Stuber 2016). In fish, the dHb transmits information from the limbic forebrain to the interpeduncular nucleus (IPN), which projects to the serotonergic RN. While the vHb is directly linked to the median raphe (MRN). So far, a direct connection with dopaminergic nuclei has not been described in fish (Amo et al. 2010). Second, in basal vertebrates such as fish the Hb presents a clear asymmetry, both anatomical (left vs right) and functional, and it has been extensively studied to investigate lateralization in brain circuits (I. Bianco and Wilson 2009). Finally, the Hb is mostly glutamatergic but some neurons in the right dHb co-release acetylcholine. These cholinergic projections are specifically post-synaptically localized in the ventral IPN (Lima et al. 2017).

In mammals the lateral Hb has attracted a great deal of attention for its involvement in sleep, in value-based decision-making, in punishment avoidance and behavioral responses to stress (Hikosaka 2010). Less is known about the role of the medial Hb, mostly because of its proximity with the ventricle (Namboodiri, Rodriguez-Romaguera, and Stuber 2016). However, this region has been linked with nicotine addiction and, upon ablation, has been shown to mediate depression-like states and impaired behavioral responses to stressors (Hikosaka 2010; Namboodiri, Rodriguez-Romaguera, and Stuber 2016).

In adult and juvenile zebrafish, manipulations of the dHb-IPN pathway affect the ability to switch behavioral strategies in various learning tasks (Cherng et al. 2020; Palumbo et al. 2020) and have established a role in mediating social hierarchy by aggression and for experience-dependent expression of fear responses (Okamoto et al. 2021; 2021). In larvae, this same pathway mediates odor attraction (Krishnan et al. 2014; Choi et al. 2021), CO2 and salt avoidance (Koide, Yabuki, and Yoshihara 2018; Herrera et al. 2021), and phototaxis (Zhang et al. 2017). Previous studies have also suggested a role of the Hb in temperature sensing in larvae (Haesemeyer et al. 2018a). Additionally,

the dHb has been proposed as a multimodal trigger network associated with state transitions during foraging behavior (Marques et al. 2020).

In previous studies, the behavioral deficits observed following dHb ablation in taxis assays were interpreted as a shift in stimulus preference (Krishnan et al. 2014; Zhang et al. 2017; Choi et al. 2021), implying that the dHb conveys information about stimulus valence to a behavioral module. The apparent discrepancy between these conclusions and my findings can be reconciled by considering the differences in the stimulus landscape used and the amount of contextual information available to the animal in the arena. In this study, I propose that instead of absolute valence, the dHb conveys a contextual relative valence signal derived from the animal's recent past, which then modulates directional choices (Figure 48). This mechanism is particularly advantageous when the sensory landscape lacks sufficient contextual cues, such as in isothermal regions of shallow or slowly changing gradients or split field arenas (Zhang et al. 2017). The role of the dHb in homeostatic navigation may serve as a functional precursor to more complex cognitive abilities observed in the adult stage of zebrafish and in mammals, such as valence processing (Amo et al. 2014b), direction-based decision-making (Cherng et al. 2020) and strategy switching (Palumbo et al. 2020; Okamoto et al. 2021).

The observation that the Hb is present in virtually all vertebrate species and it has been linked with very different behaviors suggests an important role in survival. One prominent feature is that, regardless of the task or behavior, the Hb is always involved in processing aversive information, such as pain, stress and failure. In mammals it has been proposed that the Hb acts by suppressing motor activity (Hikosaka 2010). However, my results together with many other studies in adult, juvenile and larval zebrafish suggest that the dHb could also have a role in conveying a more abstract representation of the environmental conditions surrounding the animal and how they change over time to generate expectations about the world (Figure 48).

In future studies, it would be interesting to explore whether the dHb pathway actively participates in sensorimotor transformations or acts as a global modulator, potentially through the serotonergic system, influencing brain dynamics (Marques et al. 2020; Petrucco et al. 2023).

Figure 48: The dHb as a key player for sensorimotor transformations

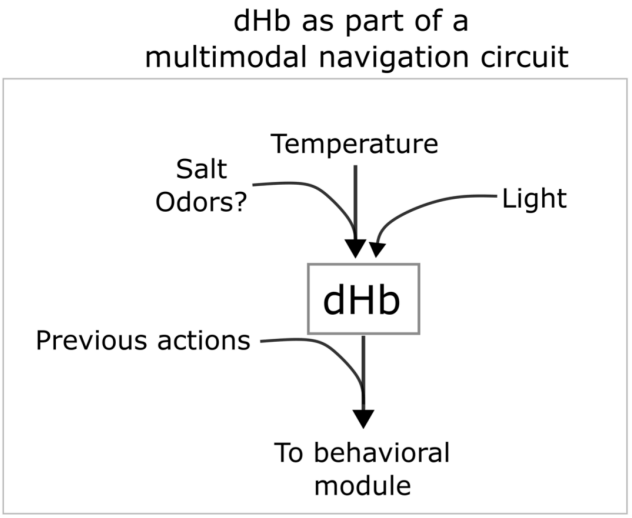

Figure 48: The dHb as a structure through which different homeostatic threats are funneled to generate a working memory able to robustly and flexibly drive homeostatic navigation

8.5.2 The IPN

The great majority of the context neurons highlighted by the imaging screen were localized in downstream areas of the Hb such as the IPN, aHB and RN. Those regions were also enriched with motor correlates. Eventually, the sensory representation of the stimulus change (i.e. the derivative) needs to instruct behavior. If the behavior was completely non-directional as in *C. elegans* one could speculate that the information from the context neurons can just suppress the activity of neurons controlling the turning rate when the conditions are improving and promote the activity in these cells when the conditions are worsening or vice versa. However, the finding that the behavioral strategy employed by the fish in homeostatic navigation has a directional component strongly supports the idea of a motor memory coupled with the sensory memory coming from the dHb. Previous studies from the Portugues laboratory have highlighted the IPN and the aHb as regions strongly correlated with fish motor activity (Dragomir, Štih, and Portugues 2020; Petrucco et al. 2023).

The IPN is mostly composed of a dense neuropil mesh, mostly consisting of the axons coming from the Hb through the Fasciculus Retroflexus, dendrites from the local interpeduncular neurons and descending fibers from the tegmentum above. Caudo-dorsally, neurons from the IPN and the MRN are not clearly anatomically separate. Moreover, in fish, the dorsal part of the IPN receives inputs from the left Hb while the ventral part is mostly targeted by the right Hb (Okamoto et al. 2021). These connections are also the ones co-releasing acetylcholine (E. Hong et al. 2013).

Observations from an electron microscopy dataset (Svara et al. 2022) have shown a high degree of compartmentalization in the ventral IPN where axons from local interneurons target the contralateral ventral IPN neuron and possibly inhibit the activity of the habenular axons through axo-axonic inhibition (Štih, Vilim 2021).Such organization is not visible for habenular afferents. Functionally speaking the activity in the ventral IPN is strongly correlated across pairs of glomeruli in the opposite hemispheres and it has been shown to respond to optic flow (Štih, Vilim 2021) and directional turning rate of fish (Dragomir, Štih, and Portugues 2020). Recently, it has also been reported that neurons from the aHb are functionally integrated in the dorsal IPN circuit and convey a signal of head direction (Petrucco et al. 2023). In my thesis I have shown that the IPN responds to different homeostatic threats - although with different dynamics- (Figure 35b), is enriched with context neurons and motor correlates. The fact that this structure is tracking both internal and external variables poses a challenge in pointing out a precise function. It is also particularly difficult to separate the individual contribution of the IPN from the Hb as the signal coming from the habenular axons is very prominent and ablations of the Hb partially disrupt activity in the IPN as well (Štih, Vilim 2021).

In future work it would be interesting to investigate whether the IPN is not involved in sensory or motor processing per se but it is rather coupling the relative valence of relevant homeostatic stimuli from the Hb, to actions that brought an improvement of conditions. It is also interesting to speculate that a parallel circuit involving the dorsal IPN could make this process more efficient by adding the information about the head direction and visual information.

8.5.3 The RN

Strikingly the IPN and the Hb project in fish, as in mammals, to the RN, which secrete serotonin. In this work I have shown that manipulating serotonin leads to a strong impairment in localizing the homeostatic setpoint (Figure 40).

Although this neurotransmitter has been discovered in humans more than 60 years ago (Rapport, Green, and Page 1948) its function remains elusive. Serotonin is a neuromodulator as its effects on the target neural circuits are usually spatially distributed and temporally extended (Doya 2002). In mammals, it modulates virtually all behavioral processes, besides having a very important role in

development (Gaspar, Cases, and Maroteaux 2003). Brainstem serotonin neurons send projections to cortical, limbic, midbrain and hindbrain regions. They widely modulate perception, memory, mood, stress responses, appetite, addiction and sexuality. Particularly in memory serotonin has been shown to modulate memory consolidation in the hippocampus acting on the sharp wave ripples (ul Haq et al. 2016; Shiozaki et al. 2023). Serotonergic neurons have also been implicated in motor control, circadian rhythms, body temperature and respiratory drive among others as well as contributing to the regulation of multiple organs in humans (for a review see (Berger, Gray, and Roth 2009)).

Although the broad effects on memory, behavior and physiology make it difficult to highlight a precise functional mechanism for serotonin, several independent lines of research provide interesting hypotheses. Serotonin is an evolutionarily conserved neuromodulator and it has maintained its role in memory. In an invertebrate model, it has recently been demonstrated that serotonin can facilitate a representation of different sensory modalities when learned together, leading to improved memory performance and a more robust and flexible representation of the environment (Okray et al. 2023).

In all taxa serotonergic neurons send and receive inputs from sensory systems, leading to a stimulus specific release of serotonin. An example is the chemo/mechanosensory neuron ADF in *C.elegans* (Iwanir et al. 2016; Liu et al. 2019; Shao et al. 2019). Serotonin can also control the gain of a sensory input; as it has been shown by enhancing the activation of interneurons suppressing odor-evoked activity in the olfactory bulb by applying broad-spectrum 5-HT receptor agonists (Petzold, Hagiwara, and Murthy 2009). Another conserved characteristic of serotonergic neurons is their involvement with internal states and behavioral output. Particularly, in behavioral strategy switching under different internal and external conditions such as deciding between exploration and exploitation in *C. elegans* and larval zebrafish (Flavell et al. 2013; Iwanir et al. 2016; Marques et al. 2020) and selecting different locomotor modes depending on the threat level in the surrounding environment (Seo et al. 2019).

To reconcile these different observations it has been proposed that, above all, serotonin acts as a global modulator by controlling how far into the future an animal looks to select the appropriate action based on the expected reward (Doya 2002). In other words, when an organism should persist in its current line of action or change its behavioral strategy. Another interesting hypothesis which, in a way, complements this idea states that serotonin helps organisms to learn and adapt to the statistics of their surrounding environment by reacting to unexpected changes (Matias et al. 2017).

Overall, most studies have focused on the sensory processing and modulation aspects of serotonin, rather than its role in shaping and instructing the selection of successful actions. In future research, it would be intriguing to investigate whether serotonergic neurons primarily influence the balance

between persisting in the current course of actions and changing behavioral strategy. For example, in the presence of intermittent sensory cues, with localized, sudden worsening of conditions, it would be interesting to explore whether the activation of serotonergic neurons affects the behavioral strategy employed to minimize homeostatic stress. Specifically, whether RN promotes the most successful behavioral sequences over time. Alternatively, serotonin may primarily act at the level of stimulus perception or directly impact different locomotion modes.

8.6 Final remarks

In conclusion, I would like to consider a potential role for homeostatic navigation in shaping brain evolution and function. A recent framework, grounded on biological findings, suggested that the brain did not evolve as an information-processing device, as Marr hypothesized in 1973, to perceive through sensors and then act. Instead, it evolved to maintain a state of relative equilibrium in its internal environment and processes, thereby preserving homeostasis (Buzsáki and Tingley 2023). This reframes the brain's purpose, suggesting that stimuli arriving from the environment to the brain aren't simply fed in the sensory input - decision-making processes - motor output chain. Instead, they support the animal in localizing favorable conditions to meet its internal needs: the real focus of the brain (Buzsáki and Tingley 2023). This view is supported by the evidence that eyes able to support image formation evolved after locomotion (Collin et al. 2009).

This hypothesis shifts our perception of the brain's purpose, from extracting a faithful representation of the external world - mainly through the eyes - , to selecting appropriate actions to reach internal homeostatic goals. It could also explain the observed asymmetry in the dHb responses to homeostatic threats versus visual inputs, as I discussed in Chapter 5 and in the Discussion. A failure in processing the relative changes in luminance is not life-threatening. However, failing to react to external or internal homeostatic threats is something an animal must quickly address using various strategies. Nevertheless, integrating visual inputs for supporting the computation of spatial primitives and cognitive maps is vital for making navigation more efficient. In this thesis, I have also presented evidence that, in an ectotherm, homeostatic threats converge onto the same circuit and may trigger the same motor output. These findings show a close relationship and a partial overlap in the processing of different homeostatic threats, a connection extensively described in mammals as well (e.g. (Nakamura, Nakamura, and Kataoka 2022).

In summary, over the course of evolution, the brain has developed the ability to perform environment-independent activities to serve cognition. However, even the most complex operations are rooted in the organism's action repertoire and homeostatic needs. Understanding how homeostatic navigation is orchestrated by the brain is, therefore, studying its most fundamental function.

8. Appendix

8.1 Abbreviations

PoA	Preoptic Area of the Hypothalamus
dHb	Dorsal Habenula
vHb	Ventral Habenula
BAT	Brown Adipose Tissue
DMH	Dorsomedial Hypothalamus
rMR	rostral Medullary Raphe region
WCxt	Worsening Context
ICxt	Improving Context
MB	Mushroom Body
DAN	Dopaminergic Neurons
OMR	Optomotor Response
OKR	Optokinetic Response
IPN	Interpeduncular Nucleus
TTA	Trial Triggered Average
PCA	Principal Component Analysis
ROI	Region of interest
mOB	Medial Olfactory bulb
aHb	Anterior Hindbrain
Pa	Pallium

mPa	medial Pallium
RN	Raphe Nuclei
MRN	Median Raphe
OT	Optic Tectum
dpf	days post fertilization
TL	Tüpfel Long Fin

8.2 Declaration of author contributions

Virginia Palieri, Ruben Portugues and Ilona C. Grunwald Kadow conceived the project and designed the experiments.

Virginia Palieri designed and built all the experimental setups for freely moving behavior, the preparation for drosophila imaging and the head-embedded system for homeostatic threats delivery under the lightsheet microscope. The latter with the help of Emanuele Paoli.

Virginia Palieri performed all the experiments on freely moving animals and analyzed the data with input from Emanuele Paoli.

Virginia Palieri performed the lightsheet experiments in drosophila and in fish. The latter with the help of Emanuele Paoli.

Emanuele Paoli analyzed and generated the plots for the whole-brain imaging dataset in fish with input from Virginia Palieri.

Virginia Palieri performed the chemogenetic ablations in fish with the help of Emanuele Paoli. Emanuele Paoli performed the experiments of laser ablations of the PoA with the help of Virginia Palieri.

9. References

Ahrens, Misha B., Jennifer M. Li, Michael B. Orger, Drew N. Robson, Alexander F. Schier, Florian Engert, and Ruben Portugues. 2012. “Brain-Wide Neuronal Dynamics during Motor Adaptation in Zebrafish.” *Nature* 485 (7399): 471–77. https://doi.org/10.1038/nature11057.

Ahrens, Misha B., Michael B. Orger, Drew N. Robson, Jennifer M. Li, and Philipp J. Keller. 2013. “Whole-Brain Functional Imaging at Cellular Resolution Using Light-Sheet Microscopy.” *Nature Methods* 10 (5): 413–20. https://doi.org/10.1038/nmeth.2434.

Alonso, Leandro M, and Eve Marder. 2020. “Temperature Compensation in a Small Rhythmic Circuit.” Edited by Frances K Skinner, Gary L Westbrook, Farzan Nadim, and Alexandre Guet-McCreight. *ELife* 9 (June): e55470. https://doi.org/10.7554/eLife.55470.

Amo, Ryunosuke, Hidenori Aizawa, Mikako Takahoko, Megumi Kobayashi, Rieko Takahashi, Tazu Aoki, and Hitoshi Okamoto. 2010. “Identification of the Zebrafish Ventral Habenula As a Homolog of the Mammalian Lateral Habenula.” *Journal of Neuroscience* 30 (4): 1566–74. https://doi.org/10.1523/JNEUROSCI.3690-09.2010.

Amo, Ryunosuke, Felipe Fredes, Masae Kinoshita, Ryo Aoki, Hidenori Aizawa, Masakazu Agetsuma, Tazu Aoki, et al. 2014a. “The Habenulo-Raphe Serotonergic Circuit Encodes an Aversive Expectation Value Essential for Adaptive Active Avoidance of Danger.” *Neuron* 84 (5): 1034–48. https://doi.org/10.1016/j.neuron.2014.10.035.

Aoki, Ichiro, and Ikue Mori. 2015. “Molecular Biology of Thermosensory Transduction in C. Elegans.” *Current Opinion in Neurobiology* 34 (October): 117–24. https://doi.org/10.1016/j.conb.2015.03.011.

Aoki, Tazu, Masae Kinoshita, Ryo Aoki, Masakazu Agetsuma, Hidenori Aizawa, Masako Yamazaki, Mikako Takahoko, et al. 2013. “Imaging of Neural Ensemble for the Retrieval of a Learned Behavioral Program.” *Neuron* 78 (5): 881–94. https://doi.org/10.1016/j.neuron.2013.04.009.

Aso, Yoshinori, Divya Sitaraman, Toshiharu Ichinose, Karla R Kaun, Katrin Vogt, Ghislain Belliart-Guérin, Pierre-Yves Plaçais, et al. 2014. “Mushroom Body Output Neurons Encode Valence and Guide Memory-Based Action Selection in Drosophila.” Edited by Liqun Luo. *ELife* 3 (December): e04580. https://doi.org/10.7554/eLife.04580.

Bang, Sunhoe, Seogang Hyun, Sung-Tae Hong, Jongkyun Kang, Kyunghwa Jeong, Joong-Jean Park, Joonho Choe, and Jongkyeong Chung. 2011. “Dopamine Signalling in Mushroom Bodies Regulates Temperature-Preference Behaviour in Drosophila.” *PLOS Genetics* 7 (3): e1001346. https://doi.org/10.1371/journal.pgen.1001346.

Barrios, Joshua P., Wei-Chun Wang, Roman England, Erica Reifenberg, and Adam D. Douglass. 2020. “Hypothalamic Dopamine Neurons Control Sensorimotor Behavior by Modulating

Brainstem Premotor Nuclei in Zebrafish." *Current Biology : CB* 30 (23): 4606-4618.e4. https://doi.org/10.1016/j.cub.2020.09.002.

Bartoszek, Ewelina Magdalena, Anna Maria Ostenrath, Suresh Kumar Jetti, Bram Serneels, Aytac Kadir Mutlu, Khac Thanh Phong Chau, and Emre Yaksi. 2021. "Ongoing Habenular Activity Is Driven by Forebrain Networks and Modulated by Olfactory Stimuli." *Current Biology* 31 (17): 3861-3874.e3. https://doi.org/10.1016/j.cub.2021.08.021.

Batchelder, Peg, Robert O. Kinney, Lori Demlow, and Carol B. Lynch. 1983. "Effects of Temperature and Social Interactions on Huddling Behavior in Mus Musculus." *Physiology & Behavior* 31 (1): 97–102. https://doi.org/10.1016/0031-9384(83)90102-6.

Berg, Howard C. 2000. "Motile Behavior of Bacteria." *Physics Today* 53 (1): 24–29. https://doi.org/10.1063/1.882934.

Berg, Howard C., and Douglas A. Brown. 1972. "Chemotaxis in Escherichia Coli Analysed by Three-Dimensional Tracking." *Nature* 239 (5374): 500–504. https://doi.org/10.1038/239500a0.

Bergemann, David, Laura Massoz, Jordane Bourdouxhe, Claudio A. Carril Pardo, Marianne L. Voz, Bernard Peers, and Isabelle Manfroid. 2018. "Nifurpirinol: A More Potent and Reliable Substrate Compared to Metronidazole for Nitroreductase-Mediated Cell Ablations." *Wound Repair and Regeneration: Official Publication of the Wound Healing Society [and] the European Tissue Repair Society* 26 (2): 238–44. https://doi.org/10.1111/wrr.12633.

Berger, Miles, John A. Gray, and Bryan L. Roth. 2009. "The Expanded Biology of Serotonin." *Annual Review of Medicine* 60: 355–66. https://doi.org/10.1146/annurev.med.60.042307.110802.

Berrigan, David, and David J. Pepin. 1995. "How Maggots Move: Allometry and Kinematics of Crawling in Larval Diptera." *Journal of Insect Physiology* 41 (4): 329–37. https://doi.org/10.1016/0022-1910(94)00113-U.

Bertotti, Giorgio. 1998. *Hysteresis in Magnetism*. Elsevier. https://doi.org/10.1016/B978-0-12-093270-2.X5048-X.

Bianco, Isaac H., Matthias Carl, Claire Russell, Jonathan DW Clarke, and Stephen W. Wilson. 2008. "Brain Asymmetry Is Encoded at the Level of Axon Terminal Morphology." *Neural Development* 3 (1): 9. https://doi.org/10.1186/1749-8104-3-9.

Bianco, Isaac, and Stephen Wilson. 2009. "The Habenular Nuclei: A Conserved Asymmetric Relay Station in the Vertebrate Brain." *Philosophical Transactions of the Royal Society of London. Series B, Biological Sciences* 364 (April): 1005–20. https://doi.org/10.1098/rstb.2008.0213.

Billman, George E. 2020. "Homeostasis: The Underappreciated and Far Too Often Ignored Central Organizing Principle of Physiology." *Frontiers in Physiology* 11 (March): 200. https://doi.org/10.3389/fphys.2020.00200.

Biron, David, Sara Wasserman, James H. Thomas, Aravinthan D. T. Samuel, and Piali Sengupta. 2008. "An Olfactory Neuron Responds Stochastically to Temperature and Modulates Caenorhabditis Elegans Thermotactic Behavior." *Proceedings of the National Academy of Sciences* 105 (31): 11002–7. https://doi.org/10.1073/pnas.0805004105.

Blessing, W. W., and E. Nalivaiko. 2001. “Raphe Magnus/Pallidus Neurons Regulate Tail but Not Mesenteric Arterial Blood Flow in Rats.” *Neuroscience* 105 (4): 923–29. https://doi.org/10.1016/s0306-4522(01)00251-2.

Budick, S.A., and D.M. O’Malley. 2000. “Locomotor Repertoire of the Larval Zebrafish: Swimming, Turning and Prey Capture.” *Journal of Experimental Biology* 203 (17): 2565–79. https://doi.org/10.1242/jeb.203.17.2565.

Buhl, Edgar, Benjamin Kottler, James J. L. Hodge, and Frank Hirth. 2021. “Thermoresponsive Motor Behavior Is Mediated by Ring Neuron Circuits in the Central Complex of Drosophila.” *Scientific Reports* 11 (January): 155. https://doi.org/10.1038/s41598-020-80103-9.

Buzsáki, György, and David Tingley. 2023. “Cognition from the Body-Brain Partnership: Exaptation of Memory.” *Annual Review of Neuroscience*, March. https://doi.org/10.1146/annurev-neuro-101222-110632.

Cannon, W. B. 1932. *The Wisdom of the Body*. The Wisdom of the Body. New York, NY, US: W W Norton & Co.

Cao, Wei Hua, and Shaun F. Morrison. 2003. “Disinhibition of Rostral Raphe Pallidus Neurons Increases Cardiac Sympathetic Nerve Activity and Heart Rate.” *Brain Research* 980 (1): 1–10. https://doi.org/10.1016/s0006-8993(03)02981-0.

Carlisle, H. J. 1966. “Behavioural Significance of Hypothalamic Temperature-Sensitive Cells.” *Nature* 209 (5030): 1324–25. https://doi.org/10.1038/2091324a0.

Carlisle, Harry J., and Mark L. Laudenslager. 1979. “Observations on the Thermoregulatory Effects of Preoptic Warming in Rats.” *Physiology & Behavior* 23 (4): 723–32. https://doi.org/10.1016/0031-9384(79)90166-5.

Carpenter, R. H. S. 2004. “Homeostasis: A Plea for a Unified Approach.” *Advances in Physiology Education* 28 (4): 180–87. https://doi.org/10.1152/advan.00012.2004.

Chen, Wei-Yu, Xiao-Lan Peng, Qiu-Sui Deng, Min-Jia Chen, Jiu-Lin Du, and Bai-Bing Zhang. 2019. “Role of Olfactorily Responsive Neurons in the Right Dorsal Habenula-Ventral Interpeduncular Nucleus Pathway in Food-Seeking Behaviors of Larval Zebrafish.” *Neuroscience* 404 (April): 259–67. https://doi.org/10.1016/j.neuroscience.2019.01.057.

Chen, Xiuye, and Florian Engert. 2014. “Navigational Strategies Underlying Phototaxis in Larval Zebrafish.” *Frontiers in Systems Neuroscience* 8. https://www.frontiersin.org/articles/10.3389/fnsys.2014.00039.

Cheng, Ruey-Kuang, Suresh J. Jesuthasan, and Trevor B. Penney. 2014. “Zebrafish Forebrain and Temporal Conditioning.” *Philosophical Transactions of the Royal Society B: Biological Sciences* 369 (1637): 20120462. https://doi.org/10.1098/rstb.2012.0462.

Cherng, Bor-Wei, Tanvir Islam, Makio Torigoe, Takashi Tsuboi, and Hitoshi Okamoto. 2020. “The Dorsal Lateral Habenula-Interpeduncular Nucleus Pathway Is Essential for Left-Right-Dependent Decision Making in Zebrafish.” *Cell Reports* 32 (11): 108143. https://doi.org/10.1016/j.celrep.2020.108143.

Choi, Jung-Hwa, Erik R. Duboue, Michelle Macurak, Jean-Michel Chanchu, and Marnie E. Halpern.

2021. “Specialized Neurons in the Right Habenula Mediate Response to Aversive Olfactory Cues.” https://elifesciences.org/articles/72345.

Cohn, Raphael, Ianessa Morantte, and Vanessa Ruta. 2015. “Coordinated and Compartmentalized Neuromodulation Shapes Sensory Processing in Drosophila.” *Cell* 163 (7): 1742–55. https://doi.org/10.1016/j.cell.2015.11.019.

Collin, Shaun P., Wayne L. Davies, Nathan S. Hart, and David M. Hunt. 2009. “The Evolution of Early Vertebrate Photoreceptors.” *Philosophical Transactions of the Royal Society B: Biological Sciences* 364 (1531): 2925–40. https://doi.org/10.1098/rstb.2009.0099.

Corradi, Laura, Matteo Bruzzone, Marco Dal Maschio, Suphansa Sawamiphak, and Alessandro Filosa. 2022. “Hypothalamic Galanin-Producing Neurons Regulate Stress in Zebrafish through a Peptidergic, Self-Inhibitory Loop.” *Current Biology: CB* 32 (7): 1497-1510.e5. https://doi.org/10.1016/j.cub.2022.02.011.

Costill, D L, and W J Fink. 1974. “Plasma Volume Changes Following Exercise and Thermal Dehydration.” *Journal of Applied Physiology* 37 (4): 521–25. https://doi.org/10.1152/jappl.1974.37.4.521.

Davies, Kelvin J. A. 2016. “Adaptive Homeostasis.” *Molecular Aspects of Medicine* 49 (June): 1–7. https://doi.org/10.1016/j.mam.2016.04.007.

Demir, Mahmut, and Hanna Salman. 2012. “Bacterial Thermotaxis by Speed Modulation.” *Biophysical Journal* 103 (8): 1683–90. https://doi.org/10.1016/j.bpj.2012.09.005.

DiMicco, Joseph A., and Dmitry V. Zaretsky. 2007. “The Dorsomedial Hypothalamus: A New Player in Thermoregulation.” *American Journal of Physiology-Regulatory, Integrative and Comparative Physiology* 292 (1): R47–63. https://doi.org/10.1152/ajpregu.00498.2006.

Doya, Kenji. 2002. “Metalearning and Neuromodulation.” *Neural Networks* 15 (4): 495–506. https://doi.org/10.1016/S0893-6080(02)00044-8.

Dragomir, Elena I., Vilim Štih, and Ruben Portugues. 2020. “Evidence Accumulation during a Sensorimotor Decision Task Revealed by Whole-Brain Imaging.” *Nature Neuroscience* 23 (1): 85–93. https://doi.org/10.1038/s41593-019-0535-8.

Dreosti, Elena, Nuria Vendrell Llopis, Matthias Carl, Emre Yaksi, and Stephen W. Wilson. 2014. “Left-Right Asymmetry Is Required for the Habenulae to Respond to Both Visual and Olfactory Stimuli.” *Current Biology* 24 (4): 440–45. https://doi.org/10.1016/j.cub.2014.01.016.

Duffy, Joseph B. 2002. “GAL4 System in Drosophila: A Fly Geneticist’s Swiss Army Knife.” *Genesis* 34 (1–2): 1–15. https://doi.org/10.1002/gene.10150.

Dunn, Timothy W, Yu Mu, Sujatha Narayan, Owen Randlett, Eva A Naumann, Chao-Tsung Yang, Alexander F Schier, Jeremy Freeman, Florian Engert, and Misha B Ahrens. 2016. “Brain-Wide Mapping of Neural Activity Controlling Zebrafish Exploratory Locomotion.” Edited by Ronald L Calabrese. *ELife* 5 (March): e12741. https://doi.org/10.7554/eLife.12741.

Easter, S. S., and G. N. Nicola. 1997. “The Development of Eye Movements in the Zebrafish (Danio Rerio).” *Developmental Psychobiology* 31 (4): 267–76.

https://doi.org/10.1002/(sici)1098-2302(199712)31:4<267::aid-dev4>3.0.co;2-p.

Falke, Joseph J., Randal B. Bass, Scott L. Butler, Stephen A. Chervitz, and Mark A. Danielson. 1997. "THE TWO-COMPONENT SIGNALING PATHWAY OF BACTERIAL CHEMOTAXIS: A Molecular View of Signal Transduction by Receptors, Kinases, and Adaptation Enzymes." *Annual Review of Cell and Developmental Biology* 13: 457–512. https://doi.org/10.1146/annurev.cellbio.13.1.457.

Fernández-Moreno, Miguel Angel, Carol L. Farr, Laurie S. Kaguni, and Rafael Garesse. 2007. "Drosophila Melanogaster as a Model System to Study Mitochondrial Biology." *Methods in Molecular Biology (Clifton, N.J.)* 372: 33–49. https://doi.org/10.1007/978-1-59745-365-3_3.

Flavell, Steven W., Navin Pokala, Evan Z. Macosko, Dirk R. Albrecht, Johannes Larsch, and Cornelia I. Bargmann. 2013. "Serotonin and the Neuropeptide PDF Initiate and Extend Opposing Behavioral States in C. Elegans." *Cell* 154 (5): 1023–35. https://doi.org/10.1016/j.cell.2013.08.001.

Fore, Stephanie, Francisca Acuña-Hinrichsen, Kadir Aytac Mutlu, Ewelina Magdalena Bartoszek, Bram Serneels, Nicholas Guy Faturos, Khac Thanh Phong Chau, et al. 2020. "Functional Properties of Habenular Neurons Are Determined by Developmental Stage and Sequential Neurogenesis." *Science Advances* 6 (36): eaaz3173. https://doi.org/10.1126/sciadv.aaz3173.

Frank, Dominic D., Genevieve C. Jouandet, Patrick J. Kearney, Lindsey J. Macpherson, and Marco Gallio. 2015. "Temperature Representation in the Drosophila Brain." *Nature* 519 (7543): 358–61. https://doi.org/10.1038/nature14284.

Füzesi, Tamás, Nuria Daviu, Jaclyn I. Wamsteeker Cusulin, Robert P. Bonin, and Jaideep S. Bains. 2016. "Hypothalamic CRH Neurons Orchestrate Complex Behaviours after Stress." *Nature Communications* 7 (1): 11937. https://doi.org/10.1038/ncomms11937.

Gale, C. C., M. Mathews, and J. Young. 1970. "Behavioral Thermoregulatory Responses to Hypothalamic Cooling and Warming in Baboons." *Physiology & Behavior* 5 (1): 1–6. https://doi.org/10.1016/0031-9384(70)90003-X.

Galili, Dana Shani, Kristina V. Dylla, Alja Lüdke, Anja B. Friedrich, Nobuhiro Yamagata, Jin Yan Hilary Wong, Chien Hsien Ho, Paul Szyszka, and Hiromu Tanimoto. 2014. "Converging Circuits Mediate Temperature and Shock Aversive Olfactory Conditioning in Drosophila." *Current Biology: CB* 24 (15): 1712–22. https://doi.org/10.1016/j.cub.2014.06.062.

Gallio, Marco, Tyler A. Ofstad, Lindsey J. Macpherson, Jing W. Wang, and Charles S. Zuker. 2011. "The Coding of Temperature in the Drosophila Brain." *Cell* 144 (4): 614–24. https://doi.org/10.1016/j.cell.2011.01.028.

Garrity, Paul A., Miriam B. Goodman, Aravinthan D. Samuel, and Piali Sengupta. 2010. "Running Hot and Cold: Behavioral Strategies, Neural Circuits, and the Molecular Machinery for Thermotaxis in C. Elegans and Drosophila." *Genes & Development* 24 (21): 2365–82. https://doi.org/10.1101/gad.1953710.

Gaspar, Patricia, Olivier Cases, and Luc Maroteaux. 2003. "The Developmental Role of Serotonin: News from Mouse Molecular Genetics." *Nature Reviews. Neuroscience* 4 (12): 1002–12. https://doi.org/10.1038/nrn1256.

Gau, Philia, Jason Poon, Carmen Ufret-Vincenty, Corey D. Snelson, Sharona E. Gordon, David W. Raible, and Ajay Dhaka. 2013. “The Zebrafish Ortholog of TRPV1 Is Required for Heat-Induced Locomotion.” *The Journal of Neuroscience* 33 (12): 5249–60. https://doi.org/10.1523/JNEUROSCI.5403-12.2013.

Giraldo, Ysabel Milton, Katherine J. Leitch, Ivo G. Ros, Timothy L. Warren, Peter T. Weir, and Michael H. Dickinson. 2018. “Sun Navigation Requires Compass Neurons in Drosophila.” *Current Biology* 28 (17): 2845-2852.e4. https://doi.org/10.1016/j.cub.2018.07.002.

Gire, David H., Vikrant Kapoor, Annie Arrighi-Allisan, Agnese Seminara, and Venkatesh N. Murthy. 2016. “Mice Develop Efficient Strategies for Foraging and Navigation Using Complex Natural Stimuli.” *Current Biology* 26 (10): 1261–73. https://doi.org/10.1016/j.cub.2016.03.040.

Glauser, Dominique A. 2013. “How and Why *Caenorhabditis elegans* Uses Distinct Escape and Avoidance Regimes to Minimize Exposure to Noxious Heat.” *Worm* 2 (4): e27285. https://doi.org/10.4161/worm.27285.

Gomez-Marin, Alex, and Matthieu Louis. 2012. “Active Sensation during Orientation Behavior in the Drosophila Larva: More Sense than Luck.” *Current Opinion in Neurobiology*, Neuroethology, 22 (2): 208–15. https://doi.org/10.1016/j.conb.2011.11.008.

Goodman, Lester. 1980. “Regulation and Control in Physiological Systms: 1960–1980.” *Annals of Biomedical Engineering* 8 (4): 281–90. https://doi.org/10.1007/BF02363432.

Green, Jonathan, Vikram Vijayan, Peter Mussells Pires, Atsuko Adachi, and Gaby Maimon. 2019. “A Neural Heading Estimate Is Compared with an Internal Goal to Guide Oriented Navigation.” *Nature Neuroscience* 22 (9): 1460–68. https://doi.org/10.1038/s41593-019-0444-x.

Haberkern, Hannah, Melanie A. Basnak, Biafra Ahanonu, David Schauder, Jeremy D. Cohen, Mark Bolstad, Christopher Bruns, and Vivek Jayaraman. 2019. “Visually Guided Behavior and Optogenetically Induced Learning in Head-Fixed Flies Exploring a Virtual Landscape.” *Current Biology* 29 (10): 1647-1659.e8. https://doi.org/10.1016/j.cub.2019.04.033.

Haesemeyer, Martin, Drew N. Robson, Jennifer M. Li, Alexander F. Schier, and Florian Engert. 2015. “The Structure and Timescales of Heat Perception in Larval Zebrafish.” *Cell Systems* 1 (5): 338–48. https://doi.org/10.1016/j.cels.2015.10.010.

Haesemeyer, Martin, Drew N. Robson, Jennifer M. Li, Alexander F. Schier, and Florian Engert. 2018a. “A Brain-Wide Circuit Model of Heat-Evoked Swimming Behavior in Larval Zebrafish.” *Neuron* 98 (4): 817-831.e6. https://doi.org/10.1016/j.neuron.2018.04.013.

Haq, Rizwan ul, Marlene L. Anderson, Jan-Oliver Hollnagel, Franziska Worschech, Muhammad Azahr Sherkheli, Christoph J. Behrens, and Uwe Heinemann. 2016. “Serotonin Dependent Masking of Hippocampal Sharp Wave Ripples.” *Neuropharmacology* 101 (February): 188–203. https://doi.org/10.1016/j.neuropharm.2015.09.026.

Harris, Charles R., K. Jarrod Millman, Stéfan J. van der Walt, Ralf Gommers, Pauli Virtanen, David Cournapeau, Eric Wieser, et al. 2020. “Array Programming with NumPy.” *Nature* 585 (7825): 357–62. https://doi.org/10.1038/s41586-020-2649-2.

Hedgecock, E M, and R L Russell. 1975. “Normal and Mutant Thermotaxis in the Nematode Caenorhabditis Elegans.” *Proceedings of the National Academy of Sciences of the United States of America* 72 (10): 4061–65.

Herrera, Kristian J., Thomas Panier, Drago Guggiana-Nilo, and Florian Engert. 2021. “Larval Zebrafish Use Olfactory Detection of Sodium and Chloride to Avoid Salt Water.” *Current Biology* 31 (4): 782-793.e3. https://doi.org/10.1016/j.cub.2020.11.051.

Hikosaka, Okihide. 2010. “The Habenula: From Stress Evasion to Value-Based Decision-Making.” *Nature Reviews. Neuroscience* 11 (7): 503–13. https://doi.org/10.1038/nrn2866.

Hong, Elim, Kirankumar Santhakumar, Courtney A. Akitake, Sang Jung Ahn, Christine Thisse, Bernard Thisse, Claire Wyart, Jean-Marie Mangin, and Marnie E. Halpern. 2013. “Cholinergic Left-Right Asymmetry in the Habenulo-Interpeduncular Pathway.” *Proceedings of the National Academy of Sciences* 110 (52): 21171–76. https://doi.org/10.1073/pnas.1319566110.

Hong, Sung-Tae, Sunhoe Bang, Seogang Hyun, Jongkyun Kang, Kyunghwa Jeong, Donggi Paik, Jongkyeong Chung, and Jaeseob Kim. 2008. “CAMP Signalling in Mushroom Bodies Modulates Temperature Preference Behaviour in Drosophila.” *Nature* 454 (7205): 771–75. https://doi.org/10.1038/nature07090.

Houtz, Jessica, Guey-Ying Liao, Juan Ji An, and Baoji Xu. 2021. “Discrete TrkB-Expressing Neurons of the Dorsomedial Hypothalamus Regulate Feeding and Thermogenesis.” *Proceedings of the National Academy of Sciences of the United States of America* 118 (4): e2017218118. https://doi.org/10.1073/pnas.2017218118.

Huang, Kuo-Hua, Misha B. Ahrens, Timothy W. Dunn, and Florian Engert. 2013. “Spinal Projection Neurons Control Turning Behaviors in Zebrafish.” *Current Biology: CB* 23 (16): 1566–73. https://doi.org/10.1016/j.cub.2013.06.044.

Hulse, Brad K., Hannah Haberkern, Romain Franconville, Daniel Turner-Evans, Shin-Ya Takemura, Tanya Wolff, Marcella Noorman, et al. 2021. “A Connectome of the Drosophila Central Complex Reveals Network Motifs Suitable for Flexible Navigation and Context-Dependent Action Selection.” *ELife* 10 (October): e66039. https://doi.org/10.7554/eLife.66039.

Hunter, John D. 2007. “Matplotlib: A 2D Graphics Environment.” *Computing in Science & Engineering* 9 (3): 90–95. https://doi.org/10.1109/MCSE.2007.55.

Iino, Yuichi, and Kazushi Yoshida. 2009. “Parallel Use of Two Behavioral Mechanisms for Chemotaxis in Caenorhabditis Elegans.” *The Journal of Neuroscience* 29 (17): 5370–80. https://doi.org/10.1523/JNEUROSCI.3633-08.2009.

Inoue, Takeshi, Taiga Yamashita, and Kiyokazu Agata. 2014. “Thermosensory Signaling by TRPM Is Processed by Brain Serotonergic Neurons to Produce Planarian Thermotaxis.” *Journal of Neuroscience* 34 (47): 15701–14. https://doi.org/10.1523/JNEUROSCI.5379-13.2014.

Iwanir, Shachar, Adam S. Brown, Stanislav Nagy, Dana Najjar, Alexander Kazakov, Kyung Suk Lee, Alon Zaslaver, Erel Levine, and David Biron. 2016. “Serotonin Promotes Exploitation in Complex Environments by Accelerating Decision-Making.” *BMC Biology* 14 (February): 9. https://doi.org/10.1186/s12915-016-0232-y.

Jetti, Suresh Kumar, Nuria Vendrell-Llopis, and Emre Yaksi. 2014. “Spontaneous Activity Governs Olfactory Representations in Spatially Organized Habenular Microcircuits.” *Current Biology* 24 (4): 434–39. https://doi.org/10.1016/j.cub.2014.01.015.

Jurado, P., E. Kodama, Y. Tanizawa, and I. Mori. 2010. “Distinct Thermal Migration Behaviors in Response to Different Thermal Gradients in Caenorhabditis Elegans.” *Genes, Brain, and Behavior* 9 (1): 120–27. https://doi.org/10.1111/j.1601-183X.2009.00549.x.

Kawashima, Takashi, Maarten F. Zwart, Chao-Tsung Yang, Brett D. Mensh, and Misha B. Ahrens. 2016. “The Serotonergic System Tracks the Outcomes of Actions to Mediate Short-Term Motor Learning.” *Cell* 167 (4): 933-946.e20. https://doi.org/10.1016/j.cell.2016.09.055.

Kermen, Florence, Luis M. Franco, Cameron Wyatt, and Emre Yaksi. 2013. “Neural Circuits Mediating Olfactory-Driven Behavior in Fish.” *Frontiers in Neural Circuits* 7 (April): 62. https://doi.org/10.3389/fncir.2013.00062.

Kerr, Jason N. D., and Winfried Denk. 2008. “Imaging in Vivo: Watching the Brain in Action.” *Nature Reviews. Neuroscience* 9 (3): 195–205. https://doi.org/10.1038/nrn2338.

Kimura, Koutarou D., Atsushi Miyawaki, Kunihiro Matsumoto, and Ikue Mori. 2004. “The C. Elegans Thermosensory Neuron AFD Responds to Warming.” *Current Biology: CB* 14 (14): 1291–95. https://doi.org/10.1016/j.cub.2004.06.060.

Kist, Andreas M., and Ruben Portugues. 2019. “Optomotor Swimming in Larval Zebrafish Is Driven by Global Whole-Field Visual Motion and Local Light-Dark Transitions.” *Cell Reports* 29 (3): 659-670.e3. https://doi.org/10.1016/j.celrep.2019.09.024.

Kludt, Eugen, Camille Okom, Alexander Brinkmann, and Detlev Schild. 2015. “Integrating Temperature with Odor Processing in the Olfactory Bulb.” *The Journal of Neuroscience* 35 (20): 7892–7902. https://doi.org/10.1523/JNEUROSCI.0571-15.2015.

Knogler, Laura D, Andreas M Kist, and Ruben Portugues. 2019. “Motor Context Dominates Output from Purkinje Cell Functional Regions during Reflexive Visuomotor Behaviours.” Edited by Indira M Raman, Ronald L Calabrese, Eva Naumann, and David L McLean. *ELife* 8 (January): e42138. https://doi.org/10.7554/eLife.42138.

Koide, Tetsuya, Yoichi Yabuki, and Yoshihiro Yoshihara. 2018. “Terminal Nerve GnRH3 Neurons Mediate Slow Avoidance of Carbon Dioxide in Larval Zebrafish.” *Cell Reports* 22 (5): 1115–23. https://doi.org/10.1016/j.celrep.2018.01.019.

Krishnan, Seetha, Ajay S. Mathuru, Caroline Kibat, Mashiur Rahman, Charlotte E. Lupton, Jim Stewart, Adam Claridge-Chang, Shih-Cheng Yen, and Suresh Jesuthasan. 2014. “The Right Dorsal Habenula Limits Attraction to an Odor in Zebrafish.” *Current Biology* 24 (11): 1167–75. https://doi.org/10.1016/j.cub.2014.03.073.

Kuhara, Atsushi, Masatoshi Okumura, Tsubasa Kimata, Yoshinori Tanizawa, Ryo Takano, Koutarou D. Kimura, Hitoshi Inada, Kunihiro Matsumoto, and Ikue Mori. 2008. “Temperature Sensing by an Olfactory Neuron in a Circuit Controlling Behavior of C. Elegans.” *Science (New York, N.Y.)* 320 (5877): 803–7. https://doi.org/10.1126/science.1148922.

Kunst, Michael, Eva Laurell, Nouwar Mokayes, Anna Kramer, Fumi Kubo, António M. Fernandes,

Dominique Förster, Marco Dal Maschio, and Herwig Baier. 2019. “A Cellular-Resolution Atlas of the Larval Zebrafish Brain.” *Neuron* 103 (1): 21-38.e5. https://doi.org/10.1016/j.neuron.2019.04.034.

Larsch, Johannes, Steven W. Flavell, Qiang Liu, Andrew Gordus, Dirk R. Albrecht, and Cornelia I. Bargmann. 2015. “A Circuit for Gradient Climbing in C. Elegans Chemotaxis.” *Cell Reports* 12 (11): 1748–60. https://doi.org/10.1016/j.celrep.2015.08.032.

Laudenslager, M. L. 1976. “Proportional Hypothalamic Control of Behavioral Thermoregulation in the Squirrel Monkey.” *Physiology & Behavior* 17 (3): 383–90. https://doi.org/10.1016/0031-9384(76)90095-0.

Le Goc, Guillaume, Julie Lafaye, Sophia Karpenko, Volker Bormuth, Raphaël Candelier, and Georges Debrégeas. 2021. “Thermal Modulation of Zebrafish Exploratory Statistics Reveals Constraints on Individual Behavioral Variability.” *BMC Biology* 19 (1): 208. https://doi.org/10.1186/s12915-021-01126-w.

Lee, Hyosang, Dong-Wook Kim, Ryan Remedios, Todd E. Anthony, Angela Chang, Linda Madisen, Hongkui Zeng, and David J. Anderson. 2014. “Scalable Control of Mounting and Attack by Esr1+ Neurons in the Ventromedial Hypothalamus.” *Nature* 509 (7502): 627–32. https://doi.org/10.1038/nature13169.

Lewis, Laurence P. C., K. P. Siju, Yoshinori Aso, Anja B. Friedrich, Alexander J. B. Bulteel, Gerald M. Rubin, and Ilona C. Grunwald Kadow. 2015. “A Higher Brain Circuit for Immediate Integration of Conflicting Sensory Information in Drosophila.” *Current Biology: CB* 25 (17): 2203–14. https://doi.org/10.1016/j.cub.2015.07.015.

Li, Yinxia, Yunli Zhao, Xu Huang, Xingfeng Lin, Yuling Guo, Daoyong Wang, Chaojun Li, and Dayong Wang. 2013. “Serotonin Control of Thermotaxis Memory Behavior in Nematode Caenorhabditis Elegans.” *PLOS ONE* 8 (11): e77779. https://doi.org/10.1371/journal.pone.0077779.

Liang, Xitong, Timothy E. Holy, and Paul H. Taghert. 2016. “Synchronous Drosophila Circadian Pacemakers Display Nonsynchronous Ca2+ Rhythms in Vivo.” *Science* 351 (6276): 976–81. https://doi.org/10.1126/science.aad3997.

Lillesaar, Christina, Christian Stigloher, Birgit Tannhäuser, Mario F. Wullimann, and Laure Bally-Cuif. 2009. “Axonal Projections Originating from Raphe Serotonergic Neurons in the Developing and Adult Zebrafish, Danio Rerio, Using Transgenics to Visualize Raphe-Specific Pet1 Expression.” *The Journal of Comparative Neurology* 512 (2): 158–82. https://doi.org/10.1002/cne.21887.

Lima, Leandro B., Debora Bueno, Fernanda Leite, Stefani Souza, Luciano Gonçalves, Isadora C. Furigo, Jose Donato, and Martin Metzger. 2017. “Afferent and Efferent Connections of the Interpeduncular Nucleus with Special Reference to Circuits Involving the Habenula and Raphe Nuclei.” *The Journal of Comparative Neurology* 525 (10): 2411–42. https://doi.org/10.1002/cne.24217.

Lin, Dayu, Maureen P. Boyle, Piotr Dollar, Hyosang Lee, E. S. Lein, Pietro Perona, and David J. Anderson. 2011. “Functional Identification of an Aggression Locus in the Mouse Hypothalamus.” *Nature* 470 (7333): 221–26. https://doi.org/10.1038/nature09736.

Liu, Hui, Li-Wei Qin, Rong Li, Ce Zhang, Umar Al-Sheikh, and Zheng-Xing Wu. 2019. “Reciprocal Modulation of 5-HT and Octopamine Regulates Pumping via Feedforward and Feedback Circuits in C. Elegans.” *Proceedings of the National Academy of Sciences* 116 (14): 7107–12. https://doi.org/10.1073/pnas.1819261116.

Lovett-Barron, Matthew, Ritchie Chen, Susanna Bradbury, Aaron S. Andalman, Mahendra Wagle, Su Guo, and Karl Deisseroth. 2020. “Multiple Convergent Hypothalamus-Brainstem Circuits Drive Defensive Behavior.” *Nature Neuroscience* 23 (8): 959–67. https://doi.org/10.1038/s41593-020-0655-1.

Luo, Linjiao, Marc Gershow, Mark Rosenzweig, KyeongJin Kang, Christopher Fang-Yen, Paul A. Garrity, and Aravinthan D. T. Samuel. 2010. “Navigational Decision Making in Drosophila Thermotaxis.” *The Journal of Neuroscience* 30 (12): 4261–72. https://doi.org/10.1523/JNEUROSCI.4090-09.2010.

Luo, Linjiao, Quan Wen, Jing Ren, Michael Hendricks, Marc Gershow, Yuqi Qin, Joel Greenwood, et al. 2014. “Dynamic Encoding of Perception, Memory, and Movement in a C. Elegans Chemotaxis Circuit.” *Neuron* 82 (5): 1115–28. https://doi.org/10.1016/j.neuron.2014.05.010.

Markov, Daniil A., Luigi Petrucco, Andreas M. Kist, and Ruben Portugues. 2021. “A Cerebellar Internal Model Calibrates a Feedback Controller Involved in Sensorimotor Control.” *Nature Communications* 12 (1): 6694. https://doi.org/10.1038/s41467-021-26988-0.

Marques, João C., Meng Li, Diane Schaak, Drew N. Robson, and Jennifer M. Li. 2020. “Internal State Dynamics Shape Brainwide Activity and Foraging Behaviour.” *Nature* 577 (7789): 239–43. https://doi.org/10.1038/s41586-019-1858-z.

Mathis, Alexander, Pranav Mamidanna, Kevin M. Cury, Taiga Abe, Venkatesh N. Murthy, Mackenzie Weygandt Mathis, and Matthias Bethge. 2018. “DeepLabCut: Markerless Pose Estimation of User-Defined Body Parts with Deep Learning.” *Nature Neuroscience* 21 (9): 1281–89. https://doi.org/10.1038/s41593-018-0209-y.

Matias, Sara, Eran Lottem, Guillaume P Dugué, and Zachary F Mainen. 2017. “Activity Patterns of Serotonin Neurons Underlying Cognitive Flexibility.” *ELife* 6 (March): e20552. https://doi.org/10.7554/eLife.20552.

McLean, David L., and Joseph R. Fetcho. 2004. “Ontogeny and Innervation Patterns of Dopaminergic, Noradrenergic, and Serotonergic Neurons in Larval Zebrafish.” *Journal of Comparative Neurology* 480 (1): 38–56. https://doi.org/10.1002/cne.20280.

Mesarović, Mihajlo D. 1964. *Views on General Systems Theory: Proceedings*. J. Wiley.

Miyasaka, Nobuhiko, Ignacio Arganda-Carreras, Noriko Wakisaka, Miwa Masuda, Uygar Sümbül, H. Sebastian Seung, and Yoshihiro Yoshihara. 2014. “Olfactory Projectome in the Zebrafish Forebrain Revealed by Genetic Single-Neuron Labelling.” *Nature Communications* 5 (1): 3639. https://doi.org/10.1038/ncomms4639.

Miyasaka, Nobuhiko, Kozo Morimoto, Tatsuya Tsubokawa, Shin-ichi Higashijima, Hitoshi Okamoto, and Yoshihiro Yoshihara. 2009. “From the Olfactory Bulb to Higher Brain Centers: Genetic Visualization of Secondary Olfactory Pathways in Zebrafish.” *The Journal of Neuroscience: The Official Journal of the Society for Neuroscience* 29 (15): 4756–67.

https://doi.org/10.1523/JNEUROSCI.0118-09.2009.

Mołoń, Mateusz, Jan Dampc, Monika Kula-Maximenko, Jacek Zebrowski, Agnieszka Mołoń, Ralph Dobler, Roma Durak, and Andrzej Skoczowski. 2020. “Effects of Temperature on Lifespan of Drosophila Melanogaster from Different Genetic Backgrounds: Links between Metabolic Rate and Longevity.” *Insects* 11 (8): 470. https://doi.org/10.3390/insects11080470.

Morgan, T. H. 1910. “SEX LIMITED INHERITANCE IN DROSOPHILA.” *Science (New York, N.Y.)* 32 (812): 120–22. https://doi.org/10.1126/science.32.812.120.

Mori, Ikue, Hiroyuki Sasakura, and Atsushi Kuhara. 2007. “Worm Thermotaxis: A Model System for Analyzing Thermosensation and Neural Plasticity.” *Current Opinion in Neurobiology*, Motor systems / Neurobiology of behaviour, 17 (6): 712–19. https://doi.org/10.1016/j.conb.2007.11.010.

Morrison, S. F., A. F. Sved, and A. M. Passerin. 1999. “GABA-Mediated Inhibition of Raphe Pallidus Neurons Regulates Sympathetic Outflow to Brown Adipose Tissue.” *The American Journal of Physiology* 276 (2): R290-297. https://doi.org/10.1152/ajpregu.1999.276.2.R290.

Mueller, Dr Thomas, and Mario Wullimann. 2015. *Atlas of Early Zebrafish Brain Development: A Tool for Molecular Neurogenetics*. Academic Press.

Nagashima, Kei, Sadamu Nakai, Mutsumi Tanaka, and Kazuyuki Kanosue. 2000. “Neuronal Circuitries Involved in Thermoregulation.” *Autonomic Neuroscience*, Fever:the role of the vagus nerve, 85 (1): 18–25. https://doi.org/10.1016/S1566-0702(00)00216-2.

Nakamura, Kazuhiro, Kiyoshi Matsumura, Shigeo Kobayashi, and Takeshi Kaneko. 2005. “Sympathetic Premotor Neurons Mediating Thermoregulatory Functions.” *Neuroscience Research* 51 (1): 1–8. https://doi.org/10.1016/j.neures.2004.09.007.

Nakamura, Kazuhiro, and Shaun F. Morrison. 2011. “Central Efferent Pathways for Cold-Defensive and Febrile Shivering.” *The Journal of Physiology* 589 (Pt 14): 3641–58. https://doi.org/10.1113/jphysiol.2011.210047.

Nakamura, Kazuhiro, Yoshiko Nakamura, and Naoya Kataoka. 2022. “A Hypothalamomedullary Network for Physiological Responses to Environmental Stresses.” *Nature Reviews Neuroscience* 23 (1): 35–52. https://doi.org/10.1038/s41583-021-00532-x.

Namboodiri, Vijay Mohan K., Jose Rodriguez-Romaguera, and Garret D. Stuber. 2016. “The Habenula.” *Current Biology* 26 (19): R873–77. https://doi.org/10.1016/j.cub.2016.08.051.

Nason, Malcolm W., and Peggy Mason. 2004. “Modulation of Sympathetic and Somatomotor Function by the Ventromedial Medulla.” *Journal of Neurophysiology* 92 (1): 510–22. https://doi.org/10.1152/jn.00089.2004.

Nath, Tanmay, Alexander Mathis, An Chi Chen, Amir Patel, Matthias Bethge, and Mackenzie Weygandt Mathis. 2019. “Using DeepLabCut for 3D Markerless Pose Estimation across Species and Behaviors.” *Nature Protocols* 14 (7): 2152–76. https://doi.org/10.1038/s41596-019-0176-0.

Okamoto, Hitoshi, Bor-Wei Cherng, Haruna Nakajo, Ming-Yi Chou, and Masae Kinoshita. 2021. “Habenula as the Experience-Dependent Controlling Switchboard of Behavior and Attention

in Social Conflict and Learning." *Current Opinion in Neurobiology* 68: 36–43. https://doi.org/10.1016/j.conb.2020.12.005.

Okray, Zeynep, Pedro F. Jacob, Ciara Stern, Kieran Desmond, Nils Otto, Clifford B. Talbot, Paola Vargas-Gutierrez, and Scott Waddell. 2023. "Multisensory Learning Binds Neurons into a Cross-Modal Memory Engram." *Nature* 617 (7962): 777–84. https://doi.org/10.1038/s41586-023-06013-8.

Orger, Michael B., Adam R. Kampff, Kristen E. Severi, Johann H. Bollmann, and Florian Engert. 2008. "Control of Visually Guided Behavior by Distinct Populations of Spinal Projection Neurons." *Nature Neuroscience* 11 (3): 327–33. https://doi.org/10.1038/nn2048.

Oteiza, Pablo, Iris Odstrcil, George Lauder, Ruben Portugues, and Florian Engert. 2017. "A Novel Mechanism for Mechanosensory-Based Rheotaxis in Larval Zebrafish." *Nature* 547 (7664): 445–48. https://doi.org/10.1038/nature23014.

Owald, David, Johannes Felsenberg, Clifford B. Talbot, Gaurav Das, Emmanuel Perisse, Wolf Huetteroth, and Scott Waddell. 2015. "Activity of Defined Mushroom Body Output Neurons Underlies Learned Olfactory Behavior in Drosophila." *Neuron* 86 (2): 417–27. https://doi.org/10.1016/j.neuron.2015.03.025.

Owald, David, and Scott Waddell. 2015. "Olfactory Learning Skews Mushroom Body Output Pathways to Steer Behavioral Choice in Drosophila." *Current Opinion in Neurobiology* 35 (December): 178–84. https://doi.org/10.1016/j.conb.2015.10.002.

Palumbo, Fabrizio, Bram Serneels, Robbrecht Pelgrims, and Emre Yaksi. 2020. "The Zebrafish Dorsolateral Habenula Is Required for Updating Learned Behaviors." *Cell Reports* 32 (8): 108054. https://doi.org/10.1016/j.celrep.2020.108054.

Panier, Thomas, Sebastian Romano, Raphaël Olive, Thomas Pietri, German Sumbre, Raphaël Candelier, and Georges Debrégeas. 2013. "Fast Functional Imaging of Multiple Brain Regions in Intact Zebrafish Larvae Using Selective Plane Illumination Microscopy." *Frontiers in Neural Circuits* 7. https://www.frontiersin.org/articles/10.3389/fncir.2013.00065.

Paricio-Montesinos, Ricardo, Frederick Schwaller, Annapoorani Udhayachandran, Florian Rau, Jan Walcher, Roberta Evangelista, Joris Vriens, Thomas Voets, James F. A. Poulet, and Gary R. Lewin. 2020. "The Sensory Coding of Warm Perception." *Neuron* 106 (5): 830-841.e3. https://doi.org/10.1016/j.neuron.2020.02.035.

Pedregosa, Fabian, Gaël Varoquaux, Alexandre Gramfort, Vincent Michel, Bertrand Thirion, Olivier Grisel, Mathieu Blondel, et al. 2012. "Scikit-Learn: Machine Learning in Python." https://doi.org/10.48550/ARXIV.1201.0490.

Petrucco, Luigi, Hagar Lavian, You Kure Wu, Fabian Svara, Vilim Štih, and Ruben Portugues. 2023. "Neural Dynamics and Architecture of the Heading Direction Circuit in Zebrafish." *Nature Neuroscience* 26 (5): 765–73. https://doi.org/10.1038/s41593-023-01308-5.

Portugues, Ruben, and Florian Engert. 2011. "Adaptive Locomotor Behavior in Larval Zebrafish." *Frontiers in Systems Neuroscience* 5. https://www.frontiersin.org/articles/10.3389/fnsys.2011.00072.

Portugues, Ruben, Kristen E Severi, Claire Wyart, and Misha B Ahrens. 2013. “Optogenetics in a Transparent Animal: Circuit Function in the Larval Zebrafish.” *Current Opinion in Neurobiology*, Neurogenetics, 23 (1): 119–26. https://doi.org/10.1016/j.conb.2012.11.001.

Prat, Ot, Luigi Petrucco, Vilim Štih, and Ruben Portugues. 2022. “Comparing the Representation of a Simple Visual Stimulus across the Cerebellar Network.” Preprint. Neuroscience. https://doi.org/10.1101/2022.09.12.507660.

Rapport, M. M., A. A. Green, and I. H. Page. 1948. “Serum Vasoconstrictor, Serotonin; Isolation and Characterization.” *The Journal of Biological Chemistry* 176 (3): 1243–51.

Reback, Jeff, Wes McKinney, Jbrockmendel, Joris Van Den Bossche, Tom Augspurger, Phillip Cloud, Gfyoung, et al. 2020. “Pandas-Dev/Pandas: Pandas 1.1.3.” Zenodo. https://zenodo.org/record/4067057.

Robson, Drew N. 2013. “Thermal Navigation in Larval Zebrafish.” In . https://www.semanticscholar.org/paper/Thermal-navigation-in-larval-zebrafish-Robson/36c1580be9de0d3ce300f04683b67e6cdea91d78.

Rohlfing, Torsten, and Calvin R. Maurer. 2003. “Nonrigid Image Registration in Shared-Memory Multiprocessor Environments with Application to Brains, Breasts, and Bees.” *IEEE Transactions on Information Technology in Biomedicine: A Publication of the IEEE Engineering in Medicine and Biology Society* 7 (1): 16–25. https://doi.org/10.1109/titb.2003.808506.

Russell, Joshua, Andrés G. Vidal-Gadea, Alex Makay, Carolyn Lanam, and Jonathan T. Pierce-Shimomura. 2014. “Humidity Sensation Requires Both Mechanosensory and Thermosensory Pathways in Caenorhabditis Elegans.” *Proceedings of the National Academy of Sciences of the United States of America* 111 (22): 8269–74. https://doi.org/10.1073/pnas.1322512111.

Satinoff, Evelyn. 1964. “Behavioral Thermoregulation in Response to Local Cooling of the Rat Brain.” *American Journal of Physiology-Legacy Content* 206 (6): 1389–94. https://doi.org/10.1152/ajplegacy.1964.206.6.1389.

Sayeed, O, and S Benzer. 1996. “Behavioral Genetics of Thermosensation and Hygrosensation in Drosophila.” *Proceedings of the National Academy of Sciences* 93 (12): 6079–84. https://doi.org/10.1073/pnas.93.12.6079.

Sayin, Sercan, Jean-Francois De Backer, K. P. Siju, Marina E. Wosniack, Laurence P. Lewis, Lisa-Marie Frisch, Benedikt Gansen, et al. 2019. “A Neural Circuit Arbitrates between Persistence and Withdrawal in Hungry Drosophila.” *Neuron* 104 (3): 544-558.e6. https://doi.org/10.1016/j.neuron.2019.07.028.

Scheffer, Louis K, C Shan Xu, Michal Januszewski, Zhiyuan Lu, Shin-ya Takemura, Kenneth J Hayworth, Gary B Huang, et al. 2020. “A Connectome and Analysis of the Adult Drosophila Central Brain.” Edited by Eve Marder, Michael B Eisen, Jason Pipkin, and Chris Q Doe. *ELife* 9 (September): e57443. https://doi.org/10.7554/eLife.57443.

Scott, Ethan K., Lindsay Mason, Aristides B. Arrenberg, Limor Ziv, Nathan J. Gosse, Tong Xiao, Neil C. Chi, Kazuhide Asakawa, Koichi Kawakami, and Herwig Baier. 2007. “Targeting Neural

Circuitry in Zebrafish Using GAL4 Enhancer Trapping." *Nature Methods* 4 (4): 323–26. https://doi.org/10.1038/nmeth1033.

Seelig, Johannes D., and Vivek Jayaraman. 2015. "Neural Dynamics for Landmark Orientation and Angular Path Integration." *Nature* 521 (7551): 186–91. https://doi.org/10.1038/nature14446.

Seo, Changwoo, Akash Guru, Michelle Jin, Brendan Ito, Brianna J. Sleezer, Yi-Yun Ho, Elias Wang, et al. 2019. "Intense Threat Switches Dorsal Raphe Serotonin Neurons to a Paradoxical Operational Mode." *Science (New York, N.Y.)* 363 (6426): 538–42. https://doi.org/10.1126/science.aau8722.

Severi, Kristen E., Ruben Portugues, João C. Marques, Donald M. O'Malley, Michael B. Orger, and Florian Engert. 2014. "Neural Control and Modulation of Swimming Speed in the Larval Zebrafish." *Neuron* 83 (3): 692–707. https://doi.org/10.1016/j.neuron.2014.06.032.

Shao, Jiajie, Xiaoyan Zhang, Hankui Cheng, Xiaomin Yue, Wenjuan Zou, and Lijun Kang. 2019. "Serotonergic Neuron ADF Modulates Avoidance Behaviors by Inhibiting Sensory Neurons in C. Elegans." *Pflugers Archiv: European Journal of Physiology* 471 (2): 357–63. https://doi.org/10.1007/s00424-018-2202-4.

Sheard, M. H., and G. K. Aghajanian. 1967. "Neural Release of Brain Serotonin and Body Temperature." *Nature* 216 (5114): 495–96. https://doi.org/10.1038/216495a0.

Shimono, Kohei, Azusa Fujimoto, Taiichi Tsuyama, Misato Yamamoto-Kochi, Motohiko Sato, Yukako Hattori, Kaoru Sugimura, Tadao Usui, Ken-ichi Kimura, and Tadashi Uemura. 2009. "Multidendritic Sensory Neurons in the Adult Drosophila Abdomen: Origins, Dendritic Morphology, and Segment- and Age-Dependent Programmed Cell Death." *Neural Development* 4 (1): 37. https://doi.org/10.1186/1749-8104-4-37.

Shiozaki, Hiromi, Nahoko Kuga, Tasuku Kayama, Yuji Ikegaya, and Takuya Sasaki. 2023. "Selective Serotonin Reuptake Inhibitors Suppress Sharp Wave Ripples in the Ventral Hippocampus." *Journal of Pharmacological Sciences* 152 (2): 136–43. https://doi.org/10.1016/j.jphs.2023.04.003.

Simões, José Miguel, Joshua I. Levy, Emanuela E. Zaharieva, Leah T. Vinson, Peixiong Zhao, Michael H. Alpert, William L. Kath, Alessia Para, and Marco Gallio. 2021. "Robustness and Plasticity in Drosophila Heat Avoidance." *Nature Communications* 12 (April): 2044. https://doi.org/10.1038/s41467-021-22322-w.

Stevens, J. C., and K. K. Choo. 1998. "Temperature Sensitivity of the Body Surface over the Life Span." *Somatosensory & Motor Research* 15 (1): 13–28. https://doi.org/10.1080/08990229870925.

Štih, Vilim. 2021. "Signatures of Motion Processing and Decisions in the Larval Zebrafish Brain." Application/pdf. Ludwig-Maximilians-Universität München. https://doi.org/10.5282/EDOC.28333.

Štih, Vilim, Diego Asua, Luigi Petrucco, Federico Puppo, and Ruben Portugues. 2022. "Sashimi." Zenodo. https://doi.org/10.5281/zenodo.5932227.

Štih, Vilim, Luigi Petrucco, Andreas M. Kist, and Ruben Portugues. 2019. "Stytra: An Open-Source,

Integrated System for Stimulation, Tracking and Closed-Loop Behavioral Experiments." *PLOS Computational Biology* 15 (4): e1006699. https://doi.org/10.1371/journal.pcbi.1006699.

Štih, Vilim, Petrucco, Luigi, Prat, Ot, Lavian, Hagar, and Portugues, Ruben. 2022. "Bouter." Zenodo. https://doi.org/10.5281/ZENODO.5931684.

Suster, Maximiliano L., Hiroshi Kikuta, Akihiro Urasaki, Kazuhide Asakawa, and Koichi Kawakami. 2009. "Transgenesis in Zebrafish with the Tol2 Transposon System." *Methods in Molecular Biology (Clifton, N.J.)* 561: 41–63. https://doi.org/10.1007/978-1-60327-019-9_3.

Svara, Fabian, Dominique Förster, Fumi Kubo, Michał Januszewski, Marco dal Maschio, Philipp J. Schubert, Jörgen Kornfeld, et al. 2022. "Automated Synapse-Level Reconstruction of Neural Circuits in the Larval Zebrafish Brain." *Nature Methods* 19 (11): 1357–66. https://doi.org/10.1038/s41592-022-01621-0.

Tan, Chan Lek, and Zachary A. Knight. 2018. "Regulation of Body Temperature by the Nervous System." *Neuron* 98 (1): 31–48. https://doi.org/10.1016/j.neuron.2018.02.022.

Terrien, Jeremy, Martine Perret, and Fabienne Aujard. 2011. "Behavioral Thermoregulation in Mammals: A Review." *Frontiers in Bioscience-Landmark* 16 (4): 1428–44. https://doi.org/10.2741/3797.

Tomchik, Seth M. 2013. "Dopaminergic Neurons Encode a Distributed, Asymmetric Representation of Temperature in Drosophila." *The Journal of Neuroscience* 33 (5): 2166–76. https://doi.org/10.1523/JNEUROSCI.3933-12.2013.

Tracey, W. Daniel, Rachel I Wilson, Gilles Laurent, and Seymour Benzer. 2003. "Painless, a Drosophila Gene Essential for Nociception." *Cell* 113 (2): 261–73. https://doi.org/10.1016/S0092-8674(03)00272-1.

Turner, Katherine J., Thomas A. Hawkins, Julián Yáñez, Ramón Anadón, Stephen W. Wilson, and Mónica Folgueira. 2016. "Afferent Connectivity of the Zebrafish Habenulae." *Frontiers in Neural Circuits* 10 (April): 30. https://doi.org/10.3389/fncir.2016.00030.

Tyrrell, Jordan J., Jackson T. Wilbourne, Alisa A. Omelchenko, Jin Yoon, and Lina Ni. 2021. "Ionotropic Receptor-Dependent Cool Cells Control the Transition of Temperature Preference in Drosophila Larvae." *PLoS Genetics* 17 (4): e1009499. https://doi.org/10.1371/journal.pgen.1009499.

Umezaki, Yujiro, Sean E. Hayley, Michelle L. Chu, Hanna W. Seo, Prasun Shah, and Fumika N. Hamada. 2018. "Feeding-State-Dependent Modulation of Temperature Preference Requires Insulin Signaling in Drosophila Warm-Sensing Neurons." *Current Biology* 28 (5): 779-787.e3. https://doi.org/10.1016/j.cub.2018.01.060.

Venken, Koen J. T., and Hugo J. Bellen. 2005. "Emerging Technologies for Gene Manipulation in Drosophila Melanogaster." *Nature Reviews. Genetics* 6 (3): 167–78. https://doi.org/10.1038/nrg1553.

Venken, Koen J. T., and Hugo J. Bellen. 2007. "Transgenesis Upgrades for Drosophila Melanogaster." *Development (Cambridge, England)* 134 (20): 3571–84. https://doi.org/10.1242/dev.005686.

Venken, Koen J. T., Julie H. Simpson, and Hugo J. Bellen. 2011. “Genetic Manipulation of Genes and Cells in the Nervous System of the Fruit Fly.” *Neuron* 72 (2): 202–30. https://doi.org/10.1016/j.neuron.2011.09.021.

Virtanen, Pauli, Ralf Gommers, Travis E. Oliphant, Matt Haberland, Tyler Reddy, David Cournapeau, Evgeni Burovski, et al. 2020. “SciPy 1.0: Fundamental Algorithms for Scientific Computing in Python.” *Nature Methods* 17 (3): 261–72. https://doi.org/10.1038/s41592-019-0686-2.

Wechsler, Samuel P., and Vikas Bhandawat. 2023. “Behavioral Algorithms and Neural Mechanisms Underlying Odor-Modulated Locomotion in Insects.” *Journal of Experimental Biology* 226 (1): jeb200261. https://doi.org/10.1242/jeb.200261.

Wee, Caroline Lei, Erin Yue Song, Robert Evan Johnson, Deepak Ailani, Owen Randlett, Ji-Yoon Kim, Maxim Nikitchenko, et al. 2019. “A Bidirectional Network for Appetite Control in Larval Zebrafish.” Edited by Ronald L Calabrese. *ELife* 8 (October): e43775. https://doi.org/10.7554/eLife.43775.

Wiener, Jan, Sara Shettleworth, Verner P. Bingman, Ken Cheng, Susan Healy, Lucia F. Jacobs, Kathryn J. Jeffery, Hanspeter A. Mallot, Randolf Menzel, and Nora S. Newcombe. 2011. “Animal Navigation: A Synthesis.” In *Animal Thinking: Contemporary Issues in Comparative Cognition*, edited by Randolf Menzel and Julia Fischer, 0. The MIT Press. https://doi.org/10.7551/mitpress/9780262016636.003.0005.

Wullimann, Mario F., and Thomas Mueller. 2004. “Teleostean and Mammalian Forebrains Contrasted: Evidence from Genes to Behavior.” *Journal of Comparative Neurology* 475 (2): 143–62. https://doi.org/10.1002/cne.20183.

Zhang, Bai-bing, Yuan-yuan Yao, He-fei Zhang, Koichi Kawakami, and Jiu-lin Du. 2017. “Left Habenula Mediates Light-Preference Behavior in Zebrafish via an Asymmetrical Visual Pathway.” *Neuron* 93 (4): 914-928.e4. https://doi.org/10.1016/j.neuron.2017.01.011.

Zhao, Zheng-Dong, Wen Z. Yang, Cuicui Gao, Xin Fu, Wen Zhang, Qian Zhou, Wanpeng Chen, et al. 2017. “A Hypothalamic Circuit That Controls Body Temperature.” *Proceedings of the National Academy of Sciences* 114 (8): 2042–47. https://doi.org/10.1073/pnas.1616255114.

To Alex: “Well, here at last, dear friends, on the shores of the Sea comes the end of our fellowship in Middle-earth. Go in peace! I will not say: do not weep; for not all tears are an evil.” ― J.R.R. Tolkien, The Return of the King

9. Acknowledgments

First and foremost, I would like to thank my two supervisors, Ruben and Ilona. Together, they managed to provide a wonderful and stimulating working environment where I had the opportunity to grow as a person and as a scientist.

I would like to, particularly, thank Ruben for seeing something in me that I wasn't able to see myself. For always giving me the opportunity to mess around and try new things. For his patience and kindness.

At the same time, I would like to thank Ilona for pushing me to always be better and take ownership of my project and my actions. She kept me focused on my goals, always giving honest and valuable feedback.

I would like to thank the people in the Portugues and Grunwald Kadow lab who have helped me over the years. Siju, who helped me take my first steps in the fly world. Jean-François, for assisting me with the fly preps. Ariane and Johanna, for being great friends and mentors. Andreas, for teaching me the most valuable lesson of the PhD: you can't be scared of breaking things. Tugce, who taught me how to embed my first fish and with whom I shared many deep conversations over the years. Elena, for her useful feedback on the conceptual framework of my project. Daniil, for his unwavering work ethics and discipline. I would like to thank Vilim for trying really hard to teach me how to produce beautiful code. Outside the lab, I thank him for the brunches, the photoshoots, the dinners, the conversations, and the many hastily executed plans.

I would like to thank Ot, Hagar, You, Younes, Amey, Anja, Shuhong, Kata, Elena, Lisa, and Laila for being great lab mates. It was a pleasure to be around all of you.

I would like to thank two very good friends from the MPI, Florian and Yana, for their support and the many silly laughs.

I want to thank Katie and Jasmine, two of the most talented cooks I have ever met.

A special mention goes to Alejandro, the only person I trust when it comes to arthropods evolution and basically everything else.

A huge thanks goes to three old friends. Francesca, who shows me on a daily basis what it means to be exceptional. Flavia and Gianluca, whose friendship I usually take for granted except when I remember how lucky I am to have them in my life.

I would like to thank Luigi with whom I shared this PhD journey. It doesn't happen often to meet someone so similar and yet so different. Thank you for all the discussions. The best part was being right.

Thank you, Ema. This project has been a constant presence in my life for the past 6 years. I feel incredibly fortunate to have had the opportunity to share it with someone as talented and kind as you. We experienced countless successes and failures together, and still I would repeat this journey all over again. Thank you for showing me what it means to feel at home.

Last but not least, I would like to thank my parents, Luigi and Isabella, because I would not be who I am if it wasn't for them. My grandma, Osanna, a true feminist and role model, and my brother, Tommaso, who is my main drive to always be the best version of myself.